

Washington University in St. Louis

Washington University Open Scholarship

All Theses and Dissertations (ETDs)

January 2009

Characterization of Ligand-Induced Conformational Changes in the EGF Receptor

Katherine Yang

Washington University in St. Louis

Follow this and additional works at: <https://openscholarship.wustl.edu/etd>

Recommended Citation

Yang, Katherine, "Characterization of Ligand-Induced Conformational Changes in the EGF Receptor" (2009). *All Theses and Dissertations (ETDs)*. 422.

<https://openscholarship.wustl.edu/etd/422>

This Dissertation is brought to you for free and open access by Washington University Open Scholarship. It has been accepted for inclusion in All Theses and Dissertations (ETDs) by an authorized administrator of Washington University Open Scholarship. For more information, please contact digital@wumail.wustl.edu.

WASHINGTON UNIVERSITY IN ST. LOUIS

Division of Biology and Biomedical Sciences

Program in Biochemistry

Dissertation Examination Committee:

Linda Pike, Chair

Ron Bose

Raphael Kopan

Timothy Lohman

David Piwnica-Worms

Philip Stahl

CHARACTERIZATION OF LIGAND-INDUCED CONFORMATIONAL CHANGES
IN THE EGF RECEPTOR

by

Katherine Sterling Yang

A dissertation presented to the
Graduate School of Arts and Sciences
of Washington University in
partial fulfillment of the
requirements for the degree
of Doctor of Philosophy

August 2009

Saint Louis, Missouri

ABSTRACT OF DISSERTATION

Characterization of ligand-induced conformational changes in the EGF receptor

by

Katherine S. Yang

Doctor of Philosophy in Biochemistry

Washington University in St. Louis, 2009

Professor Linda Pike, Chairperson

The epidermal growth factor (EGF) receptor is a classical receptor tyrosine kinase that mediates cellular processes such as proliferation, migration, and differentiation in response to growth factor stimulation. Crystal structures of the EGF receptor suggest that its activation is associated with extensive conformational changes in both the extracellular and intracellular domains. However, evidence of these structural dynamics in intact cells has been lacking. This thesis describes the characterization of sequential ligand-induced conformational changes in the EGF receptor in live cells in real time using luciferase fragment complementation imaging. We find that these conformational changes are unique to the full-length activated EGF receptor. These studies identified a novel conformational change that was dependent on MAP kinase activation and desensitization of the EGF receptor. It has been unclear how MAP kinase desensitizes the EGF receptor following activation. Mutational analysis was done to identify residues involved in the MAP kinase-mediated EGF receptor desensitization. We use these analyses to provide a structural explanation for the MAP kinase-mediated desensitization of the EGF receptor. The luciferase complementation assay was further utilized to test

the ability of different ligands for the EGF receptor family to induce dimer formation and intracellular domain conformational changes.

ACKNOWLEDGEMENTS

The work presented in this thesis was supported by the Division of Biology and Biomedical Sciences and the National Institutes of Health grant 5R01GM064491-07 and 5R01GM082824-02 to Professor Linda Pike.

I dedicate this work to my mentor, Linda Pike, my family, and of course my husband Rob. Without their continued support and willingness to help me, this work would not have been possible.

Table of Contents

Abstract of Dissertation	ii
Acknowledgements	iv
Table of Contents	v
List of Tables	viii
List of Figures	ix
List of Abbreviations	xi
CHAPTER 1. Introduction to the EGF Receptor Family	1
Discovery of EGF and its Receptor	1
Nomenclature and Domain Organization of the EGF Receptor Family	3
Ligand-Induced EGF Receptor Dimer Formation	4
Structure-Based Activation Mechanism for the EGF Receptor.....	5
Higher Order EGF Receptor Oligomers	8
Ligands for the EGF Receptor Family.....	9
Ligand-Induced EGF Receptor Signaling.....	11
Mechanism of EGF Receptor Deactivation	12
Figures.....	15
CHAPTER 2. Luciferase Fragment Complementation Imaging of Conformational Changes in the EGF Receptor	20
Introduction.....	20
Results.....	21
<i>EGF induces a rapid increase in luciferase complementation in ΔC-EGFR- NLuc/CLuc cells</i>	21
<i>EGF elicits a rapid but transient decrease in luciferase activity in full-length EGFR- NLuc/CLuc cells</i>	22
<i>The decrease in luciferase activity is dependent on EGF receptor kinase activity ..</i>	24
<i>MAP kinase activity is required for the recovery of luciferase complementation</i>	28
Discussion	29
Experimental Procedures	36
Reagents.....	36
DNA Constructs.....	36
Cell lines	38
Kinase activation and Western Blotting	39
¹²⁵ I-EGF Binding	39
Luciferase complementation imaging.....	39
Data Analysis	40
Figures.....	41

CHAPTER 3. MAP Kinase Desensitizes the EGF Receptor by Blocking Allosteric Activation of the Kinase Domain	53
Introduction.....	53
Results.....	55
<i>EGF induces enhanced phosphorylation and internalization of the T669A-EGF receptor</i>	55
<i>Mutation of acidic amino acids in the C-lobe of the EGF receptor kinase domain result in elevated autophosphorylation independent of MAP kinase activity</i>	56
<i>T669R-, T669E-, and T669D-EGF receptor mutants display enhanced autophosphorylation</i>	59
<i>Asp-950 is important in stabilizing the asymmetric kinase domain interface</i>	60
<i>Autophosphorylation is recovered in cells expressing the triple EGF receptor mutant, D950A/D960A/E961A</i>	61
<i>Asp-960 and Glu-961 are required to observe a recovery in luciferase activity</i>	62
<i>Mutation of Asp-950 leads to a rapid increase in luciferase activity</i>	63
Discussion	64
Experimental Procedures	72
Reagents	72
DNA Constructs	73
Cell Lines	75
Kinase activation and Western Blotting	76
¹²⁵ I-EGF Internalization	76
Luciferase complementation imaging.....	77
Data Analysis	77
Figures.....	78
CHAPTER 4. Examining the Differential Effects of the EGF Family of Growth Factors using the Luciferase Fragment Complementation Imaging Assay	90
Introduction.....	90
Results.....	92
<i>Identification of the saturation point in luciferase activity following stimulation with EGF, BTC, or AR in ΔC-EGF receptor cells</i>	92
<i>Ability of EGF, BTC, and AR to saturate ΔC-EGF receptor/ΔC-ErbB2 hetero-dimerization</i>	94
<i>Ability of EGF, BTC, and AR to induce homo- and hetero-dimerization</i>	98
<i>BTC enhances the recovery in luciferase activity in the full-length EGF receptor</i> ..	99
Discussion	100
Experimental Procedures	104
Reagents	104
DNA constructs	104
Cell Lines	105
Luciferase complementation imaging.....	105
Data Analysis	106
Tables.....	106
Figures.....	107
CHAPTER 5. Discussion and Future Directions	117

Contributions to the EGF receptor field.....	117
Future Directions	118
References	121

List of Tables

Chapter 4

Table 4.1. Comparison of the Y_{\max} and EC_{50} values following stimulation with EGF or BTC in cells expressing ΔC -EGFR-NLuc/CLuc or ΔC -EGFR-NLuc/ ΔC -ErbB2-CLuc.	107
Table 4.2. Comparison of the effects of EGF, BTC, and AR on cells expressing ΔC -EGFR-NLuc/CLuc or ΔC -EGFR-NLuc/ ΔC -ErbB2-CLuc.	107

List of Figures

Chapter 1

Figure 1.1. Domain organization of the EGF receptor.	15
Figure 1.2. Schematic representation for the ligand-induced dimerization and activation of the EGF receptor.	15
Figure 1.3. Schematic representation of the EGF receptor extracellular domain monomer and dimer.	16
Figure 1.4. Schematic representation of the EGF receptor kinase domain asymmetric dimer.	16
Figure 1.5. Crystal structure of the intracellular juxtamembrane and kinase domains of ErbB4 (Her4) and the EGF receptor.	17
Figure 1.6. Ligands for the EGF receptor family.	18
Figure 1.7. Ligand-induced EGF receptor autophosphorylation and downstream signaling.	19

Chapter 2

Figure 2.1. Reconstitution of luciferase activity and ¹²⁵ I-EGF binding in ΔC-EGFR-NLuc/CLuc CHO cells.	41
Figure 2.2. Characterization of the full-length EGFR-NLuc and EGFR-CLuc.	42
Figure 2.3. Reconstitution of luciferase activity in response to EGF in EGFR-NLuc/CLuc cells.	43
Figure 2.4. Competition of basal luciferase complementation using unlabeled wild type EGF receptor.	44
Figure 2.5. Comparison of the rate of EGF receptor autophosphorylation to the EGF-stimulated decrease in luciferase activity.	44
Figure 2.6. Inhibition of EGF receptor autophosphorylation and MAP kinase activation following pre-treatment with AG1478 or Erlotinib.	45
Figure 2.7. Effect of a kinase inhibitor on reconstituted luciferase activity.	46
Figure 2.8. Effect of TPA treatment on EGF receptor autophosphorylation and luciferase activity in EGFR-NLuc/CLuc cells.	47
Figure 2.9. Effect of the protein kinase C activator, calmidazolium, on EGF receptor autophosphorylation and reconstituted luciferase activity.	48
Figure 2.10. Expression of kinase-dead EGF receptor and the effect on reconstituted luciferase activity.	49
Figure 2.11. Effect of truncation of the C-terminal tail of the EGF receptor on reconstituted luciferase activity.	49
Figure 2.12. Contribution of MAP kinase activation to the recovery of reconstituted luciferase activity.	50
Figure 2.13. Effect of mutation of Thr-669 of the EGF receptor on reconstituted luciferase activity.	51
Figure 2.14. Model for intracellular domain conformational changes observed using luciferase fragment complementation imaging of the full-length EGF receptor.	52

Chapter 3

Figure 3.1. Effect of Thr-669 mutation on EGF receptor autophosphorylation and internalization.	78
Figure 3.2. Crystal structure of the EGF receptor juxtamembrane and kinase domain asymmetric dimer interface, highlighting the residues surrounding Thr-669.....	79
Figure 3.3. EGF receptor autophosphorylation in wild type, T669A, and D960A/E961A mutants.....	80
Figure 3.4. Effect of blocking MAP kinase activation on wild type or T669A-EGF receptor autophosphorylation.....	81
Figure 3.5. Dose-response to EGF in cells expressing wild type, T669A, T669R, T669D, and T669E-EGF receptor mutants.....	82
Figure 3.6. EGF receptor autophosphorylation in cells expressing wild type, D950A, D950A/D960A/E961A, L680N, or D950A/L680N mutations.....	83
Figure 3.7. EGF dose response in cells expressing wild type or T669A/D950A EGF receptors.....	84
Figure 3.8. Reconstitution of luciferase activity in cells expressing wild type, T669A, or D960A/E961A luciferase constructs.....	85
Figure 3.9. Reconstitution of luciferase activity in cells expressing D950A and K721A EGF receptor luciferase constructs.....	86
Figure 3.10. Sequence alignment of the region surrounding EGF receptor Thr-669 and the acidic amino acids Asp-950, Asp-960, and Glu-961.....	87
Figure 3.11. Model for the mechanism of MAP kinase-mediated EGF receptor desensitization.....	89

Chapter 4

Figure 4.1. Complexity of the EGF receptor family signaling network.....	108
Figure 4.2. Ability of EGF, BTC, and AR to induce an increase in luciferase activity in Δ C-EGF receptor cells.....	109
Figure 4.3. Dose-response to EGF, BTC, and AR in Δ C-EGF receptor cells.....	110
Figure 4.4. Characterization of Δ C-ErbB2-NLuc and Δ C-ErbB2-CLuc constructs..	111
Figure 4.5. Ligand-induced increase in luciferase activity in Δ C-EGF receptor/ Δ C-ErbB2 cells.....	112
Figure 4.6. Dose-response to EGF and BTC in Δ C-EGF receptor/ Δ C-ErbB2 cells	113
Figure 4.7. Ligand-induced changes in luciferase activity in cells expressing Δ C-EGF receptor alone or in addition to Δ C-ErbB2.....	114
Figure 4.8. Effect of EGF and BTC on the ligand-induced conformational changes in the full-length EGF receptor.....	115
Figure 4.9. Model for differential regulation of EGF receptor dimerization, signaling, and biological effect mediated by different ligands.....	116

List of Abbreviations

NGF	Nerve Growth Factor
EGF	Epidermal Growth Factor
BTC	Betacellulin
AR	Amphiregulin
ADAM	A Disintegrin Associated Metalloproteinase
Grb2	Growth Factor Receptor Bound Protein 2
SOS	Son of Sevenless
MAP Kinase	Mitogen-Activated Protein Kinase
SH2	Src-Homology 2 Domain
PTB	Protein Tyrosine Binding-Domain
NLuc	N-terminal Firefly Luciferase
CLuc	C-terminal Firefly Luciferase
TPA	12-O-tetradecanoylphorbol 13-acetate

CHAPTER 1. Introduction to the EGF Receptor Family

Discovery of EGF and its Receptor

The epidermal growth factor (EGF) was first discovered in 1962 by Professor Stanley Cohen. The route to this discovery began with the discovery of nerve growth factor (NGF). While working in the lab of Professor Viktor Hamburger, Dr. Rita Levi-Montalcini observed that when a fragment of mouse tumor (Sarcoma 180) was grafted onto the body wall of chick embryos, both sympathetic and sensory fibers entered the tumor and extended to tissues that they normally should not reach (1). After several confirmatory experiments, Dr. Levi-Montalcini and Professor Hamburger hypothesized that this phenomenon was due to a diffusible agent that was released from the tumor, resulting in the stimulation of nerve cell growth (2, 3).

Professor Stanley Cohen, a postdoc in the Hamburger lab at the time, further advanced the remarkable story when he discovered that crude extract from the mouse tumors could be inactivated by protease but not Dnase or RNase. These observations led him to think that the diffusible agent was a protein (4), but the possibility of it being a virus was also raised by Professor Arthur Kornberg. In an attempt to test the virus hypothesis, Professor Stanley Cohen used partially purified phosphodiesterase from snake venom (which would have degraded all known nucleic acids including those of viruses) in the absence and presence of his crude tumor extract to examine the effect on chick ganglions in culture. To his surprise, partially purified phosphodiesterase alone resulted in a massive growth of nerve fibers in a single day. Further experiments showed that this growth resulted from the presence of an additional protein in the impure

phosphodiesterase preparation, and that it in its purified form was much more potent in stimulating nerve growth. This protein was the nerve growth factor or NGF (5).

Puzzled by the lack of an apparent connection between nerve growth, tumors and snake venom, Professor Cohen wondered about the source of the snake venom—the salivary glands. He subsequently tested crude extracts of the salivary gland from male mice and observed that these mice-extracts were just as potent in inducing nerve outgrowth. Furthermore, when these crude extracts were injected daily into newborn mice the sympathetic ganglion were enlarged. Even more surprisingly, the mice opened their eyes 5-7 days earlier than normal and their teeth erupted earlier, a phenomenon that could not be induced by purified NGF..

Professor Cohen went on to pursue the question why crude extracts from the male mouse salivary gland induced early eyelid opening in the mouse as a faculty at Vanderbilt. By examining histological sections of the eyelid area from control and treated animals, it was clear that early eyelid opening was due to enhanced epidermal growth and keratinization. The 53-amino acid disulfide linked protein responsible was purified from the mouse salivary gland using the eyelid-opening functional assay and was initially referred to as tooth-lid factor (6).

To address whether this tooth-lid factor was acting directly or indirectly via a secondary mechanism, the tooth-lid factor was added directly to organ cultures of chick embryonic skin. This led to a direct effect in which there was an increase in both epidermal cell number and size, resulting in a renaming of tooth-lid factor to epidermal growth factor (EGF) (7).

The prevailing theory at the time was that protein hormones do not enter cells, but rather bind to cell surface receptors to exert their effect and then dissociate. The next major discovery was the identification and isolation of the receptor for EGF. An explosion of research into the EGF receptor then followed. Among the major discoveries were that 1) EGF addition to A431 cell membrane preparations resulted in incorporation of ^{32}P -ATP into the protein of membranes (8); 2) many proteins were phosphorylated in A431 membranes, particularly a protein of 170kDa (9); 3) the purified 170kDa protein bound EGF, had protein kinase activity that was dependent on ATP and EGF and was itself phosphorylated (10-15); and finally that 4) the EGF receptor was a tyrosine kinase (16).

The initial identification of EGF and its receptor won Professor Cohen the Nobel prize in 1986. His groundbreaking research into the field of growth factors and their receptors has shaped nearly 50 years of research to date, and has led to the identification of nearly 60 receptor tyrosine kinases. The remainder of this introduction will focus on the biology of the EGF receptor.

Nomenclature and Domain Organization of the EGF Receptor Family

The EGF receptor (ErbB1/HER1) is the founding member of the ErbB or human EGF receptor (HER) subfamily of receptor tyrosine kinases. This subfamily consists of three additional members: ErbB2/HER2/Neu, ErbB3/HER3, and ErbB4/HER4. The ErbB nomenclature derives from the high homology between the family members and the avian erythroblastosis virus v-erb-B transforming protein (17). The ErbB members are

highly homologous (40-45% sequence identity) (18) and all share similar domain organizations.

The EGF receptor consists of an extracellular ligand-binding domain, a single-pass α -helical transmembrane domain, and an intracellular domain with tyrosine kinase activity (19) (Figure 1.1). Approximately half of the receptor constitutes the extracellular domain (amino acids 1-621). The remainder of the EGF receptor is comprised of the transmembrane domain (amino acids 622-644), the intracellular juxtamembrane domain (amino acids 645-685), the tyrosine kinase domain (amino acids 686-960), and the C-terminal tail (amino acids 961-1186) (Figure 1.1).

Ligand-Induced EGF Receptor Dimer Formation

The canonical view of EGF receptor activation postulates that in the absence of ligand, the receptor exists as an inactive monomer in cell membranes (challenges to this hypothesis will be discussed later in the introduction). Upon ligand binding to the extracellular domain, EGF receptor dimers are formed leading to stimulation of the protein tyrosine kinase activity (Figure 1.2). Initial studies indicating that the EGF receptor dimerizes upon ligand binding demonstrated that addition of EGF leads to conversion of the receptor from a low molecular weight to a higher molecular weight state (20). Additionally, covalently cross-linking ^{125}I -EGF to its receptor results in a slower electrophoretic migration, which is competed by addition of unlabeled EGF (20). Further chemical crosslinking studies showed that EGF induces EGF receptor dimerization in Triton X-100-solubilized receptor preparations (21, 22), membrane preparations (23), and in intact cells (24-26).

Dimerization of the EGF receptor stimulates the protein tyrosine kinase activity, which leads to an intermolecular autophosphorylation mechanism of tyrosine residues on the C-terminal tail of the receptor (Figure 1.2). Several lines of evidence support the intermolecular phosphorylation mechanism as opposed to an intramolecular or truly self-phosphorylation process. First, EGF receptor cross-linking using bivalent antibodies stimulates receptor autophosphorylation, with no autophosphorylation observed in the absence of antibodies or using monovalent forms of the antibodies (27, 28). Second, simply immobilizing the EGF receptor on solid matrices prevents EGF from activating the receptor kinase activity (27). Finally, in experiments where cells expressed a kinase-dead EGF receptor and a kinase-active EGF receptor that lacks the amino-terminal 63 amino acids (and two autphosphorylation sites), the kinase-dead EGF receptor was observed to be in the phosphorylated state. This phosphorylation could only result from an intermolecular process mediated by the truncated/kinase-active EGF receptor since the kinase-dead EGF receptor completely lacks catalytic activity (29, 30). Taken together, these data support the ligand-induced dimerization and activation mechanism for the EGF receptor.

Structure-Based Activation Mechanism for the EGF Receptor

Recent crystal structures of the EGF receptor extracellular domain have provided invaluable insights into the structural aspects of the activation mechanism. The EGF receptor extracellular domain consists of four subdomains: I, II, III, and IV (Figure 1.3). Subdomains I and III are homologous and together form the primary ligand binding site (red in Figure 1.3). Subdomains II and IV are homologous cysteine-rich regions (19)

(green in Figure 1.3). In the absence of ligand, the EGF receptor monomer exists in a tethered/closed conformation (31) (Figure 1.3). The EGF receptor monomer is held in this tethered conformation primarily through a β -hairpin/loop in subdomain II that interacts with a similar loop in subdomain IV. One of the required residues for this interaction is Y246 in subdomain II (31). This tethered conformation of the EGF receptor is thought to have low affinity for ligand because the ligand cannot simultaneously bind subdomains I and III (31).

Ligand binding to the EGF receptor disrupts the intramolecular tether and promotes a dramatic conformational change in which the EGF receptor adopts an open/extended conformation (31-33) (Figure 1.3). The β -hairpin/loop from subdomain II, referred to as the dimerization arm, mediates formation of back-to-back EGF receptor dimer (32, 33) (Figure 1.3). In the extended, dimerized conformation, Y246 is crucial to formation of the EGF receptor/EGF receptor intermolecular contacts in the dimer. Mutation of this residue to D, F, or W abolishes EGF receptor dimer formation as measured by chemical crosslinking (34). Moreover, the integrity of this residue is required to observe EGF receptor autophosphorylation, providing a structural basis for the observed intermolecular phosphorylation mechanism (34).

Recently it has been demonstrated that the EGF receptor kinase domain can also form dimers (35). X-ray crystallography work has shown that the kinase domain of the EGF receptor forms an asymmetric dimer in which the N-lobe of one kinase contacts the C-lobe of a second kinase (35) (Figure 1.4). In this configuration, one of the monomers (acceptor in Figure 1.4) becomes activated and is able to phosphorylate the C-terminal tail of the second monomer (donor in Figure 1.4). Mutation of residues in the dimer

interface of either the N-lobe (eg L680N) or the C-lobe (eg V924R) block the ability of EGF to stimulate kinase activation (35). Together these data imply an allosteric mechanism for activation of the EGF receptor kinase domain. Through an unknown mechanism, these kinase domains may re-order, so that phosphorylation of the other kinase monomer in the dimer can occur (donor becomes acceptor and vice versa in Figure 1.4).

The intracellular juxtamembrane region has also been hypothesized to play a critical role in activating the kinase domain (Figure 1.1). Thiel and Carpenter first demonstrated the necessity for this domain by utilizing an intracellular domain (ICD) construct that is constitutively autophosphorylated (36). Deletion of amino acids 645-662 or 645-676 resulted in a dramatic reduction in EGF receptor autophosphorylation. Similar results were obtained when these deletion mutants were introduced into the ligand-regulated full-length EGF receptor that was expressed in NIH 3T3 cells.

Structurally, insight on the juxtamembrane region was first gained from the asymmetric kinase domain crystal structure of ErbB4 bound to a thienopyrimidine analog inhibitor, a structure that included the C-terminal portion of the juxtamembrane region of ErbB4 (EGF receptor amino acids 664-961) (37). Further analysis of the asymmetric dimer in this structure by Jura et al. showed that the juxtamembrane region of the acceptor kinase forms a cradle around the C-lobe of the donor kinase in the asymmetric unit (Figure 1.5A) (38). A recent crystal structure of the EGF receptor kinase domain where the entire juxtamembrane region (amino acids 652-994) was visible revealed a similar “cradling” orientation (Figure 1.5B) (39). In both of these reports, mutagenesis of the ICD construct (39) or the full-length EGF receptor (38) in the C-terminal portion

of the juxtamembrane domain (amino acids 664-682) significantly impaired autophosphorylation of the EGF receptor. In addition, Jura et al. demonstrated using mutagenesis that residues in the C-lobe of the donor kinase that contact the juxtamembrane domain of the acceptor kinase are also required for full autophosphorylation of the EGF receptor (38). These findings suggest that the juxtamembrane region is important for formation of the asymmetric dimer interface and required for full activation of the EGF receptor.

While there is ample structural information for the extracellular and tyrosine kinase domains of the EGF receptor, there is little structural information for the C-terminal tail. This is likely due to the conformational flexibility of this region. Indeed, hydrodynamic studies have shown that upon autophosphorylation of the C-terminal tail, the EGF receptor intracellular domain adopts a more extended conformation than in the absence of autophosphorylation (40). Additional studies using FRET suggest that the C-terminal tail and the EGF receptor tyrosine kinase domain separate to form a more extended molecule following autophosphorylation (41).

Higher Order EGF Receptor Oligomers

There is evidence that the EGF receptor forms higher order oligomers both in the absence and presence of ligand. Using image correlation microscopy of an EGF receptor-GFP chimera, studies have shown that the EGF receptor undergoes a dimer-tetramer transition upon stimulation with ligand (42). Recent studies from our lab using fluorescence intensity cluster analysis support the notion that the EGF receptor may exist in preformed dimers and higher order oligomers in the absence of ligand (43).

Studies utilizing FRET microscopy with fluorescently labeled EGF demonstrated that the receptor bound EGF molecules are capable of significant energy transfer. However, these data contradicted the known structure of EGF receptor dimers (Figure 1.3), where the two bound EGF molecules are too far apart (100Å) to undergo the observed significant energy transfer. Thus, the authors hypothesized that FRET occurred due to clustering of the EGF receptor, most likely in side-by-side tetramers (44). Other studies using lifetime-based FRET microscopy suggest that in the absence of ligand, the EGF receptor may exist in large clusters, with up to 30 receptors per cluster (45). These clusters may enable rapid receptor activation on ligand binding.

Together these studies provide evidence for the existence of a higher-order signaling complex within the EGF receptor system. The nature of higher order EGF receptor oligomers is not fully understood and the structural requirements for such an oligomer have not been addressed.

Ligands for the EGF Receptor Family

In order to engage the EGF receptor in signaling inside the cell, the receptor must first be activated by a small, soluble growth factor outside the cell. There are 11 known ligands that bind to the extracellular domains of the EGF receptor family (46, 47) (Figure 1.6A). These ligands can be subdivided into three groups based on their receptor specificity: 1) EGF, TGF- α , Amphiregulin (AR), and Epigen all bind the EGF receptor, 2) Betacellulin (BTC), Heparin-binding EGF, and Epiregulin all bind the EGF receptor and ErbB4, 3) the Neuregulins (of which there are multiple isoforms) bind to ErbB3 or

ErbB4 (46-48). It is interesting to note that no ligand has yet been found that binds to ErbB2.

All ligands for the EGF receptor family are synthesized as transmembrane precursors that are cleaved by the ADAM (A Disintegrin And Metalloproteinase) family of metalloproteinases (49). This cleavage leads to release of the “mature” or soluble protein into the cell matrix or cell culture (Figure 1.6B). Ligands for the EGF receptor family also have at least one EGF-like motif, which is defined by the presence of six spatially conserved cysteine residues (CX7 CX4-5 CX10-13 CXCX8 C). These cysteines then form three disulfide bonds (C1-3, C2-4, C5-6) (49).

The ligands for the EGF receptor family have different binding affinity and specificity (47, 50). They also induce different phosphorylation patterns of the signaling tyrosine residues which consequently leads to diversification of signaling pathways activated and gene expression patterns (47). While these differential outputs are not yet fully understood, part of the distinction may lie in the conformation of the receptor bound to ligand. The subdomain II dimerization arm in the EGF receptor extracellular domain adopts slightly different conformations when bound to EGF versus TGF- α , which may reflect differences in one of the ligand binding subdomains (III) (32, 33, 47). Differences in ligand-binding to the extracellular domain may be transmitted to the intracellular domain, resulting in slightly different interfaces for the tyrosine kinase domains and eventually leading to the observed differential outputs (47).

Ligand-Induced EGF Receptor Signaling

Ligand binding to the EGF receptor promotes a conformational change in the extracellular domain that exposes residues essential for dimerization (31-34, 51-53). Formation of EGF receptor dimers brings into close proximity the tyrosine kinase domains so that they can form the activating asymmetric dimer interface (35, 46, 54). This enhances the catalytic activity of the EGF receptor kinase, resulting in autophosphorylation in trans on five regulatory tyrosine residues in the ~200 amino acid C-terminal tail (55-60) (Figure 1.7A). In addition to autophosphorylation, the EGF receptor can also be transphosphorylated on its tyrosine residues by other kinases, such as Src (61-63) (Figure 1.7A).

The phosphorylated C-terminal tail tyrosine residues of the EGF receptor serve as association sites for signaling or adaptor proteins. The pattern and sequence context of the phosphorylated tyrosine residues discriminates which Src homology 2 (SH2) and phosphotyrosine binding (PTB) domain-containing proteins bind to the EGF receptor (56, 64) (Figure 1.7A). SH2 modules are typically 100 amino acids long and recognize phosphorylated tyrosines in the context of the 3-6 amino acids downstream of the phosphorylated tyrosine. In contrast, PTB modules are typically 150 amino acids long and recognize phosphorylated tyrosines by the amino acids just upstream (64, 65). The SH2 and PTB domain-containing proteins that bind to the EGF receptor phosphorylated tyrosine residues ultimately determines which signaling pathways are activated and the biological outcome from the external cue (cell proliferation, survival, migration, etc.) (48, 57, 64, 66). The SH2 and PTB domain-containing proteins serve as adaptors, enabling

EGF receptor signaling inside the cell. Association with the EGF receptor facilitates formation of an ordered multicomponent signaling complex (48, 56, 57, 64, 66).

Several signaling pathways are activated by the EGF receptor, but the focus of this introduction will be on the Ras/mitogen activated protein (MAP) kinase pathway. Following autophosphorylation of the EGF receptor on tyrosine residues, growth factor receptor-bound protein 2 (Grb2) docks directly to tyrosines 1068 or 1086, or associates indirectly via Shc (56, 67-69) (Figure 1.7A and B). Grb2 is constitutively bound to the guanine nucleotide exchange factor Son of Sevenless (SOS) (70) so that binding of Grb2 to the EGF receptor relocalizes the complex to the plasma membrane. This causes exchange of GDP for GTP on the membrane-bound protein Ras, thereby activating Ras (71-74). Activated Ras in turn activates the serine-threonine kinase Raf (75-77), which phosphorylates the threonine/tyrosine kinase MEK (78, 79). Finally, MEK activates MAP kinase through phosphorylation on threonine and tyrosine residues, inducing nuclear translocation and the phosphorylation and activation of nuclear transcription factors that lead to cellular proliferation (56, 69, 80).

Mechanism of EGF Receptor Deactivation

Following activation, negative regulation of EGF receptor signaling must ensue to prevent “over-signaling” from the receptor. Failure in proper EGF receptor de-regulation often leads to heightened oncogenic potential (81). Long-term regulation is mediated by internalization and subsequent irreversible degradation of the receptor (82-84). This process was first described by Carpenter and Cohen in studies demonstrating that ¹²⁵I-EGF binds to the EGF receptor and is subsequently removed from the cell surface and

degraded by lysosomes (85). Long-term regulation of EGF receptor signaling, later termed “EGF-induced down-regulation of the EGF receptor”, serves as a major negative regulatory mechanism (84).

Independent of receptor internalization and degradation, the EGF receptor also undergoes a rapid negative regulatory component, termed desensitization, that is associated with a loss of protein tyrosine kinase activity (86-88). Desensitization can occur through binding of negative regulatory proteins to the EGF receptor. The best characterized example is the protein MIG-6 (also known as gene 33 or receptor-associated late transducer/RALT). MIG-6 is transcriptionally induced by the EGF receptor via the Ras pathway and has been shown through crystallography work to bind to the C-lobe of the EGF receptor kinase domain to block formation of the activating asymmetric dimer (81, 89-92). Binding of MIG-6 to the EGF receptor effectively blocks activation of the EGF receptor without blocking the catalytic activity.

In addition to specific negative regulators, several proteins activated by the EGF receptor signaling pathways also play significant roles in the desensitization process. Previous work suggests that phosphorylation of the EGF receptor on two threonine residues within the intracellular juxtamembrane region may be involved in the rapid loss of tyrosine kinase activity (93, 94). Of these two sites, the major site of threonine phosphorylation on the EGF receptor is Thr-669 (95). Phosphorylation of this site is mediated by a feedback loop: the EGF receptor activates MAP kinase, which in turn directly phosphorylates the EGF receptor on Thr-669 (96-98). Mutation of Thr-669 to Ala is associated enhanced EGF receptor phosphorylation (94). These data suggest that phosphorylation of Thr-669 is associated with EGF receptor desensitization. The

mechanism by which phosphorylated Thr-669 blocks receptor kinase activity is not understood. Overall, the pathways and proteins that negatively regulate EGF receptor signaling are poorly understood and much work remains to understand how these pathways function and how they may be exploited or modified to evolve new therapies targeting the EGF receptor.

The work presented in this thesis will examine several conformational changes in the EGF receptor, as well as the implications of these conformational changes. Chapter 2 will describe how a luciferase fragment complementation imaging assay was developed and utilized in the context of the EGF receptor system to follow ligand-induced conformation changes. This type of analysis has not been possible using existing assays. One of the major implications of these results will be described in Chapter 3, with the mechanistic explanation for MAP kinase-mediated EGF receptor desensitization. Finally, Chapter 4 will delve into one aspect of the wide-range of utility of luciferase fragment complementation imaging of the EGF receptor by focusing on the effects of EGF-like growth factors. A discussion of the global implications of these results and potential future studies based on these results will be addressed in Chapter 5.

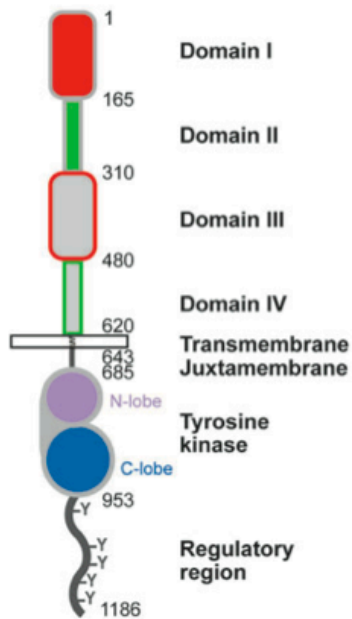


Figure 1.1. Domain organization of the EGF receptor. The extracellular domain consists of four subdomains (I-IV). This is followed by an α -helical transmembrane domain and then the intracellular juxtamembrane domain. The tyrosine kinase domain contains the catalytic activity of the receptor, while the C-terminal tail contains regulatory tyrosine residues (52).

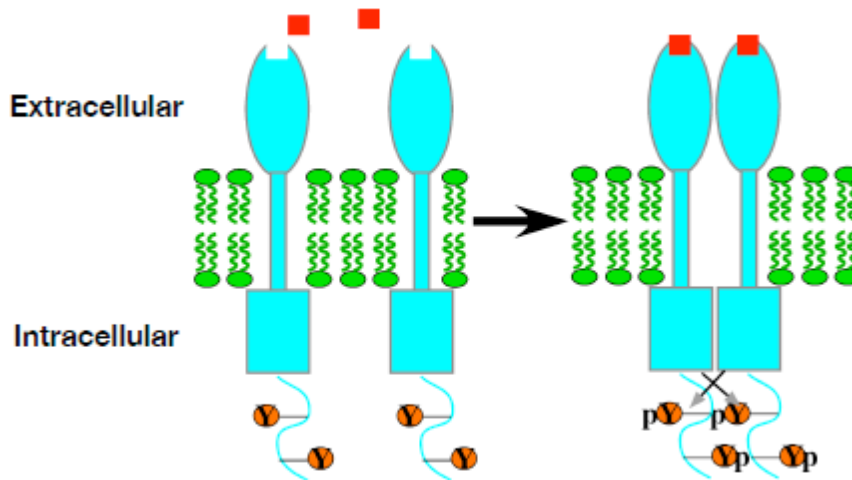


Figure 1.2. Schematic representation for the ligand-induced dimerization and activation of the EGF receptor. In the absence of ligand, the EGF receptor is thought to exist as an inactive monomer (left panel). Binding of ligand induces EGF receptor dimer formation, bringing into proximity the tyrosine kinase domains of the EGF receptor and resulting in enhanced kinase activity (right panel). This results in autophosphorylation in trans of tyrosine residues in the C-terminal tail of the receptor, as well as phosphorylation of several protein substrates.

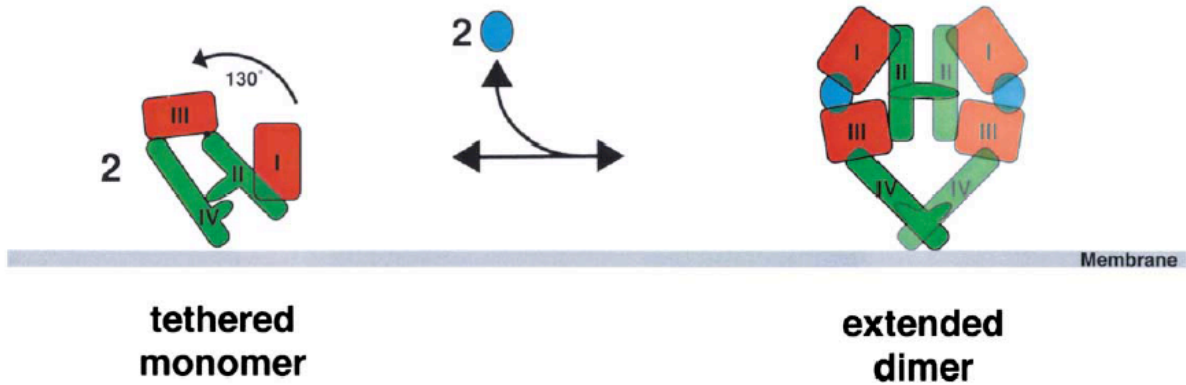


Figure 1.3. Schematic representation of the EGF receptor extracellular domain monomer and dimer. In the absence of ligand, the EGFR monomer is held in a tethered/closed conformation through contacts between subdomains II and IV. Ligand binding between subdomains I and III induces a dramatic conformational change that disrupts the intramolecular tether and exposes a dimerization arm in subdomain II. This dimerization arm mediates the formation of a back-to-back EGFR dimer. Figure adapted from Burgess et al. (53).

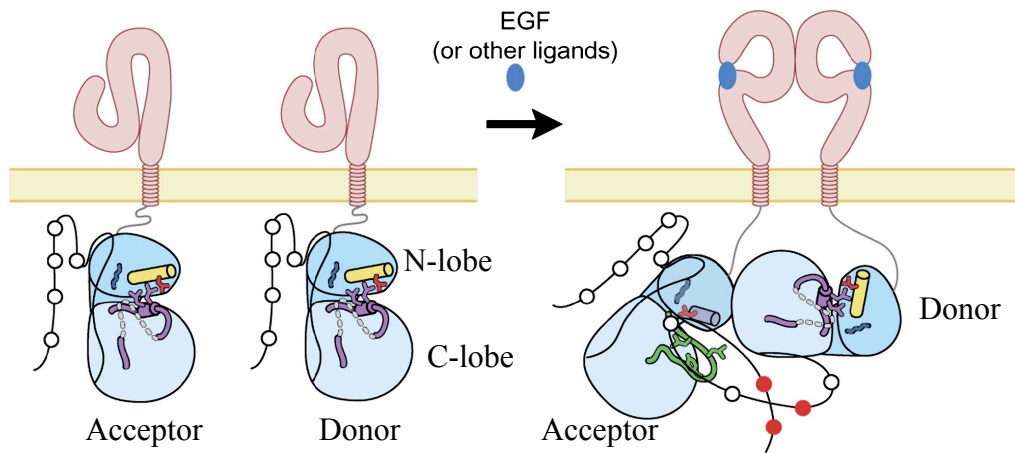


Figure 1.4. Schematic representation of the EGF receptor kinase domain asymmetric dimer. Upon ligand binding to the extracellular domain, the EGF receptor undergoes a conformational change that results in formation of an extracellular domain dimer. This dimer is thought to bring into close contact the kinase domains from each monomer. X-ray crystallography and mutational studies have demonstrated that the asymmetric dimer is required for EGF stimulation of kinase activity. Figure adapted from Zhang et al. (35).

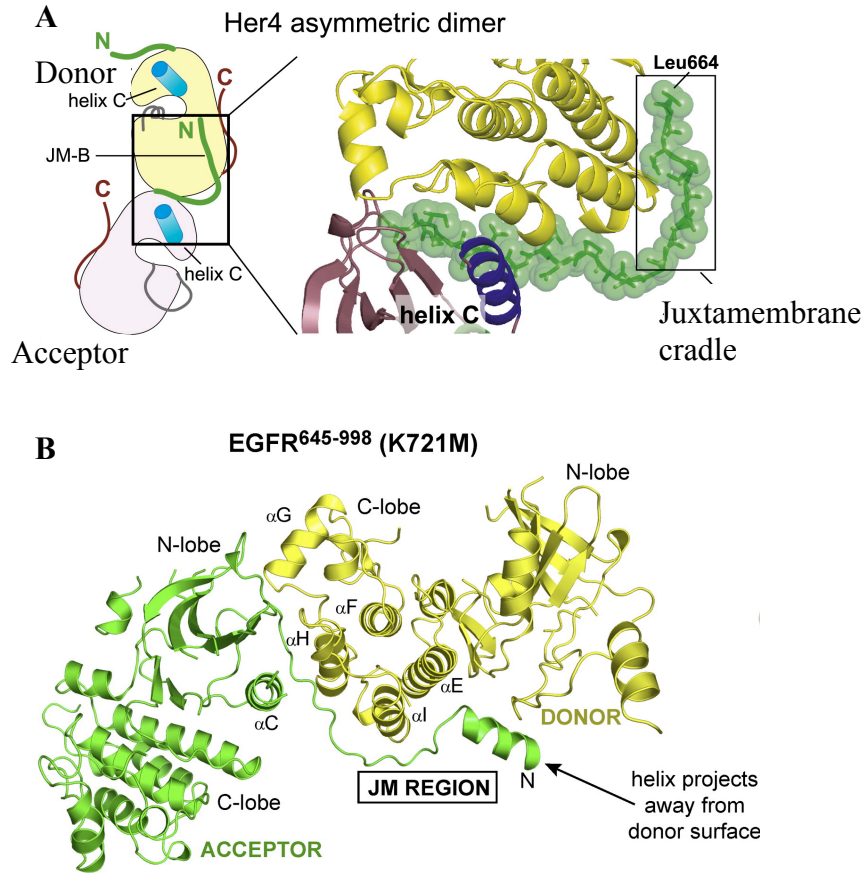


Figure 1.5. Crystal structure of the intracellular juxtamembrane and kinase domains of ErbB4 (Her4) and the EGF receptor. A) Cartoon depiction of the ErbB4 (Her4) asymmetric dimer including 20 amino acids from the intracellular juxtamembrane region. The cradle formed by the juxtamembrane domain of the acceptor kinase is magnified in the right panel (38). B) Crystal structure of the kinase-dead (K721M) EGF receptor juxtamembrane and kinase domains in the asymmetric dimer. Similar to ErbB4, the juxtamembrane region of the acceptor kinase cradles the C-lobe of the donor kinase (39).

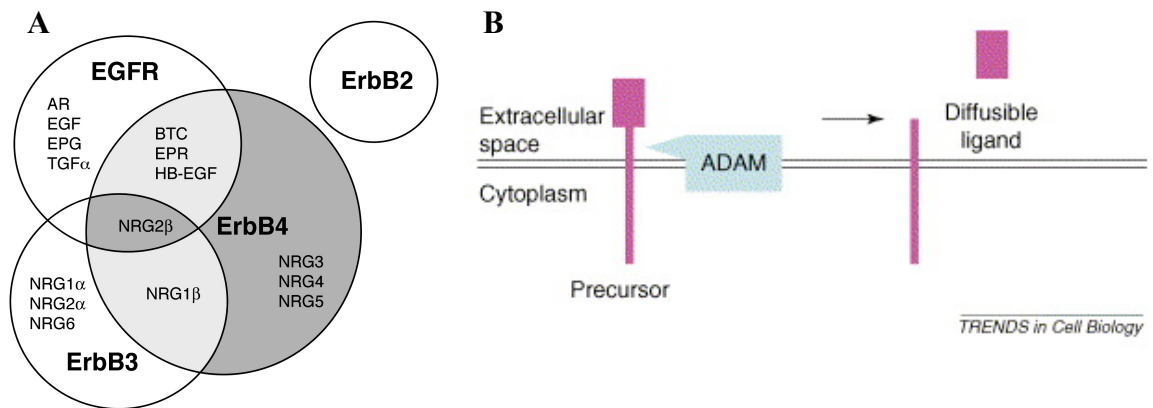


Figure 1.6. Ligands for the EGF receptor family. A) Ven diagram depicting the specificity of various EGF-like ligands for members of the EGF receptor family (47). B) ADAMs (A Disintegrin Activated Metalloproteinase) are responsible for the proteolytic processing of the transmembrane precursors for the EGF receptor family of ligands. This releases a soluble “mature” peptide growth factor that binds to members of the EGF receptor family (46).

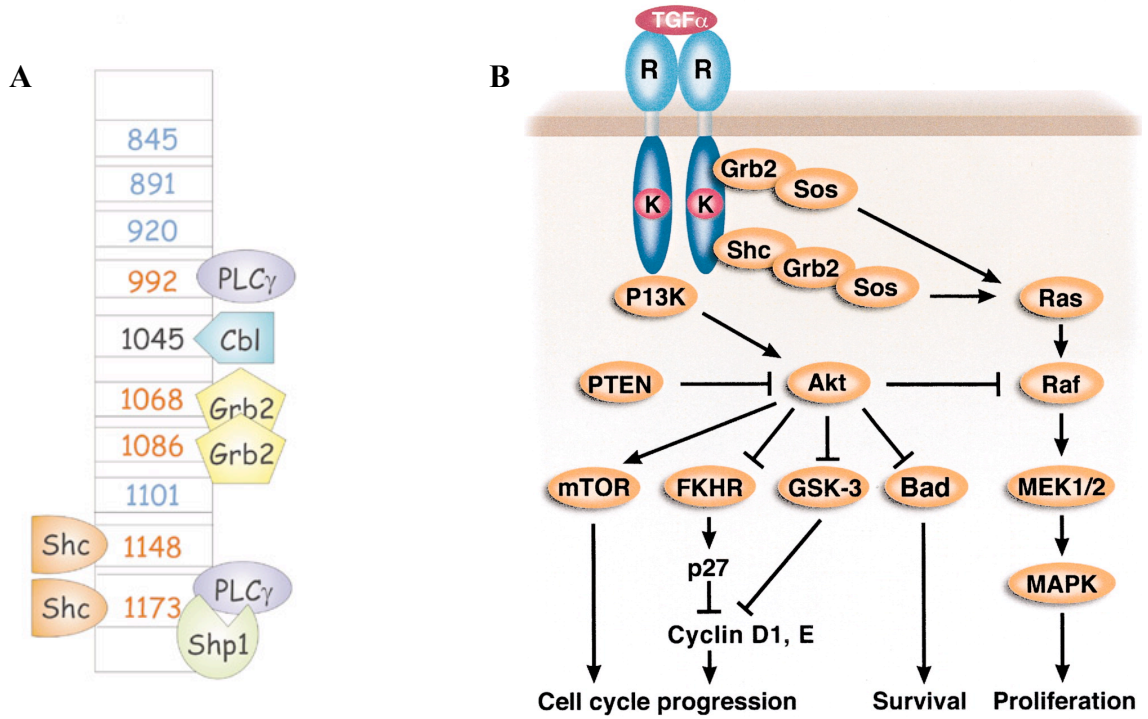


Figure 1.7. Ligand-induced EGF receptor autophosphorylation and downstream signaling. A) Schematic of the EGF receptor C-terminal tail phosphorylation sites and association of SH2 and PTB domain-containing proteins. Autophosphorylation sites are shown in red, while transphosphorylation sites mediated by Src are shown in blue (64). B) Simplified view of the signaling pathways activated by ligand binding to the EGF receptor (69).

CHAPTER 2. Luciferase Fragment Complementation Imaging of Conformational Changes in the EGF Receptor

Introduction

Activation of the EGF receptor is thought to be associated with several dramatic conformational changes in the extracellular and kinase domains, as well as the C-terminal tail (31-33, 35, 40, 99). While evidence from crystal structures and purified systems suggests that the EGF receptor undergoes several conformational changes during the process of activation, these changes have not been observed in intact cells. Thus, the relevance of these findings to the physiological situation is not clear. This problem was addressed using a luciferase fragment complementation imaging assay (100) to image EGF receptor dimerization and ligand induced conformational changes in real time in live cells.

In the context of an EGF receptor lacking the entire cytoplasmic domain, luciferase fragment complementation accurately reports on the kinetics of EGF receptor dimerization. When used with the full-length EGF receptor, the system reveals sequential conformational changes in the EGF receptor that are dependent on receptor autophosphorylation as well as phosphorylation of the receptor by MAP kinase. Our data demonstrate the utility of the luciferase system for in vivo imaging of EGF receptor dimerization and intracellular domain conformational changes. The data presented in this chapter suggest that phosphorylation of the receptor by MAP kinase determines the final conformation adopted by the activated EGF receptor.

Results

EGF induces a rapid increase in luciferase complementation in Δ C-EGFR-NLuc/CLuc cells

The firefly luciferase complementation system utilizes two fragments of luciferase termed NLuc and CLuc. These fragments are inactive by themselves but are capable of reconstituting an active luciferase if the fragments are brought into close proximity (100, 101). Initially, the luciferase fragments were independently fused to the C-terminus of an EGF receptor lacking the entire cytoplasmic domain yielding the Δ C-EGFR-NLuc and Δ C-EGFR-CLuc cDNA constructs. CHO-K1 Tet-On cells were transfected with Δ C-EGFR-NLuc and a line that stably expressed Δ C-EGFR-NLuc in a doxycycline-inducible manner was selected. Twenty four hours prior to use, these cells were transiently transfected with Δ C-EGFR-CLuc. These cells are referred to as Δ C-EGFR-NLuc/CLuc CHO cells.

For imaging experiments, cells were first incubated with luciferin for 20 min at 37°C to allow equilibration of the intracellular and extracellular pools of this substrate. This preincubation assures a stable baseline during the subsequent 20 min observation period (Figure 2.1A). Luciferase activity was measured by monitoring the photon flux from Δ C-EGFR-NLuc/CLuc co-expressing CHO cells. Readings were taken approximately every 30 sec, providing a continuous readout of luciferase activity through bioluminescence imaging of live cells.

Luciferase activity was detectable in cells co-expressing Δ C-EGFR-NLuc and Δ C-EGFR-CLuc even in the absence of added EGF (Figure 2.1A open circles). This suggests the presence of receptor-receptor interactions in the basal state. The addition of

10 nM EGF led to a rapid increase in light production that plateaued between 10 and 15 min (Figure 2.1A, closed circles). Both the rate and extent of ligand-induced dimer formation were dependent on the concentration of EGF (Figure 2.1B). This increase in luciferase complementation following EGF stimulation is consistent with the canonical model of EGF-induced dimerization of its receptor (20). Importantly, the rate of dimer formation detected by luciferase fragment complementation was similar to the rate of ^{125}I -EGF binding observed in these cells (Figure 2.1C, 1nM EGF: $0.14 \pm 0.015 \text{ min}^{-1}$ for luciferase versus $0.15 \pm 0.02 \text{ min}^{-1}$ for binding; 10 nM EGF: $0.30 \pm 0.03 \text{ min}^{-1}$ for luciferase versus $0.42 \pm 0.13 \text{ min}^{-1}$ for binding). This indicates that this imaging technique accurately reflects the kinetics of ligand-induced dimerization of the EGF receptor.

EGF elicits a rapid but transient decrease in luciferase activity in full-length EGFR-NLuc/CLuc cells

To assess the contribution of the cytoplasmic domain of the EGF receptor to receptor-receptor interactions, the NLuc and CLuc fragments were independently fused to the C-terminus of the full-length EGF receptor. To ensure that equal levels of the two chimeric receptors were expressed, a double-stable CHO-K1 Tet-On cell line was established that will be referred to as the EGFR-NLuc/CLuc cell line. In this cell line, EGFR-CLuc was constitutively expressed while EGFR-NLuc was expressed from a doxycycline inducible plasmid. This allowed adjustment of EGFR-NLuc expression levels to match those of EGFR-CLuc.

As shown in Figure 2.2A, Scatchard analysis of ^{125}I -EGF binding to the uninduced EGFR-NLuc/CLuc cells indicated that EGFR-CLuc was expressed at a level

of ~100,000 receptors per cell. When the cells were treated with 1 $\mu\text{g/ml}$ doxycycline, binding experiments demonstrated the presence of ~200,000 EGF receptors per cell. These data suggest that under these conditions, EGFR-NLuc and EGFR-CLuc are expressed at roughly equivalent levels of approximately 100,000 receptors/cell. As can be seen from Figure 2.2A, both Scatchard plots were curvilinear, demonstrating that these receptor fusion proteins retain this characteristic feature of EGF binding to the wild type receptor (102).

The effect of the luciferase fragments on the kinase activity of the EGF receptor was determined independently in CHO cells that expressed only the EGFR-NLuc or the EGFR-CLuc receptors. The data in Figure 2.2B show that EGF stimulated the autophosphorylation of both EGFR-NLuc and EGFR-CLuc, indicating that both receptors retain kinase function. EGFR-NLuc showed two distinct bands, both of which were phosphorylated and both of which react with anti-luciferase antibodies (Figure 2.2C). This suggests that the lower molecular weight form is not the result of proteolytic removal of the luciferase fragment. It is possible that differences in glycosylation may be responsible for the different forms. Both NLuc- and CLuc-EGF receptors mediated the activation of MAP kinase (Figure 2.2B). Thus, addition of the luciferase fragments did not substantially alter the biochemical behavior of the EGF receptor.

When EGFR-NLuc/CLuc cells were incubated with luciferin, light production was observed in the absence of EGF (Figure 2.3A). At least a portion of this basal light production is due to receptor-receptor specific interactions, since the basal luciferase activity is decreased upon transient transfection of cDNA for the unlabeled EGF receptor (Figure 2.4). In contrast to the results obtained with the truncated ΔC -EGF receptor,

addition of EGF to EGFR-NLuc/CLuc cells resulted in a rapid, but transient, decrease in luciferase activity (Figure 2.3B-2.3G). The decrease was observed at the earliest time point following EGF addition and reached a nadir 2 to 4 min after EGF stimulation. Subsequently, light production recovered to essentially the same level as that observed prior to EGF addition.

Because EGF induces a variety of changes in ion transport and metabolic pathways, it was possible that the decrease in light production observed after the addition of EGF was due to changes in pH or some other metabolite within the cells. To examine this possibility, HeLa cells that express endogenous EGF receptors were transfected with FRB-NLuc and its binding partner CLuc-FKBP (100). Treatment of these cells with rapamycin induces interaction of FRB and FKBP leading to enhanced luciferase activity. In this system, addition of EGF failed to alter the level of complementation stimulated by rapamycin (Figure 2.3H). This suggests that the EGF-induced decrease in luciferase activity observed in the EGFR-NLuc/CLuc cells is not due to a non-specific effect on luciferase fragment complementation arising from metabolic changes stimulated by the growth factor.

The decrease in luciferase activity is dependent on EGF receptor kinase activity

Figure 2.5 compares the time course of EGF-stimulated receptor autophosphorylation with that of the EGF-induced decrease in luciferase activity in EGFR-NLuc/CLuc cells. As can be seen from the figure, maximal autophosphorylation occurred within 30 sec after the addition of EGF. By contrast, the decrease in luciferase activity required 2 to 4 min to reach its nadir. Thus, receptor activation precedes the

agonist-induced decrease in luciferase activity. This suggests that the decrease in luciferase activity might be a consequence of receptor tyrosine kinase activation.

To assess the involvement of receptor kinase activity in the decreased luciferase complementation, EGFR-NLuc/CLuc cells were incubated with 5 μ M erlotinib or 10 μ M AG1478 to inhibit receptor tyrosine kinase activity. Inhibition of EGF receptor kinase activity was confirmed using Western blot analysis with an anti-phosphotyrosine antibody (Figure 2.6). Treatment with erlotinib or AG1478 induced a ~3-fold increase in basal luciferase activity indicating that they enhanced the interaction between EGF receptors under resting conditions (Figure 2.7A). This increase was specific for the EGF receptor, since treatment of HeLa cells expressing FRB-NLuc and CLuc-FKBP with erlotinib or AG1478 did not alter light production (Figure 2.7B). As expected, stimulation with EGF led to a transient decrease in luciferase activity in control cells (Figure 2.7C and D). However, this effect was largely eliminated in cells pre-treated with erlotinib or AG1478 (Figure 2.7C and D).

To further test the hypothesis that an active EGF receptor kinase is required to observe the decrease in luciferase activity, EGF receptor autophosphorylation was indirectly blocked. Cells were treated with inhibitors of proteins that modulate EGF receptor function. 12-O-tetradecanoylphorbol 13-acetate (TPA) has been reported to block activation of the EGF receptor kinase (103). This was confirmed by pre-treatment of cells with TPA followed by addition of 10 nM EGF and Western blot with an anti-phosphotyrosine antibody (Figure 2.8A). When compared to control cells, TPA does not influence the basal light production in the luciferase complementation assay (Figure 2.8B). Similar to the EGF receptor-specific tyrosine kinase inhibitors, addition of TPA in

the luciferase complementation assay was also able to block the transient decrease and recovery in light production that was observed after 10 nM EGF stimulation (Figure 2.8C). EGF receptor autophosphorylation can also be inhibited by calmodulin antagonists such as calmidazolium, although the exact mechanism remains unknown (104-106). Pre-treatment with calmidazolium decreased EGF receptor autophosphorylation as measured by Western blot by ~50% (Figure 2.9A). Pre-treatment with calmidazolium increased the basal light production in EGFR-NLuc/CLuc CHO cells by ~6-fold (Figure 2.9B). Calmidazolium did not affect the light production in HeLa cells expressing FRB-NLuc and CLuc-FKBP (Figure 2.9C). Pre-treatment with calmidazolium, followed by addition of 10 nM EGF partially blocked the decrease in luciferase activity, consistent with an incomplete inhibition of EGF receptor autophosphorylation (Figure 2.9D). These results further support the hypothesis that an active EGF receptor kinase is required to observe the decrease in luciferase activity.

Because the effect of erlotinib, AG1478, and calmidazolium on basal luciferase complementation complicated the interpretation of the effects on the EGF-stimulated decrease in luciferase activity, the requirement for EGF receptor tyrosine kinase activity was further examined using the K721A-EGF receptor. The K721A mutation abolishes the tyrosine kinase activity of the EGF receptor (107). The NLuc and CLuc fragments were fused to the C-terminus of the K721A-EGF receptor and were transiently transfected into CHO cells. As was seen for the wild type EGF receptor, erlotinib enhanced basal luciferase activity in this kinase-dead EGF receptor mutant (Figure 2.10A). However, in contrast to the situation with wild type receptor, addition of EGF to the K721A-EGF receptor led to an increase in luciferase activity (Figure 2.10B), similar

to that seen in the Δ C-EGF receptor (Figure 2.1). Erlotinib enhanced the EGF-stimulated increase in luciferase activity in the K721A-EGF receptor system suggesting that the effect of this tyrosine kinase inhibitor is independent of the effects elicited by EGF. These data confirm the involvement of receptor tyrosine kinase activity in the ligand-induced decrease in luciferase complementation.

The observed decrease in luciferase activity is consistent with the hypothesis that EGF induces a conformational change in the receptor that leads to separation of the luciferase fragments. To determine whether the EGF-stimulated decrease in luciferase complementation was due to movement of the C-terminal tails of the receptors or involved changes in the relative positions of the kinase domains, the luciferase fragments were fused to an EGF receptor truncated at residue 973 just beyond the kinase domain. The constructs were expressed in CHO cells. Luciferase activity was detectable in these cells in the absence of EGF (Figure 2.11A). Treatment of the c'973-EGFR-NLuc/CLuc cells with EGF led to a decrease in luciferase activity that was somewhat smaller than that observed for the wild type EGF receptor (Figure 2.11B). While there was some recovery of luciferase activity over time, it was slower and less extensive than that seen for the wild type receptor. Thus, while the effect of EGF was apparent in the truncated receptor it was significantly dampened compared to that observed with the wild type receptor. These data suggest that EGF induces movement of the kinase domains relative to each other but in the full-length receptor, this is amplified by conformational changes that lead to the separation of the C-terminal tails of the receptors.

MAP kinase activity is required for the recovery of luciferase complementation

The recovery of luciferase activity after treatment of EGFR-NLuc/CLuc cells with EGF occurred over a time course that was similar to that of the activation of MAP kinase by EGF (Figure 2.12, top left). MAP kinase is known to catalyze the phosphorylation of the EGF receptor on Thr-669 (108, 109) and the phosphorylation of this residue on the EGF receptor paralleled the activation of MAP kinase in EGFR-NLuc/CLuc cells (Figure 2.12, top left).

To determine whether the activation of MAP kinase played a role in the recovery of luciferase complementation, EGFR-NLuc/CLuc cells were pre-treated with the MEK inhibitor, U0126, to block the activation of MAP kinase. As shown in Figure 2.13, top right, U0126 completely prevented both the activation of MAP kinase and the phosphorylation of Thr-669. When cells were pretreated with U0126 prior to assay of luciferase activity, U0126 had little effect on basal light production (Figure 2.12, bottom left). However, this inhibitor completely blocked the recovery of luciferase activity after the EGF-stimulated decrease (Figure 2.12, bottom right). The initial decrease was of a greater magnitude than that seen in control cells and there was no recovery toward baseline levels over the 20 min observation period. These data indicate that MAP kinase activity is involved in the recovery phase of luciferase complementation.

The requirement for MAP kinase activation in the recovery of luciferase activity was further examined using the T669A-EGF receptor. The T669A mutation removes the MAP kinase phosphorylation site from the EGF receptor (108-110). The NLuc and CLuc fragments were fused to the C-terminus of the T669A-EGF receptor and the constructs were transiently transfected into CHO cells. As a control, wild type NLuc and CLuc

EGF receptors were also transiently transfected into CHO cells. As shown in Figure 2.13A, the wild-type EGF receptor displayed basal luciferase activity which was relatively stable over the 20 min time course of the experiment. Addition of EGF led to a rapid decrease followed by a slow recovery of luciferase activity (Figure 2.13B). The T669A-EGF receptor also displayed basal luciferase activity (Figure 2.13C). But in this mutant, treatment with EGF led to a decrease in luciferase complementation with no significant recovery back towards baseline levels of activity (Figure 2.13D). Furthermore, the decrease observed in the T669A-EGFR-NLuc/CLuc cells was greater in magnitude than that observed in the wild-type EGFR-NLuc/CLuc cells (Figure 2.13B and D). This pattern was similar to that seen in cells expressing wild type EGFR-NLuc/CLuc cells but treated with U0126 (Figure 2.12). These data suggest that the recovery in luciferase complementation is a result of the phosphorylation of the EGF receptor on Thr-669 by MAP kinase.

Discussion

The use of firefly luciferase for enzyme complementation has allowed continuous monitoring of reversible conformational changes in the EGF receptor. When the luciferase fragments were fused to EGF receptors that contained only the extracellular and transmembrane domains of the receptor, the system permitted the direct imaging of EGF receptor dimerization in real time in living cells. The observed rate of receptor dimerization paralleled the rate of ligand binding suggesting that the luciferase complementation system responds rapidly to changes in proximity of the fragments, allowing an accurate temporal read-out of receptor dimerization in vivo. Previous studies that employed a β -galactosidase complementation system reported dimerization rates that

were 5- to 10-fold slower than those observed here (*111, 112*). The time lag between ligand binding and receptor dimerization, as measured by the β -galactosidase assay, is likely due to the fact that the β -galactosidase assay must be performed *ex vivo* on lysed cells and is susceptible to artifacts resulting from the slow, continuous accumulation of product over time. Thus, the β -galactosidase system is suboptimal for monitoring rapid and dynamic changes in protein-protein interactions.

When the luciferase fragments were fused to the full-length EGF receptor, substantially different results were obtained than with the truncated EGF receptor. A significant basal luciferase activity was observed, suggesting that the unstimulated EGF receptor exists in a conformation in which the C-terminal tails of the two monomers are in close proximity to each other. This is consistent with previous reports that some fraction of cell-surface EGF receptors exist as pre-formed dimers (*42, 113-115*). Addition of the tyrosine kinase inhibitors erlotinib and AG1478 significantly increased the basal luciferase activity. This is in agreement with the observation that the level of inactive, pre-formed EGF receptor dimers is increased by treatment of cells with 4-anilinoquinazoline tyrosine kinase inhibitors (*116-119*). Our finding that erlotinib also enhanced basal luciferase complementation in the kinase-dead K721A-EGF receptor system suggests that the effects of erlotinib are due solely to the binding of the inhibitor and do not require an active tyrosine kinase. Calmidazolium, an antagonist of calmodulin, also led to a significant increase in the basal luciferase activity. While the exact mechanism is not known, previous studies suggest that in addition to blocking calmodulin activity, these types of inhibitors can also bind to the plasma and internal membranes of the cell (*105*). This binding may change the electrostatic surface potential,

disrupt EGF receptor interactions with the membrane in the basal state, and result in enhanced accessibility of the luciferase fragments for one another (120).

Addition of EGF to the EGFR-NLuc/CLuc cells resulted in a biphasic response to the ligand. Initially, EGF stimulated a rapid decrease in luciferase activity. This was followed by a slower recovery back to baseline levels of luciferase complementation. These findings are interpreted as the presence of two sequential, ligand-induced conformational changes in the EGF receptor.

For several reasons, we do not feel that the observed changes are related to internalization and/or degradation of the EGF receptor. First, the initial decrease in luciferase activity occurs much more rapidly than the degradation of the EGF receptor. Thus, it seems unlikely that the loss of luciferase activity is due to the loss of receptors. Furthermore, the decrease in luciferase activity is reversible indicating that it cannot be due to an irreversible process such as proteolysis of the receptor. The recovery phase could arise from clustering of the receptors in coated pits for internalization. However, both U0126 treatment and the T669A mutation lead to enhanced receptor internalization (121) and would thus be expected to promote the recovery phase. However, they actually led to its ablation. It therefore seems probable that the observed changes in luciferase activity are the result of conformational changes in the EGF receptor.

Treatment with EGF initially led to a rapid decrease in luciferase activity consistent with the hypothesis that a conformational change had occurred that resulted in the separation of the luciferase fragments. The decrease in luciferase activity was dependent on the concentration of EGF and reached its maximum 2 to 4 min after the addition of EGF. This is well after receptor autophosphorylation has peaked, suggesting

that this conformational change occurs as a result of receptor autophosphorylation rather than concomitant with kinase activation.

Consistent with this hypothesis, treatment of the cells with erlotinib, AG1478, TPA, or calmidazolium blocked the decrease in light production. More importantly, mutation of the receptor to the kinase-dead K721A variant abolished the decrease in luciferase activity and actually led to a system in which EGF stimulated an increase in light production. This demonstrates that: i) the conformational dynamics reported by the luciferase fragment complementation assay are the result of receptor tyrosine kinase activity; and, ii) EGF does induce dimer formation in the context of the full-length EGF receptor but its effects are masked by conformational changes within the intracellular domain. The observation that tyrosine kinase inhibitors erlotinib and AG1478 blocked the decrease in luciferase activity but did not reveal the increase in receptor dimer formation in the wild type receptor may be due to the presence of residual kinase activity in the inhibitor-treated cells. A low level of kinase activity would promote a decrease in complementation thereby offsetting the increase in luciferase activity induced by EGF receptor dimerization.

It is noteworthy that EGF stimulated dimerization of the kinase-dead EGF receptor in the presence of erlotinib enhanced receptor-receptor interactions. This suggests that the effects of EGF and erlotinib on the formation of receptor dimers occur through independent mechanisms. Presumably, EGF induces dimerization of the extracellular domains while erlotinib promotes kinase-kinase interactions within the intracellular domain (58, 122-124). Whether these mechanisms can work additively within the same receptor dimer (or tetramer) is unclear. However, the fact that EGF

stimulated luciferase complementation in receptors that were fully saturated with erlotinib suggests that this is likely the case.

The EGF receptor is extensively autophosphorylated on its C-terminal tail (55, 58-60) and previous studies on the isolated cytoplasmic domain of the receptor suggested that the C-terminal tail adopts a more extended conformation following phosphorylation (40, 41, 99). It was therefore possible that the decrease in luciferase activity was due to a phosphorylation-induced change in the position of the C-terminal tails within the activated EGF receptor dimer with no movement of the kinase domains. Fusion of the luciferase fragments to a truncated EGF receptor lacking the C-terminal tail resulted in a system in which both the initial decrease and the subsequent recovery of luciferase complementation were visible but noticeably dampened. This suggests that ligand binding induces a change in the relative positions of the kinase domains that separates the luciferase fragments. While changes in the C-terminal tails may also contribute to this effect in the full-length receptor, the C-terminal tails seem to be relatively more important in the recovery phase of luciferase complementation.

Luciferase fragment complementation identified a second ligand-induced conformational change in the EGF receptor that followed the tyrosine phosphorylation-dependent separation of the C-terminal tails. This second phase was marked by the recovery of luciferase activity back to baseline levels. The recovery phase occurred over a time course that was similar to the activation of MAP kinase, a downstream signaling pathway stimulated by EGF. Inhibition of MAP kinase activation abolished the recovery of luciferase activity suggesting that a MAP kinase-catalyzed phosphorylation event is responsible for the increase in luciferase activity.

MAP kinase is known to phosphorylate the EGF receptor on Thr-669 (108-110). When the luciferase fragments were fused to the T669A-EGF receptor, EGF stimulated a decrease in luciferase activity but the recovery phase was completely ablated. These data are consistent with the interpretation that phosphorylation of the EGF receptor on Thr-669 by MAP kinase induces a conformational change in the receptor that allows the re-establishment of complementation between the luciferase fragments.

Recent studies have demonstrated that phosphorylation of the EGF receptor on Thr-669 leads to desensitization of the receptor (121). Our data suggest that this functional change in the EGF receptor is likely to be the result of a conformational change in the receptor. We hypothesize that phosphorylation of the EGF receptor on Thr-669 by MAP kinase induces a re-orientation of the kinase domains that results in the adoption of a post-activated conformation of the receptor in which the C-terminal tails are once again in close proximity. The relationship between the resting and the post-activated conformations of the receptor is not clear. However, because the activated receptor would be phosphorylated, ubiquitinated and bound to a variety of interacting molecules, it seems likely that the final conformation of the activated receptor would differ substantially from that of an unstimulated receptor.

The data presented here are consistent with the model shown in Figure 2.14. A significant basal photon flux was observed, indicating the presence of receptor-receptor interactions in the inactive state (Figure 2.14A). Following addition of ligand, a rapid decrease in luciferase activity was observed, indicating a separation of the luciferase fragments (Figure 2.14B). This likely represents formation of the activating asymmetric kinase dimer, which places the luciferase fragments in a position where they cannot

complement. Finally, a recovery in luciferase activity to baseline levels was observed that indicates the luciferase fragments can again complement (Figure 2.14C). This recovery was entirely dependent on the MAP kinase-mediated phosphorylation of the EGF receptor on Thr-669, indicating that this modification alters the final conformation adopted by the EGF receptor.

Li et al. (125) recently reported the use of luciferase fragment complementation to study EGF receptor interactions. These workers reported that EGF did not elicit any change in the photon flux in cells expressing NLuc and CLuc fused to the full-length EGF receptor. However, their protocol involved treatment of their cells with EGF for 15 min prior to imaging. Thus, they only observed the system after it had recovered back to baseline levels of luciferase complementation and failed to see the early dynamics that follow ligand binding.

Our data demonstrate the utility of luciferase fragment complementation imaging for monitoring reversible conformational changes in the EGF receptor in real time in living cells. Utilizing this approach, we developed an assay for assessing dimerization of the EGF receptor in intact cells using either C-terminally truncated or kinase-dead receptors. This assay is superior to the chemical cross-linking studies normally used as it is more sensitive and yields accurate information on the temporal progress of the dimerization reaction. The ability to generate temporal information allowed us to identify two sequential ligand-induced changes in the conformation of the full-length EGF receptor. These observations reveal structural dynamics in the activated EGF receptor and provide insight into how MAP kinase may induce desensitization of the EGF receptor.

Experimental Procedures

Reagents—Murine EGF was purchased from Biomedical Technologies, Inc. and was dissolved in sterile water. U0126, AG1478, and calmidazolium were purchased from EMD Chemicals and were dissolved in DMSO. Erlotinib was obtained from OSI Pharmaceuticals and was dissolved in DMSO. 12-O-tetradecanoylphorbol 13-acetate (TPA, Sigma) was dissolved in DMSO. Rapamycin was dissolved in DMSO and was kindly provided by Dr. D. Piwnica-Worms (Washington University, St. Louis, MO). Doxycycline was purchased from Clontech and was dissolved in sterile water. D-Luciferin (Biosynth) was dissolved in PBS and coelenterazine (Sigma) was dissolved in ethanol. The MAP kinase antibody was from Upstate and the phospho-specific MAP kinase and luciferase antibodies were from Promega. The phosphotyrosine antibody (PY20) was from BD Biosciences. The phospho-Tyr1173 and phospho-Thr669 specific antibodies were from Upstate. The EGF receptor was detected using Erbitux (ImClone) or a mixture of antibodies from Cell Signaling and Santa Cruz.

DNA Constructs—To generate the EGFR-NLuc construct, Notch full-length-NLuc (NFL-NLuc, kindly provided by Dr. R. Kopan Washington University, St. Louis, MO) was digested with BsiWI and XbaI. A flexible Gly-Ser rich linker was generated (amino acid sequence WPRSYASRGGGSSGGG) (100) containing SacII, BsiWI, and XbaI sites. The linker was ligated into the NFL-NLuc construct using the BsiWI and XbaI sites. An EGFR-GFP construct (126) was digested with SacII and XbaI and was ligated into the NFL-NLuc construct to generate EGFR-NLuc in pcDNA3.1 TOPO (Invitrogen). EGFR-NLuc was ligated into MCS1 of the pBI-Tet vector (Clontech) using the NheI and EcoRV sites.

EGFR-CLuc was constructed by ligating NFL-CLuc (kindly provided by Dr. R. Kopan Washington University, St. Louis, MO) into EGFR-NLuc using the HindIII and BsiWI restriction sites. EGFR-CLuc was cloned into pcDNA6/V5-His B (Invitrogen) using the BstEII and EcoRV sites in the EGFR pcDNA6/V5-His B construct. To make the Δ C-EGFR-NLuc and CLuc constructs, a BsiWI site was inserted in the Δ C-EGFR (127) (pBI-Tet) construct using QuikChange site-directed mutagenesis (Stratagene). EGFR-NLuc (pBI-Tet) and EGFR-CLuc (pcDNA6/V5-His B) were digested with NheI and BsiWI and Δ C-EGFR was ligated into these sites. This resulted in the following linker DYKAYASRGGGSSGGG (100). To make the c'973-EGFR-NLuc and CLuc constructs, a BsiWI site was inserted into the EGFR (pcDNA5.FRT) following amino acid 973 using QuikChange site-directed mutagenesis. The DNA was digested with NheI and BsiWI and cloned into the EGFR-CLuc (pcDNA6/V5-His B) or EGFR-NLuc (pBI-Tet) constructs, resulting in the following linker YASRGGGSSGGG (100). The K721A-EGFR-CLuc construct was made using QuikChange site-directed mutagenesis (Stratagene) in the EGFR-CLuc pcDNA6/V5-His B construct. The K721A-EGFR-NLuc construct was made by digesting EGFR-NLuc (pcDNA3.1 TOPO) with BstEII and KpnI. The insert was ligated into the K721A pcDNA5.FRT (Invitrogen) construct digested with the same enzymes. The T669A-EGFR-CLuc construct was made using QuikChange site-directed mutagenesis (Stratagene) in the EGFR-CLuc pcDNA6/V5-His B construct. The T669A-EGFR-NLuc construct was made by digesting EGFR-NLuc (pcDNA3.1 TOPO) with BstEII and KpnI. The insert was ligated into the T669A pcDNA5.FRT (Invitrogen) construct digested with the same enzymes. All mutations were verified by sequencing.

The FRB-NLuc and CLuc-FKBP constructs were kindly provided by Dr. D. Piwnica-Worms (100) (Washington University, St. Louis, MO).

Cell lines—CHO-K1 Tet-On cells (Clontech) were cotransfected with pTK-Hyg (Clontech) and EGFR-NLuc (pBI-Tet MCSI) using Lipofectamine 2000 (Invitrogen). Stable clones were isolated by selection in 400 µg/ml hygromycin (Invitrogen). A double-stable cell line was established by transfecting EGFR-CLuc (pcDNA6/V5-HisB) into EGFR-NLuc cells using Lipofectamine 2000 and selecting in 10 µg/ml blasticidin-S (Invitrogen). Double-stable lines were grown in DMEM containing 10% FBS, 1000 µg/ml penicillin/streptomycin, 100 µg/ml G418, 50 µg/ml hygromycin, and 2 µg/ml blasticidin-S. ΔC-EGFR-NLuc (pBI-Tet MCSI) and c'973-EGFR-NLuc (pBI-Tet MCSI) were stably expressed as described above for EGFR-NLuc. Cells were maintained in DMEM containing 10% FBS, 1000µg/ml penicillin/streptomycin, 200µg/ml G418, and 100µg/ml hygromycin. ΔC-EGFR-CLuc (pcDNA6/V5-His B) and c'973-EGFR-CLuc (pcDNA6/V5-His B) were transiently transfected into the appropriate parental cell line 24 hr prior to luciferase complementation imaging using Lipofectamine 2000 (Invitrogen). The K721A-EGFR-NLuc/K721A-EGFR-CLuc constructs and the T669A-EGFR-NLuc/T669A-EGFR-CLuc constructs were transiently transfected into CHO-K1 Tet-On cells 24 hours prior to luciferase complementation imaging using Lipofectamine 2000. To assess the transfection efficiency, cells were co-transfected with renilla luciferase (pRLuc-N1, Packard Bioscience). FI CHO cells were purchased from Invitrogen and were co-transfected with wild type EGFR (pcDNA5.FRT) and pOG44. Stable clones were selected in F-12 media containing 10% FBS, 1000 µg/ml penicillin/streptomycin,

and 400 µg/ml hygromycin. Cell lines were maintained in F-12 containing 100 µg/ml hygromycin.

Kinase activation and Western Blotting—EGFR-NLuc/CLuc or FI CHO EGFR cells were grown to confluence in 35 mm dishes. Cells were serum-starved in DMEM containing 1 mg/ml BSA for 3 hr. Culture medium was removed and cells were washed twice in ice-cold PBS and then scraped into RIPA buffer (150 mM NaCl, 10 mM Tris pH 7.2, 0.1% sodium dodecylsulfate, 1% Triton X-100, 17 mM deoxycholate, and 2.7 mM EDTA) containing 20 mM p-nitrophenyl phosphate, 1 mM sodium orthovanadate, and protease inhibitors. Equal amounts of protein (BCA assay, Pierce) were loaded onto a 9% SDS-polyacrylamide gel and then transferred to PVDF (Millipore) or nitrocellulose (Osmonics, Inc.). Western blots were blocked for 1 hour in TBST/10% nonfat milk. The blots were incubated in primary antibody for 1 hr, washed in TBST/0.1% BSA, incubated in secondary antibody for 45 min and washed three times in TBST/0.1% BSA. Western blots were detected using the ECL reagent from GE Healthcare.

¹²⁵I-EGF Binding—Murine EGF was radioiodinated and ligand binding assays were performed as described previously (102).

Luciferase complementation imaging—Cells were plated 48 hr prior to use at 5 x10³ cells per well in DMEM containing doxycycline in a black-walled 96-well plate. On the day of the assay, cells were serum-starved for 3 hr and then incubated for 20 min in 175 µl DMEM without phenol red, containing 1 mg/ml BSA, 25 mM Hepes, and 0.6 mg/ml D-luciferin at 37°C. To establish a baseline, cell radiance (photons/second/cm²/sr) was measured using a cooled CCD camera and imaging system at 37°C (IVIS 50; Caliper) (30 sec exposure; binning, 8; no filter; f-stop, 1; field of view, 12 cm). EGF was

added in a volume of 25 μ l in the same media (DMEM, 1mg/ml BSA, 25mM Hepes, 0.6mg/ml D-Luciferin). Radiance was measured sequentially as described above. For the Δ C-EGFR, c'973-EGFR, K721A-EGFR, and T669A-EGFR experiments involving transient transfection, the transfection efficiency was assessed by monitoring renilla luciferase expression. Media was replaced on cells with DMEM (no phenol red) containing 1 mg/ml BSA, 25 mM Hepes, and 400 nM coelenterazine. Radiance was immediately measured as described above except the filter was set to <510.

Data Analysis—Data was collected in quadruplicate for each condition. A flat-field correction was done to correct for differences in the baseline photon flux. Light production expressed as photon flux (photons/sec) was determined from regions-of-interest defined over wells using LIVINGIMAGE (Xenogen) and IGOR (Wavemetrics) software. Changes in photon flux were calculated by subtracting values from untreated cells from those of EGF-treated cells. Standard errors were determined using the formula for the unpooled standard error.

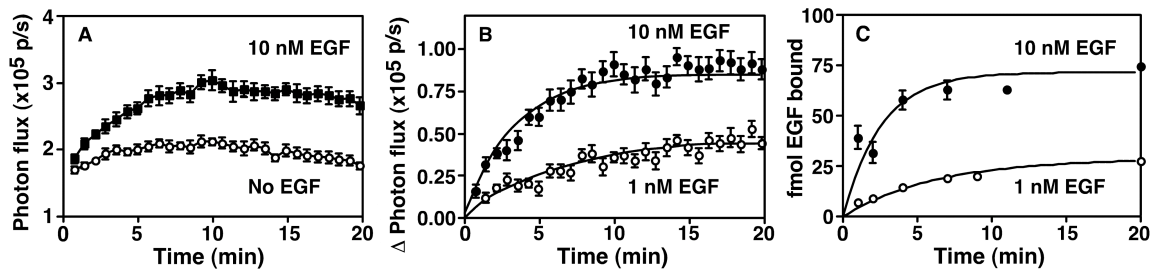
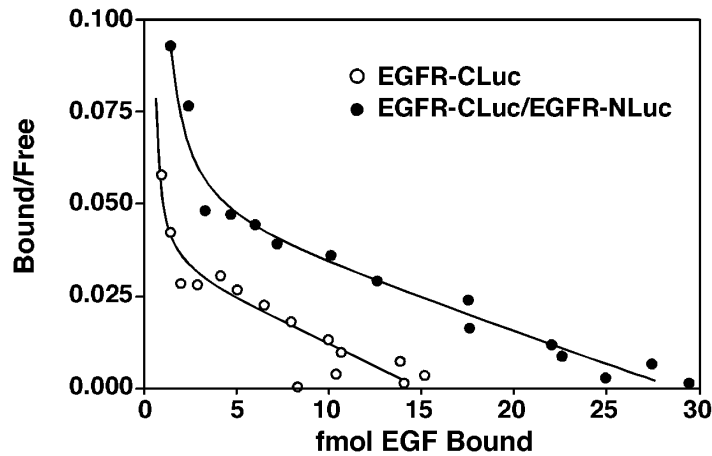
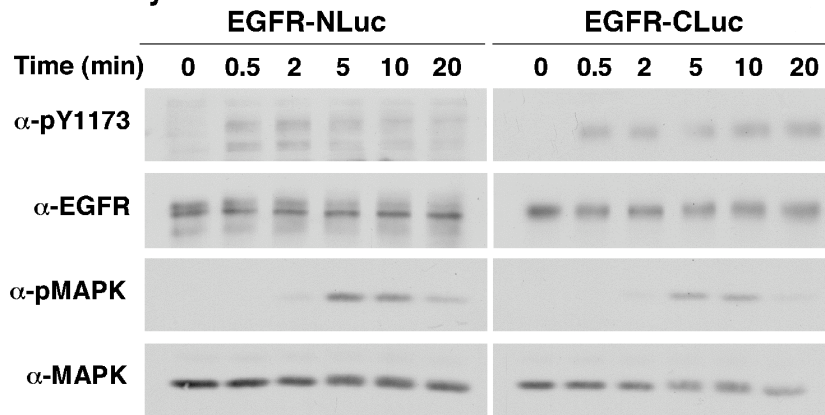


Figure 2.1. Reconstitution of luciferase activity and ¹²⁵I-EGF binding in ΔC-EGFR-NLuc/CLuc CHO cells. ΔC-EGFR-NLuc CHO cells were plated 48 hr prior to imaging in DMEM containing 1 μg/ml doxycycline. 24 hrs before imaging, cells were transiently transfected with cDNA encoding ΔC-EGFR-CLuc. On the day of imaging, cells were pre-incubated for 20 min with 0.6 mg/ml D-luciferin. A) Photon flux (photons/sec; p/s) in the absence of agonist stimulation (open circles) or in the presence of 10 nM EGF (closed squares). B) Change in photon flux over time in cells stimulated with 1 nM (open circles, association rate $0.14 \pm 0.015 \text{ min}^{-1}$) or 10 nM (closed circles, association rate $0.30 \pm 0.03 \text{ min}^{-1}$) EGF. C) Time course of ¹²⁵I-EGF binding to cells expressing ΔC-EGFR-NLuc at 37° C using 1 nM (open circles, association rate $0.15 \pm 0.02 \text{ min}^{-1}$) or 10 nM (closed circles, association rate $0.42 \pm 0.13 \text{ min}^{-1}$) EGF. Error bars represent the standard error of four independent measurements for each condition. The one-phase exponential association was fit in B and C using non-linear least squares analysis with the GraphPad Prism software.

A. ¹²⁵I-EGF Binding



B. Activity



C. Luciferase antibody

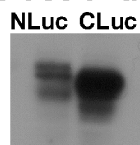


Figure 2.2. Characterization of the full-length EGFR-NLuc and EGFR-CLuc. A) Scatchard analysis of ¹²⁵I-EGF binding to CHO cells stably expressing EGFR-CLuc (no doxycycline, open circles) or EGFR-NLuc/CLuc (closed circles) in which EGFR-NLuc expression had been induced by the addition of 1 μ g/ml doxycycline for 48 hrs. Data were fit to a two-site binding hyperbola using nonlinear regression from the GraphPad Prism software. B) CHO cells stably expressing either EGFR-NLuc or EGFR-CLuc were stimulated with 10 nM EGF at 37°C for the indicated lengths of time. Western blot analysis was performed with the indicated antibodies. C) CHO cells stably expressing either EGFR-NLuc (1 μ g/ml doxycycline for 48 hrs) or EGFR-CLuc were lysed and Western blot analysis was performed with an anti-luciferase antibody.

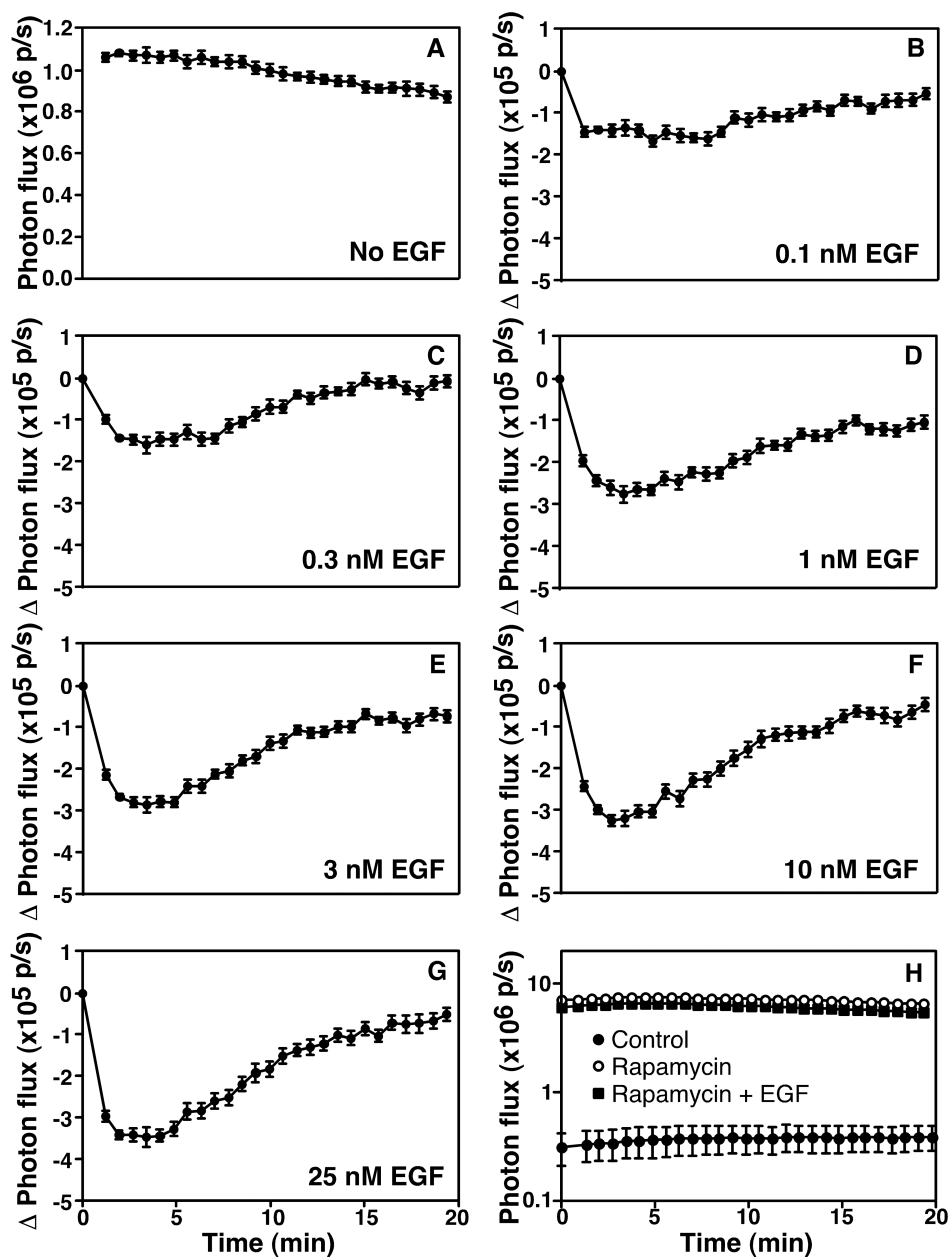


Figure 2.3. Reconstitution of luciferase activity in response to EGF in EGFR-NLuc/CLuc cells. EGFR-NLuc/CLuc cells were plated into DMEM containing 1 μ g/ml doxycycline 48 hr prior to imaging. Before collecting data, cells were incubated for 20 min with 0.6 mg/ml D-luciferin. A) Photon flux (photons/sec; p/s) in the absence of ligand. B-G) Change in photon flux following addition of varying concentrations of EGF. H) HeLa cells were plated 48 hrs prior to bioluminescence imaging in DMEM. Cells were transiently transfected with FRB-NLuc and CLuc-FKBP (100) 24 hrs prior to imaging. Cells were pre-treated with rapamycin (80 nM for 5 hrs). Before collecting data, cells were incubated for 20 min with 0.6 mg/ml D-luciferin. Photon flux was immediately measured over time after the addition of vehicle, 10 nM EGF, or rapamycin. Error bars represent the standard error of four independent measurements for each condition.

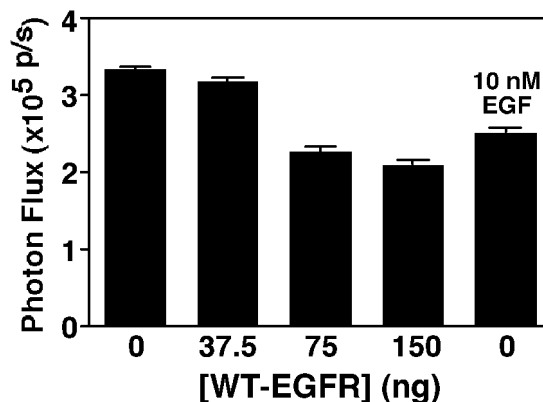


Figure 2.4. Competition of basal luciferase complementation using unlabeled wild type EGF receptor. EGFR-NLuc/CLuc cells were plated in DMEM containing 1 μ g/ml doxycycline 48 hrs prior to imaging. Cells were transiently transfected with empty vector (pcDNA5.FRT) or unlabeled wild type EGF receptor 24 hrs prior to imaging. Before collecting data, cells were serum starved for 3 hrs and then were incubated for 20 min in 0.6 mg/ml D-luciferin. The maximum photon flux (photons/sec; p/s) is shown for several concentrations of wild type unlabeled EGF receptor or after cells were stimulated with 10 nM EGF.

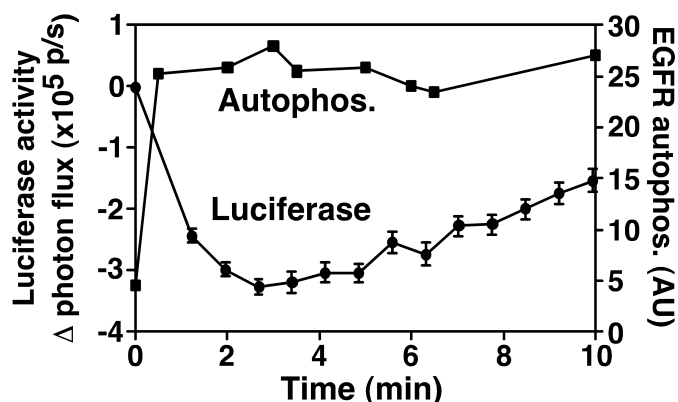


Figure 2.5. Comparison of the rate of EGF receptor autophosphorylation to the EGF-stimulated decrease in luciferase activity. For the EGF receptor autophosphorylation, EGFR-NLuc/CLuc cells were plated in 6-well dishes in DMEM containing 1 μ g/ml doxycycline 48 hrs prior to assay. On the day of assay, cells were serum starved for 3 hrs before stimulation with 10 nM EGF for the indicated lengths of time. Cells were lysed and equal proteins were loaded on a 9% SDS-PAGE gel. Proteins were transferred and Western blot analysis was done with a phosphotyrosine antibody (pY20, BD Biosciences). Densitometric analysis was done using Image J (NIH). For luciferase imaging, EGFR-NLuc/CLuc cells were plated in DMEM containing 1 μ g/ml doxycycline 48 hrs prior to imaging. Before collecting data, cells were incubated for 20 min with 0.6 mg/ml D-Luciferin. Photon flux (photons/sec; p/s) was measured after addition of 10 nM EGF. Error bars represent the standard error of four independent measurements for each condition.

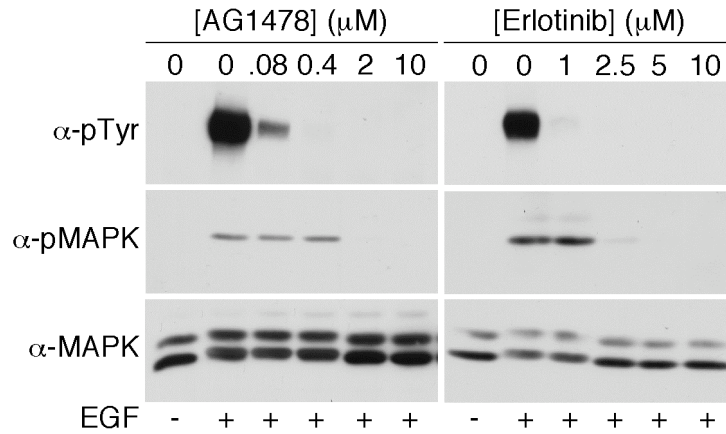


Figure 2.6. Inhibition of EGF receptor autophosphorylation and MAP kinase activation following pre-treatment with AG1478 or Erlotinib. FI CHO cells stably expressing the EGF receptor were plated 48 hrs prior to assay in 6-well dishes. On the day of the assay, cells were serum starved 3 hrs. Cells were pre-treated with the indicated concentrations of AG1478 for 20 min or with erlotinib for 1 hr. 25 nM EGF was added for 3 min, cells were lysed, and equal proteins were loaded on a 9% SDS-PAGE gel. Western blot analysis was done with the indicated antibodies.

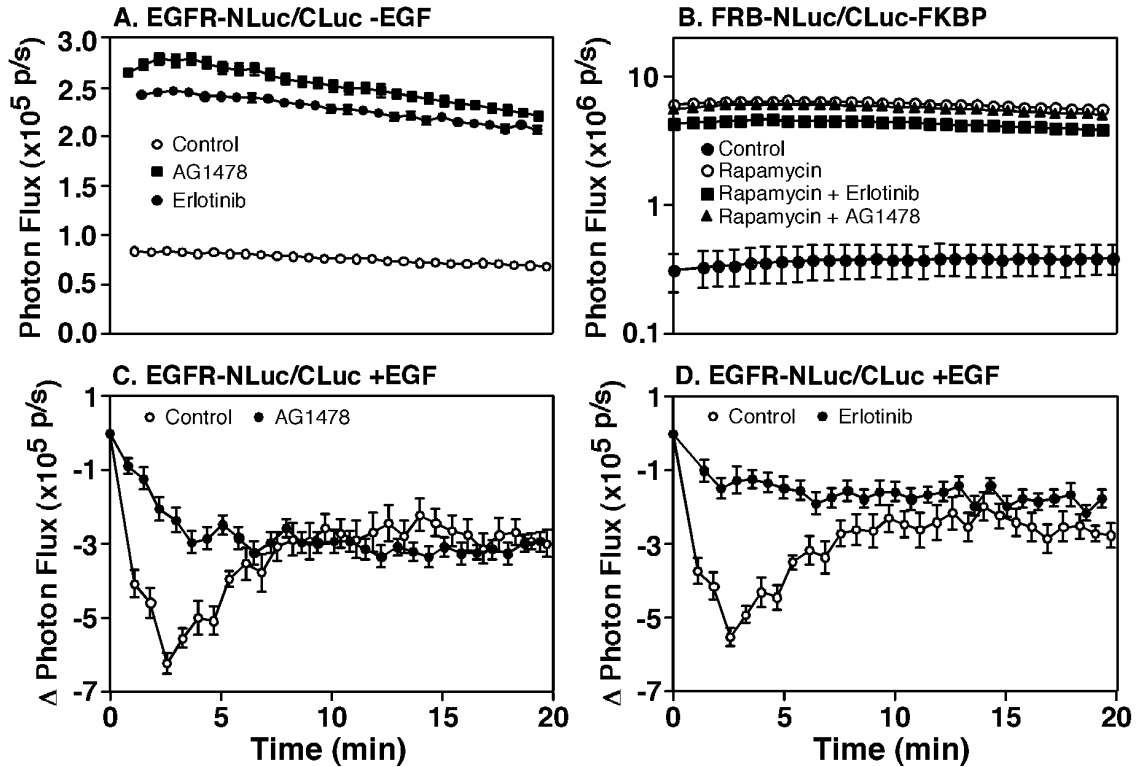


Figure 2.7. Effect of a kinase inhibitor on reconstituted luciferase activity. A) EGFR-NLuc/CLuc cells were plated in DMEM containing 1 μ g/ml doxycycline 48 hrs prior to imaging. EGFR-NLuc/CLuc CHO cells were treated with vehicle or 5 μ M erlotinib for 1 hr prior to imaging. Cells were treated for 20 min with 0.6 mg/ml D-Luciferin prior to imaging. A) Basal luciferase activity in photon flux (photons/sec; p/s). Control values were corrected independently by the baseline for erlotinib or AG1478. B) HeLa cells were plated 48 hrs prior to bioluminescence imaging in DMEM. Cells were transiently transfected with FRB-NLuc and CLuc-FKBP (100) 24 hrs prior to imaging. Cells were pre-treated with rapamycin (80 nM for 5 hrs). Before collecting data, cells were incubated for 20 min with 0.6 mg/ml D-luciferin. Photon flux was immediately measured over time after the addition of vehicle, 5 μ M erlotinib, 10 μ M AG1478, or rapamycin. The control in this experiment is also used in Figure 2.3H. C and D) Luciferase activity in EGFR-NLuc/CLuc cells as in (A) treated with 10 nM EGF in the absence or presence of 10 μ M AG1478 (C) or 5 μ M erlotinib (D) pre-treatment. Error bars represent the standard error of four independent measurements for each condition.

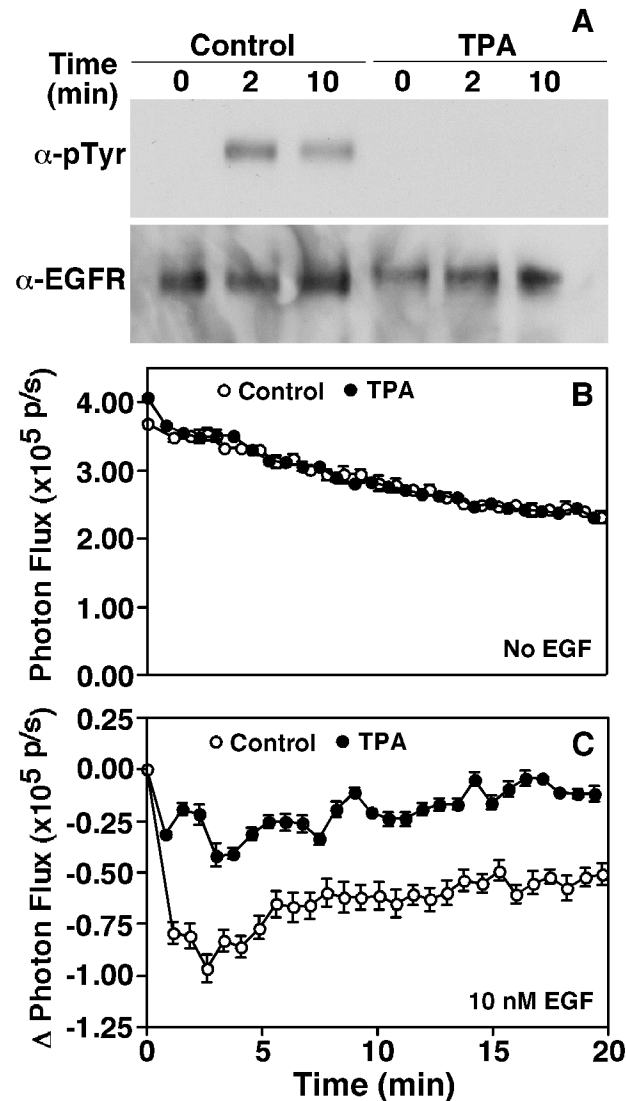


Figure 2.8. Effect of TPA treatment on EGF receptor autophosphorylation and luciferase activity in EGFR-NLuc/CLuc cells. EGFR-NLuc/CLuc cells were plated in DMEM containing 1 μ g/ml doxycycline 48 hrs prior to assay or imaging. Cells were serum starved 3 hrs on the day of assay, followed by pre-treatment for 20 min in vehicle or 100 nM TPA. A) Cells were stimulated with 10 nM EGF for the indicated lengths of time and were then lysed. Equal proteins were loaded on a 9% SDS-PAGE gel and Western blot analysis was done with the indicated antibodies. B and C) Prior to luciferase complementation imaging, cells were incubated for 20 min in DMEM containing 0.6 mg/ml D-luciferin and DMSO (vehicle) or 100 nM TPA. Photon flux (photons/sec; p/s) was immediately measured after addition of vehicle (B) or 10 nM EGF (C).

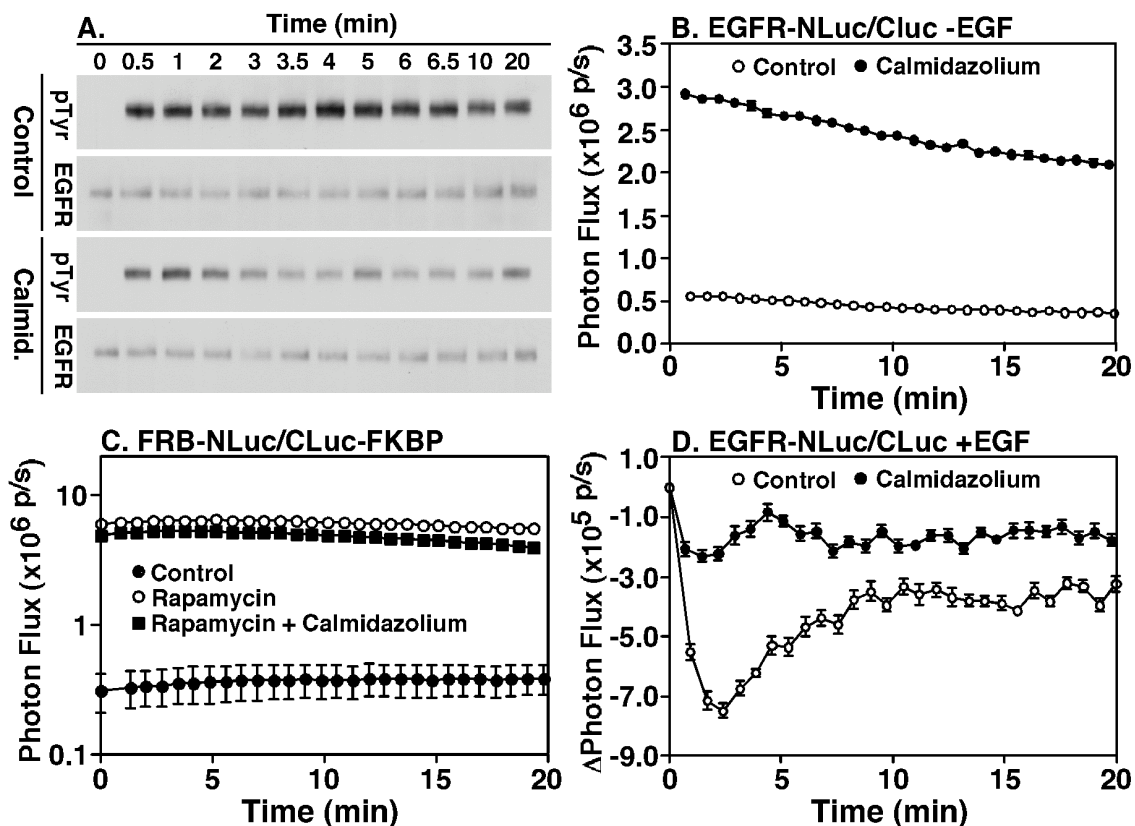


Figure 2.9. Effect of the protein kinase C activator, calmidazolium, on EGFR receptor autophosphorylation and reconstituted luciferase activity. EGFR-NLuc/CLuc or HeLa cells were plated in DMEM containing $1\mu\text{g/ml}$ doxycycline 48 hrs prior to assay or imaging. Cells were serum starved 3 hrs on the day of assay, followed by pre-treatment for 20 min in vehicle or $10\mu\text{M}$ calmidazolium. A) Cells were stimulated with 10 nM EGF for the indicated lengths of time. Cells were lysed, equal proteins were loaded on a 9% SDS-PAGE gel and Western blot analysis was done with the indicated antibodies. B) Prior to luciferase complementation imaging, cells were incubated for 20 min in DMEM containing 0.6 mg/ml D-luciferin and DMSO (vehicle) or $10\mu\text{M}$ calmidazolium. Photon flux (photons/sec; p/s) was immediately measured. Control values were corrected independently by the baseline for calmidazolium. C) HeLa cells were transiently transfected with FRB-NLuc and CLuc-FKBP (100) 24 hrs prior to imaging. Cells were pre-treated with rapamycin (80 nM for 5 hrs). Before collecting data, cells were incubated for 20 min with 0.6 mg/ml D-luciferin. Photon flux was immediately measured over time after the addition of vehicle, $10\mu\text{M}$ calmidazolium, or rapamycin. The control in this experiment is also used in Figure 2.3H. D) EGFR-NLuc/CLuc cells were treated as in (B) except that photon flux was measured after addition of 10 nM EGF. Error bars represent the standard error of at least four independent measurements.

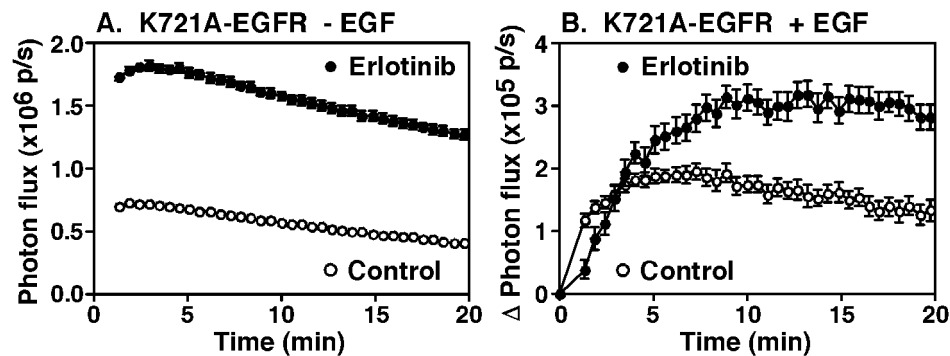


Figure 2.10. Expression of kinase-dead EGF receptor and the effect on reconstituted luciferase activity. CHO-K1 Tet-On cells were plated in DMEM 48 hrs prior to luciferase imaging. Cells were transiently transfected with cDNA for K721A-EGFR-NLuc and K721A-EGFR-CLuc 24 hrs prior to imaging. Prior to imaging, cells were serum starved 2 hrs, pre-treated for 1 hr in media containing vehicle or 5 μ M erlotinib, and then treated for 20 min with 0.6 mg/ml D-Luciferin. A) Basal photon flux (photons/sec; p/s). Control values were corrected independently by the baseline for erlotinib. B) Luciferase activity in cells treated with 10 nM EGF. Error bars represent the standard error of four independent measurements for each condition.

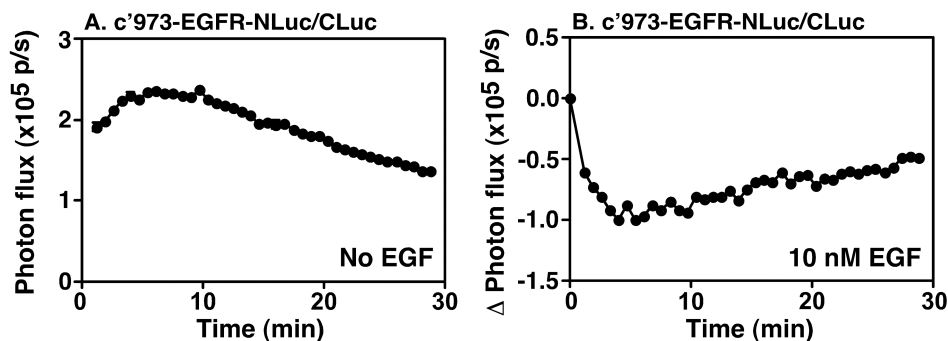


Figure 2.11. Effect of truncation of the C-terminal tail of the EGF receptor on reconstituted luciferase activity. CHO cells stably expressing c'973-EGFR-NLuc were plated in DMEM containing 2 μ g/ml doxycycline 48 hrs prior to luciferase imaging. Cells were transiently transfected with c'973-EGFR-CLuc 24 hrs prior to imaging. Cells were treated for 20 min with 0.6 mg/ml D-Luciferin prior to imaging. A) Basal photon flux (photons/sec; p/s). B) Luciferase activity in cells treated with 10 nM EGF. Error bars represent the standard error of four independent measurements for each condition.

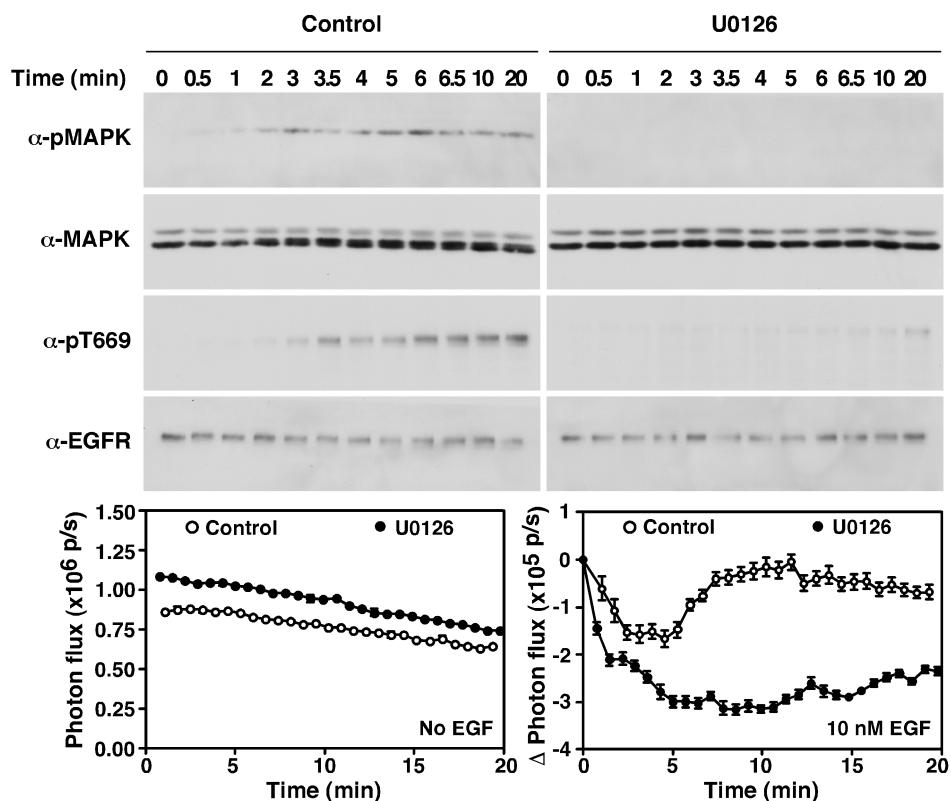


Figure 2.12. Contribution of MAP kinase activation to the recovery of reconstituted luciferase activity. EGFR-NLuc/CLuc cells were plated 48 hrs prior to assay in DMEM containing 1 μ g/ml doxycycline. Cells were serum starved for 3 hrs prior to assay. EGFR-NLuc/CLuc cells were pre-treated with vehicle (control, top left) or 10 μ M U0126 (top right) for 20 min prior to addition of 10 nM EGF at time = 0. Western blot analysis was performed with the indicated antibodies. For the luciferase imaging, EGFR-NLuc/CLuc cells were plated 48 hrs before imaging in DMEM containing 1 μ g/ml doxycycline. EGFR-NLuc/CLuc cells were pre-treated with vehicle (control) or 10 μ M U0126 for 20 min (both in the presence of 0.6 mg/ml D-Luciferin). The photon flux in the absence of ligand (bottom left) or after addition of 10 nM EGF (bottom right) was monitored over time. Error bars represent the standard error of four independent measurements for each condition.

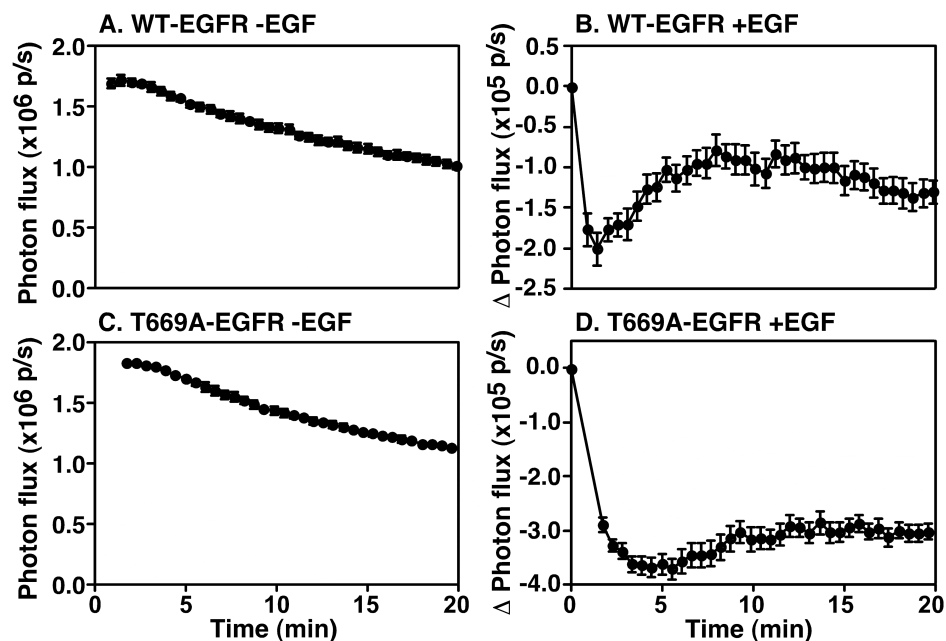


Figure 2.13. Effect of mutation of Thr-669 of the EGF receptor on reconstituted luciferase activity. Panels A-B) CHO-K1 Tet-On cells were transiently transfected with EGFR-NLuc and EGFR-CLuc 24 hrs prior to imaging. Cells were treated for 20 min with 0.6 mg/ml D-Luciferin prior to imaging. A) Basal photon flux (photons/sec; p/s). B) Luciferase activity in cells treated with 10 nM EGF. Panels C-D) CHO-K1 Tet-On cells were transiently transfected with T669A-EGFR-NLuc and T669A-EGFR-CLuc 24 hrs prior to imaging. Cells were treated for 20 min with 0.6 mg/ml D-Luciferin prior to imaging. C) Photon flux (photons/sec; p/s) in the absence of ligand. D) Change in photon flux following addition of 10 nM EGF. Error bars represent the standard error of four independent measurements for each condition.

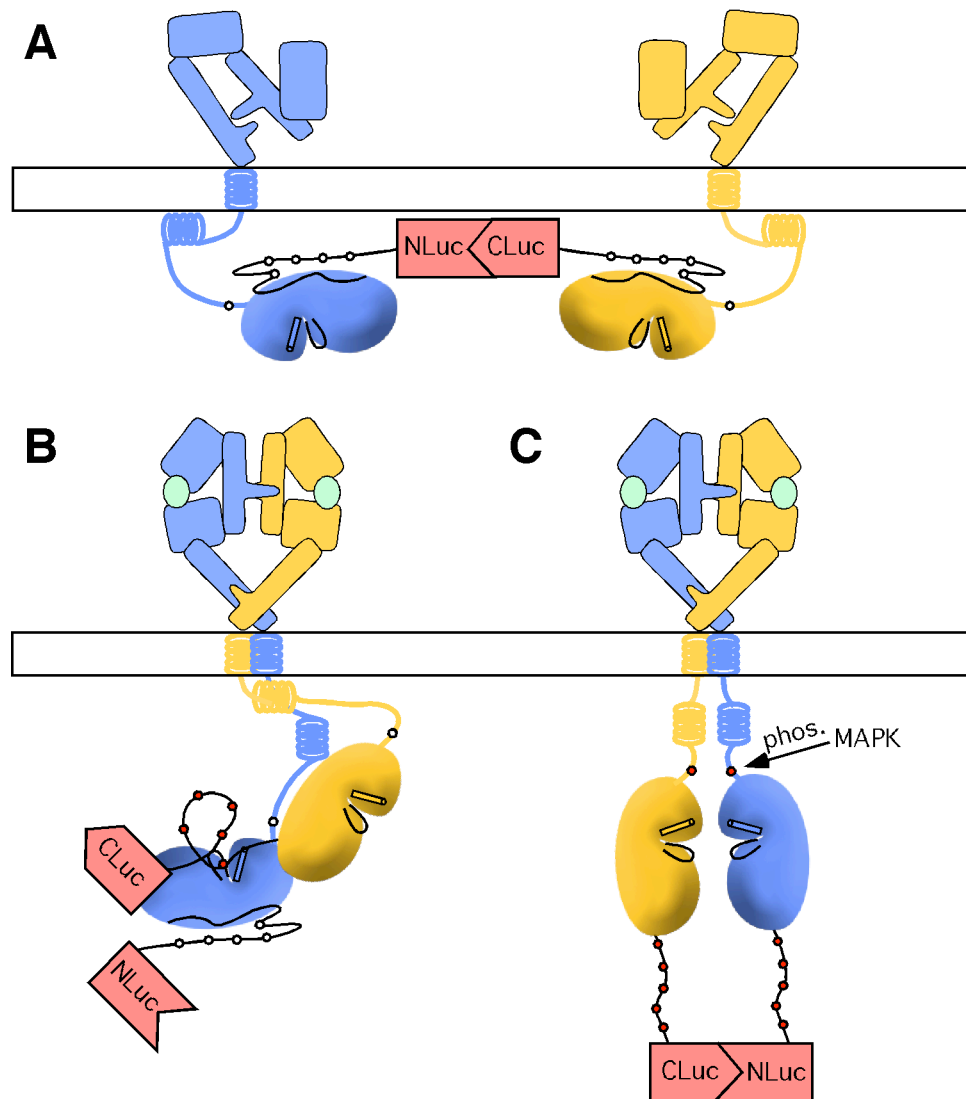


Figure 2.14. Model for intracellular domain conformational changes observed using luciferase fragment complementation imaging of the full-length EGF receptor. A) In the absence of ligand, a significant photon flux is observed, indicating the presence of basal receptor-receptor interactions. B) Addition of ligand induces formation of the activating asymmetric EGF receptor kinase dimer. Transition to this conformational state separates the luciferase fragments, placing them in a conformation where interaction is no longer possible, resulting in the observed decrease in luciferase activity. C) Following the ligand-induced decrease in luciferase activity, a recovery is observed that is dependent on MAP kinase activity and the presence of an intact EGF receptor Thr-669 that can be phosphorylated. White circles represent unphosphorylated residues, while red circles indicate the presence of phosphorylation.

CHAPTER 3. MAP Kinase Desensitizes the EGF Receptor by Blocking Allosteric Activation of the Kinase Domain

Introduction

Following activation, the EGF receptor is desensitized in order to dampen receptor signaling. Long-term desensitization is mediated by internalization and degradation of the receptor (82, 83). In addition, there exists a more rapid desensitization mechanism thought to be mediated by a reduction in protein tyrosine kinase activity (86-88). More specifically, previous work suggests that this rapid desensitization mechanism relies on phosphorylation of the EGF receptor on two threonine residues (Thr-654 and Thr-669) within the intracellular juxtamembrane region (93, 94). Of these two sites, Thr-669 is the major site of threonine phosphorylation in the EGF receptor (95). Phosphorylation of this site is mediated by a feedback loop: the EGF receptor activates MAP kinase, which in turn directly phosphorylates the EGF receptor on Thr-669 (96-98). Mutation of Thr-669 to Ala is associated with enhanced EGF receptor phosphorylation (94). Despite recognition that phosphorylation of Thr-669 is associated with EGF receptor desensitization, the mechanism by which phosphorylated Thr-669 blocks receptor kinase activity is not understood.

Recent studies by two groups highlights the importance of the intracellular juxtamembrane region in activation of the EGF receptor kinase domain (36, 38, 39). These studies were discussed in detail earlier and so will not be repeated here. The important finding of these studies was that activation of the EGF receptor kinase domain, through formation of the asymmetric dimer, relies on additional contacts mediated by the

intracellular juxtamembrane domain of the acceptor kinase and the C-lobe of the donor kinase.

In Chapter 2, luciferase fragment complementation imaging identified sequential ligand-induced conformational changes in the EGF receptor. The final conformation adopted by the EGF receptor was dependent on MAP kinase activation. The time course of this conformational change followed the time course of activation of MAP kinase and EGF receptor Thr-669 phosphorylation. These data suggested that desensitization of the EGF receptor through phosphorylation on Thr-669 may result in a re-orientation of the kinase domains that leads to a loss in tyrosine kinase activity.

The aim of this chapter is to describe mechanistically how MAP kinase mediates desensitization of the EGF receptor. Acidic residues were identified in the C-lobe of the donor kinase domain that are in proximity to Thr-669 of the activator kinase domain. We hypothesized that when Thr-669 is phosphorylated by MAP kinase, a charge repulsion exists that blocks the allosteric activation mechanism of the kinase domain, resulting in a loss of tyrosine kinase activity. Mutations in the kinase domain of either Thr-669 or C-lobe acidic residues to alanines resulted in an enhancement of EGF receptor autphosphorylation and reduced sensitivity to MAP kinase activation compared to the wild type receptor. Luciferase fragment complementation imaging of these mutants showed that upon EGF stimulation, there was an initial rapid decrease in luciferase activity similar to the wild type receptor. However, the subsequent recovery of luciferase activity observed in wild type receptor was completely ablated.

Results

EGF induces enhanced phosphorylation and internalization of the T669A-EGF receptor

MAP kinase has been shown to phosphorylate the EGF receptor on Thr-669 (97, 98). As shown in Figure 3.1A, treatment of cells expressing the wild type EGF receptor with EGF leads to a dose-dependent increase in the level of receptor autophosphorylation. This is associated with the activation of MAP kinase and the concomitant phosphorylation of the EGF receptor on Thr-669.

MAP kinase is also activated in response to EGF in cells expressing the T669A-EGF receptor (Figure 3.1A). As expected, there is no phosphorylation of this receptor on Thr-669. However, there is a clear increase in the level of EGF receptor autophosphorylation as compared to that seen in the wild type EGF receptor. These data are consistent with previous reports (94) and suggest that phosphorylation of the EGF receptor on Thr-669 leads to a desensitization of the tyrosine kinase activity of the EGF receptor.

The ability of the T669A-EGF receptor to mediate internalization of ^{125}I -EGF was next examined. Cells were incubated at 37°C with 1 nM ^{125}I -EGF for varying lengths of time. The amount of internalized ^{125}I -EGF/surface ^{125}I -EGF was plotted versus the length of incubation time to determine the internalization rate (Figure 3.1B). Both the wild-type and T669A-EGF receptors mediated internalization of EGF, however, the rate of internalization of the T669A-EGF receptor was faster compared to the wild-type EGF receptor ($0.078 \pm 0.004 \text{ min}^{-1}$ versus $0.052 \pm 0.003 \text{ min}^{-1}$, respectively). This is consistent with the observation that the T669A-EGF receptor has increased

autophosphorylation compared to the wild-type EGF receptor and is therefore likely to internalize at an increased rate.

Mutation of acidic amino acids in the C-lobe of the EGF receptor kinase domain result in elevated autophosphorylation independent of MAP kinase activity

Thr-669 is in the intracellular juxtamembrane domain of the EGF receptor, just upstream of the tyrosine kinase domain (Figure 3.2). Several recent studies (36, 38, 39) have shown that the juxtamembrane domain participates in the activation of the tyrosine kinase. In particular, the juxtamembrane domain of the acceptor kinase interacts with the C-lobe of the donor kinase to stabilize the asymmetric dimer interface. Phosphorylation of Thr-669 could desensitize the EGF receptor kinase by destabilizing the activating asymmetric dimer interface.

Examination of the asymmetric dimer formed by a recent EGF receptor kinase domain structure (39) as well as that of the homologous ErbB4 kinase (37) showed that Thr-669 lies in close proximity to several acidic amino acids (Asp-950, Asp-960 and Glu-961) in the C-lobe of the donor kinase (Figure 3.2). The unphosphorylated Thr-669 could interact favorably with these residues. When a kinase with a phosphorylated Thr-669 attempts to adopt the acceptor position, the highly negatively-charged phosphate group would lead to charge repulsion and would preclude formation of the activating asymmetric dimer.

To determine whether Asp-950, Asp-960 and/or Glu-961 were involved in the mechanism of MAP kinase-dependent desensitization of the EGF receptor, these residues were mutated to alanine and their effect on EGF receptor autophosphorylation assessed. EGF receptors with a single-point mutation (D950A), a double mutation

(D960A/E961A), or a triple mutation (D950A/D960A/E961A) to the acidic residues were stably expressed in cells. The results of these studies are shown in Figures 3.3-3.6.

Figure 3.3A compares the dose response to EGF in cells expressing the wild type EGF receptor, the T669A-EGF receptor and the D960A/E961A-EGF receptor. While EGF stimulated the phosphorylation of the receptor in all cell lines, autophosphorylation of the EGF receptor was substantially higher in cells expressing the T669A- and D960A/E961A-EGF receptors.

To determine whether the difference in the level of EGF receptor autophosphorylation in the wild type as compared to the D960A/E961A-EGF receptors was related to the phosphorylation of the receptor by MAP kinase, cells were treated without or with the MEK inhibitor, U0126, prior to stimulation by EGF. As shown in Figure 3.3B, treatment of all three cell lines with EGF led to the activation of MAP kinase and this was completely blocked by pretreatment with U0126. In the wild type EGF receptor, stimulation with EGF resulted in receptor autophosphorylation as well as phosphorylation of the receptor on Thr-669. Pretreatment with U0126 abolished phosphorylation of the receptor on Thr-669 and was associated with an increase in EGF receptor autophosphorylation. Due to the absence of the MAP kinase phosphorylation site, the T669A-EGF receptor was not phosphorylated at residue 669 in either the absence or presence of U0126. Consistent with the lack of phosphorylation at this site, pretreatment of these cells with U0126 did not alter the level of EGF receptor autophosphorylation in the T669A-EGF receptor-expressing cells.

In contrast to the T669A-EGF receptor, the D960A/E961A-EGF receptor was extensively phosphorylated at Thr-669 and this was abolished by pretreatment with

U0126. Despite the major change in the level of Thr-669 phosphorylation, there was only a modest increase in the level of EGF receptor autophosphorylation. These data suggest that like the T669A mutation, the D960A/E961A mutation suppresses the effect of MAP kinase phosphorylation on the activity of the EGF receptor.

The wild type EGF receptor exhibited enhanced autophosphorylation when MAP kinase activation was blocked. However, the increase in autophosphorylation did not reach the level of autophosphorylation observed in the T669A-EGF receptor (Figure 3.3B), suggesting possible alternative mechanisms of wild type EGF receptor desensitization. To determine if similar levels of autophosphorylation could be observed in the wild type EGF receptor as compared to the T669A-EGF receptor in the absence of MAP kinase activation, we examined the autophosphorylation after stimulation with higher concentrations of ligand. As shown in Figure 3.4, when the EGF receptor was pre-treated with U0126 and then stimulated with 10 nM, as opposed to 1 nM EGF, an additional increase in autophosphorylation was observed.

As shown previously and in Figure 3.4, the autophosphorylation of the T669A-EGF receptor was higher than the wild type receptor when MAP kinase was active. However, when MAP kinase activation was blocked, the levels of autophosphorylation between the wild type and T669A-EGF receptor were indistinguishable after stimulation with 10 nM, but not 1 nM EGF (Figure 3.4). This is similar to the results observed by Li et al. when wild type and T669A-EGF receptors were stimulated with 1 nM EGF for longer lengths of time (94). These results suggest a possible shift of ligand-induced activation for the T669A-EGF receptor compared to the wild type EGF receptor.

T669R-, T669E-, and T669D-EGF receptor mutants display enhanced autophosphorylation

Mutation of Thr-669 to Ala appears to block the MAP kinase-mediated desensitization mechanism of the EGF receptor. To further test this hypothesis, additional mutations to the Thr-669 site were constructed. First, Thr-669 was mutated to Arg, which would eliminate any charge repulsion with the acidic amino acids in the C-lobe of the donor kinase. Thr-669 was also mutated to Asp and Glu to attempt to mimic the effects of phosphorylation at this site.

Figure 3.5 compares the dose-response to EGF in cells expressing the wild type, T669A-, T669R-, T669D-, and T669E-EGF receptors. Addition of EGF to cells expressing the wild type EGF receptor resulted in a dose-dependent increase in autophosphorylation, MAP kinase activation, and EGF receptor Thr-669 phosphorylation. Similar to the results in Figures 3.1 and 3.3, the T669A-EGF receptor exhibited enhanced EGF receptor autophosphorylation and an absence of Thr-669 phosphorylation (Figure 3.5A). When the T669R-EGF receptor was expressed in CHO cells, addition of EGF resulted in enhanced autophosphorylation compared to both the wild type and T669A-EGF receptors, despite similar levels of receptor expression (Figure 3.5A). These data are consistent with MAP kinase desensitizing the EGF receptor by establishing a charge repulsion that makes formation of the asymmetric dimer interface unfavorable.

Similar to the other Thr-669 mutations, when the T669D-EGF receptors and T669E-EGF receptors were expressed in CHO cells and stimulated with EGF, an increase in autophosphorylation was observed compared to the wild type EGF receptor (Figure

3.5B). Consistent with mutation of the Thr-669 phosphorylation site, the T669D- and T669E-EGF receptors did not react with the phospho-Thr-669 antibody, while the wild type EGF receptor did. Mutation of Thr-669 to an acidic residue was expected to lead to decreased autophosphorylation by mimicking the presence of Thr-669 phosphorylation. Instead an increase in autophosphorylation was observed that may reflect an inability of these amino acids to mimic a phosphorylated amino acid.

Asp-950 is important in stabilizing the asymmetric kinase domain interface

Figure 3.6A compares the dose response to EGF in cells expressing the wild type, D950A-, or D950A/D960A/E961A- triple mutant EGF receptors. Substitution of Asp-950 with alanine markedly impaired the ability of EGF to stimulate autophosphorylation of the D950A-EGF receptor. This result is consistent with Jura et al. who have recently reported that mutation of Asp-950 to Ala leads to impaired EGF receptor autophosphorylation (38). This inhibition was largely overcome when the D950A mutation was combined with the D960A/E961A mutation in the triple mutant, resulting in autophosphorylation levels near the wild type EGF receptor.

The decrease in receptor autophosphorylation seen in the D950A-EGF receptor suggests that Asp-950 may actually serve to stabilize the asymmetric dimer interface and that its mutation destabilizes this interface. Inspection of the EGF receptor kinase domain structure (39) suggests that Asp-950 of the donor kinase could form a potential hydrogen bond with Ser-671 in the juxtamembrane domain of the acceptor kinase. If so, the D950A-EGF receptor mutant would exhibit decreased activity because of its compromised ability to serve as a donor kinase. However, it could still serve as an acceptor kinase since its N-lobe is intact.

To test this hypothesis, the D950A-EGF receptor was expressed alone or in combination with the L680N-EGF receptor. The L680N mutation is in the N-lobe of the kinase domain and it blocks the ability of this receptor to serve as an acceptor kinase (35). However, the receptor can still serve as a donor kinase. As shown in Figure 3.6B, when expressed alone, the EGF-stimulated autophosphorylation of the D950A-EGF receptor was low. Likewise, when expressed alone, the L680N-EGF receptor did not undergo significant autophosphorylation. However, when the D950A-EGF receptor and the L680N-EGF receptor were expressed together, EGF stimulated a marked increase in the autophosphorylation of the EGF receptor. This is consistent with the interpretation that the L680N-EGF receptor served as the donor kinase to activate the D950A-EGF receptor.

Autophosphorylation is recovered in cells expressing the triple EGF receptor mutant, D950A/D960A/E961A

The recovery in receptor autophosphorylation in the D950A/D960A/E961A-EGF receptor suggests that mutation of Asp-950 to Ala is destabilizing, but mutation of Asp-960/Glu-961 to Ala enables re-stabilization of the asymmetric dimer interface. To determine if this recovery is dependent on the MAP kinase-mediated effects through phosphorylation on Thr-669, a double-mutant was established in which both Thr-669 and Asp-950 were mutated to Ala (T669A/D950A-EGF receptor). Addition of varying concentrations of EGF resulted in a dose-dependent increase in autophosphorylation in cells expressing the wild type EGF receptor (Figure 3.7). However, autophosphorylation was still severely impaired in the T669A/D950A EGF receptor double-mutant,

suggesting the recovery observed in the D950A/D960A/E961A-EGF receptor mutant is independent of the effects of MAP kinase phosphorylation on Thr-669.

Asp-960 and Glu-961 are required to observe a recovery in luciferase activity

As described in Chapter 2, firefly luciferase can be divided into an N-terminal fragment (NLuc) and a C-terminal fragment (CLuc), each of which are inactive (100, 101). However, when brought into proximity, the two fragments complement each other, producing an active luciferase enzyme. Thus, luciferase fragment complementation can be used to detect the proximity of two molecules tagged with the different luciferase fragments. These studies can be done in real time in intact cells which allows for continuous imaging of changes in the proximity or conformation of the tagged protein.

Chapter 2 demonstrated that when the NLuc and CLuc fragments were fused to the carboxy-terminus of the full length EGF receptor this system could be used to image conformational changes in the EGF receptor that occur in response to EGF (128). Figure 3.8A and B show the results of such a control experiment using the wild type EGF receptor. As previously reported, significant luciferase activity was observed in the absence of EGF indicating the presence of pre-formed dimers (Figure 3.8A). Upon addition of 10 nM EGF (Figure 3.8B), there was a rapid decrease in luciferase activity followed by a somewhat slower recovery back to baseline levels. The results in Chapter 2 demonstrated that the initial decline in luciferase complementation occurs as a consequence of the autophosphorylation of the EGF receptor while the recovery phase is a result of the phosphorylation of the EGF receptor on Thr-669 by MAP kinase.

These data are recapitulated in Figure 3.8C and D which show luciferase fragment complementation in the T669A-EGF receptor mutant. Like the wild type receptor, the

T669A-EGF receptor showed substantial basal luciferase activity (Figure 3.8C). Also like the wild type receptor, addition of EGF induced a rapid decrease in luciferase activity (Figure 3.8D). However, the subsequent recovery phase was absent in sharp contrast to wild type EGF receptor. Luciferase activity reached a lower plateau and remains that way for the duration of the experiment. This was due to the loss of the MAP kinase phosphorylation site in the T669A-EGF receptor.

As can be seen in Figures 3.8E and F, luciferase fragment complementation in the D960A/E961A-EGF receptor exhibited the same pattern as that seen in the T669A-EGF receptor—EGF stimulated a rapid decline in luciferase activity with no recovery. These data indicate that the D960A/E961A-EGF receptor does not undergo the MAP kinase-dependent conformational change that gives rise to the recovery phase in luciferase fragment complementation. Thus, the data confirm that this mutant is insensitive to the effects of MAP kinase phosphorylation.

Mutation of Asp-950 leads to a rapid increase in luciferase activity

The pattern of luciferase fragment complementation is different in cells expressing the K721A-kinase-dead EGF receptor (Figure 3.9A and B). In this case, there is no decrease in luciferase complementation because this initial decline requires autophosphorylation of the receptor (Chapter 2, Figures 2.7-2.9). Instead, there is an increase due to enhanced dimerization of the receptor mediated by the extracellular domains. The pattern of luciferase fragment complementation in the D950A-EGF receptor is similar to that seen in the K721A-EGF receptor, consistent with its severely compromised kinase activity (Figure 3.9C and D).

Discussion

Expression of an EGF receptor mutant lacking the MAP kinase phosphorylation site, T669A-EGF receptor, led to enhanced autophosphorylation and internalization compared to the wild type receptor. Li et al. observed a similar increase in EGF receptor autophosphorylation and degradation using the same mutation (94). This is consistent with a role for this residue in the rapid MAP kinase-mediated desensitization mechanism.

In Chapter 2, luciferase complementation imaging of cells pre-treated with an inhibitor to block MAP kinase activation or of cells expressing the T669A mutation displayed a decrease but no recovery in luciferase activity (Figures 2.12 and 2.13). These results were interpreted as MAP kinase phosphorylation on the EGF receptor at Thr-669 being critical for the final conformation adopted by the EGF receptor. In this Chapter, the goal was to understand mechanistically how MAP kinase desensitization alters the conformational state of the EGF receptor.

Recent crystal structures of the EGF receptor provided structural insight into the potential mechanism for MAP kinase-mediated EGF receptor desensitization. These crystal structures reveal the location of Thr-669, which lies in the intracellular juxtamembrane region, between the transmembrane and kinase domains (37, 39). Inspection of these crystal structures indicated a region of negatively charged amino acids (Asp-950, Asp-960, and Glu-961) in the C-lobe of the donor kinase (Figure 3.2) that could unfavorably interact with a phosphorylated Thr-669, leading to an inability to form the activating asymmetric dimer and hence a desensitization of EGF receptor kinase activity.

When Asp-960 and Glu-961 were both mutated to Ala (D960A/E961A-EGF receptor), enhanced autophosphorylation was observed compared to the wild type EGF receptor, indicating a loss of desensitization. Pre-treatment of cells with a MEK inhibitor to block MAP kinase activation resulted in an increase in wild type EGF receptor autophosphorylation, indicating a loss of receptor desensitization. In contrast, T669A- and D960A/E961A-EGF receptor mutants were insensitive to the MEK inhibitor, suggesting that the receptors already lacked the desensitization mechanism. Li et al. showed similar results with the wild type and T669A-EGF receptor using a different MEK inhibitor (94).

The D960A/E961A-EGF receptor did show a small increase in autophosphorylation in the presence of the inhibitor to block MAP kinase activation, albeit this increase was significantly less than that observed for the wild type EGF receptor under identical conditions. This small increase may reflect the involvement of additional residues in the MAP kinase-mediated EGF receptor desensitization.

Because the D960A/E961A-EGF receptor mutant exhibited increased autophosphorylation in comparison to the T669A-EGF receptor, it is possible that in addition to desensitization, these residues are important for additional regulatory mechanisms. Both Asp-960 and Glu-961 are located at the junction between the EGF receptor kinase domain and C-terminal tail. Further inspection of crystal structures of the EGF receptor kinase domain C-lobe indicate that Asp-960 may form an intramolecular hydrogen-bond to Ser-787 (35, 37-39, 129-131). Thus, Asp-960 may not function in MAP kinase-mediated desensitization; rather it may function as a pivot point for movement of the C-terminal tail while it undergoes autophosphorylation.

A recent study by Jura et al. determined a crystal structure of the EGF receptor kinase domain with a longer portion of the C-terminal tail than was previously observed (amino acids 960-990) (38). The position of the C-terminal tail suggests that it may be autoinhibitory and requires displacement by the intracellular juxtamembrane domain during formation of the asymmetric dimer. Because Asp-960 is located at the junction of the kinase and C-terminal tail domains, it may be the pivot point for this displacement. Mutation of Asp-960 so it can no longer hydrogen-bond with Ser-787 would facilitate displacement of the C-terminal tail, possibly leading to enhanced EGF receptor autophosphorylation. If this is the case, then the D960A/E961A-EGF receptor double mutant would exhibit enhanced autophosphorylation compared to the wild type EGF receptor and the T669A-EGF receptor for two reasons: 1) an inability to undergo MAP kinase-mediated desensitization through charge repulsion between phospho-Thr-669 and Glu-961, and 2) facilitated displacement of the C-terminal tail due to mutation of the Asp-960/Ser-787 hydrogen-bond. The dual effects of the D960A/E961A-EGF receptor would explain why autophosphorylation is enhanced compared to the T669A-EGF receptor and why the wild type EGF receptor with desensitization blocked cannot attain autophosphorylation levels comparable to the D960A/E961A-EGF receptor.

Luciferase complementation imaging of the full-length EGF receptor captured a series of ligand-induced conformational changes by the intracellular domain (Chapter 2, Figure 2.3). The final conformation adopted by the EGF receptor was shown to be dependent on MAP kinase activity because blocking MAP kinase activation completely abolished the recovery in luciferase activity (Figure 2.12). Additionally, mutation of the Thr-669 phosphorylation site eliminated the recovery but not the decrease in luciferase

activity (Figure 2.13 and 3.8). Similar results were obtained when the D960A/E961A-EGF receptor luciferase constructs were expressed in cells, indicating that this mutant behaves similarly to the Thr-669 mutant that lacks the MAP kinase phosphorylation site. Together these data suggest Asp-960 and/or Glu-961 play a significant role in MAP kinase-mediated EGF receptor desensitization, possibly by blocking formation of the allosteric asymmetric dimer.

When Thr-669 was mutated to Arg, enhanced autophosphorylation was observed compared to the wild-type EGF receptor. This is consistent with a favorable interaction between the Arg-669 and Asp-960/Glu-961. However, mutation of Thr-669 to Asp and Glu to mimic constitutive phosphorylation did not have the expected result. Instead of observing the expected decrease in autophosphorylation due to charge repulsion between the negatively charged Asp- or Glu-669 and Asp-960/Glu-961, an increase in autophosphorylation compared to the wild type EGF receptor was observed. This is consistent with data reported by Morrison et al. in which Thr-669 was mutated to Glu and an increase in autophosphorylation compared to the wild type EGF receptor was observed (132). However, these data are not consistent with a recent report by Red Brewer et al., in which the intracellular domain of the T669D-EGF receptor showed decreased autophosphorylation compared to the wild type EGF receptor, whereas the T669A-EGF receptor exhibited enhanced autophosphorylation (39). These observed differences may be due to a lack of signaling in the intracellular domain constructs utilized by Red Brewer et al., rendering MAP kinase inactive and therefore blocking one of the EGF receptor desensitization mechanisms. Alternatively, there may be additional structural constraints imposed by the EGF receptor extracellular and transmembrane domains that allow the

receptor to overcome the negative charge imposed by the T669D- and T669E-EGF receptor mutations.

While the increased autophosphorylation observed in the T669D- and T669E-EGF receptor mutants was unexpected, it does not necessarily contradict the hypothesis that Thr-669 phosphorylation by MAP kinase desensitizes the EGF receptor by blocking formation of the asymmetric dimer interface. Attempts in other systems to mimic serine or threonine phosphorylation using either Aspartic or Glutamic acid have also generated mixed results (133, 134). For example, phosphorylation of rhodopsin's C-terminal tail is required for binding of and induction of a conformational change in arrestin. Studies using Surface Plasmon Resonance with either a phosphorylated rhodopsin C-terminal tail peptide or one in which all the serine/threonine residues were substituted with Glutamic acid yielded opposing results in the ability to bind arrestin. These and other studies indicate that the ability of Glutamic and Aspartic acid to mimic constitutive phosphorylation is system-dependent.

In this system, replacement of Thr-669 with Asp or Glu does not appear to be enough to mimic the effects of phosphorylation. The effects of serine/threonine phosphorylation may be particularly difficult to mimic because surface-exposed Glutamic acid side chains can occupy several positions due to the flexibility of this sidechain (134). The increased phosphorylation observed in the T669D- and T669E-EGF receptor mutants is therefore expected if the charge on these amino acids is not enough to lead to charge repulsion with Asp-960/Glu-961. These mutants lack the "cue" to desensitize the receptor, resulting in enhanced autophosphorylation.

The mutations described in this chapter identified Asp-950 as a residue important for stabilization of the asymmetric dimer interface. When the D950A-EGF receptor was expressed in cells, severely impaired autophosphorylation was observed compared to the wild type EGF receptor. Similar results were obtained by Jura et al. when Asp-950 was mutated to Ala (38). These data are consistent with the D950A-EGF receptor being unable to function as a donor kinase in the asymmetric dimer. This hypothesis is further supported here by demonstrating that D950A- and L680N-EGF receptors expressed independently had little kinase activity, but activity was restored when the receptors were co-expressed in the same cells.

A rapid increase in luciferase activity was observed both in the kinase-dead EGF receptor and the EGF receptor lacking the intracellular domain (Chapter 2, Figures 2.1 and 2.10). Similar results were observed when luciferase complementation imaging of the D950A-EGF receptor was examined, consistent with the lack of kinase activity in this mutant. Luciferase complementation imaging further supports that the D950A-EGF receptor plays an important role in proper formation of the asymmetric dimer interface.

Surprisingly, in stark contrast to the D950A-EGF receptor, autophosphorylation of the D950A/D960A/E961A-EGF receptor recovered to near wild type levels. This recovery was independent of the MAP kinase-mediated desensitization mechanism since expression of the T669A/D960A-EGF receptor retained little kinase activity. The Asp-950 residue is stabilizing in the context of the asymmetric dimer interface and mutation of this residue is destabilizing. When mutated in conjunction with Asp-960 and Glu-961, the “imperfect” asymmetric dimer interface formed by the Asp-950 mutant may recover kinase activity because the C-terminal tail may be displaced more easily when the

potential “pivot” formed by the Asp-960 is loosened through mutation to Ala. This scenario would allow asymmetric dimer formation and autophosphorylation to near wild type levels, despite a non-ideal asymmetric dimer interface.

The potential role of Asp-960 as a pivot point during movement of the C-terminal tail may explain why mutation of Ser-787 has been reported in lung cancer patients. Na et al. reported mutation of Ser-787 to Phe (135), which would remove the hydrogen bond between this residue and Asp-960, possibly causing easier displacement of the EGF receptor C-terminal tail and enhanced EGF receptor kinase activation and signaling. However, these results are purely speculative in the absence of: 1) confirmation that S787F-EGF receptor displays enhanced phosphorylation and 2) this mutation has been identified in additional patients and/or is linked more clearly to cancer progression.

In a sequence alignment of the EGF receptor family members, Thr-669 and the MAP kinase consensus sequence for phosphorylation (P X T/S P) is conserved among all members, except ErbB3 (Figure 3.10). While the significance of this is unknown, it is noteworthy that ErbB3 is the only intrinsically kinase-dead member of the EGF receptor (48, 57, 66). This may reflect the redundant nature of the MAP kinase desensitization mechanism because the kinase-dead nature of ErbB3 limits the pool of kinase domains that can serve as an activated acceptor. Additionally, ErbB3 signals better via the PI3-kinase pathway due to multiple docking sites in its C-terminal tail (48), possibly reducing the impact of the MAP kinase pathway, as well as need for a desensitization mechanism via this pathway. In addition to conservation of the Thr-669 site, the presence of negatively charged amino acids in the region of the EGF receptor Asp-960 and Glu-961 is also conserved among all family members and among various species (Figure 3.10).

Based on the data described in this chapter, a model for the MAP kinase-mediated desensitization of the EGF receptor was established. Figure 3.11 depicts a cartoon representation of this model. Ligand binding to the EGF receptor extracellular domain induces a large conformational change, enabling dimerization and subsequent asymmetric kinase domain dimerization. The juxtamembrane domain of the acceptor kinase domain in the dimer may displace the C-terminal tail of the donor kinase domain to form the optimal asymmetric dimer interface/juxtamembrane domain cradle (Figure 3.11A to B). The activating asymmetric dimer leads to acceptor activation and phosphorylation of the C-terminal tail of the donor kinase. This enhances signal complex formation and leads to activation of the MAP kinase pathway, followed by feedback signaling through MAP kinase phosphorylation on the EGF receptor Thr-669 (Figure 3.11 C to D). Following phosphorylation of the initial donor kinase C-terminal tail, the kinase domains may switch roles so that the donor becomes the acceptor and vice versa (Figure 3.11D). As the kinase domains switch roles, the original donor kinase with a phosphorylated Thr-669 will try to displace the C-terminal tail of the original acceptor kinase (now adopting the donor position). Because of the highly negatively charged phosphate group on Thr-669, a charge repulsion with Asp-960 and/or Glu-961 exists, making it difficult for the original donor to adopt the acceptor position/form a proper asymmetric dimer interface. This leads to a dissociation of this attempted asymmetric dimer without phosphorylation of the original acceptor's C-terminal tail (Figure 3.11E). MAP kinase desensitizes the EGF receptor kinase activity by making the monomer with a phosphorylated Thr-669 a poor acceptor kinase. This mechanism would lead to decreased autophosphorylation because of the limited pool of kinases that can function as acceptors. Several questions remain to

be answered based on this model. For example, it is not known which Thr-669 residue is phosphorylated. Figure 3.11 depicts the phospho-Thr-669 as the original donor kinase simply because it seems likely that the Thr-669 phosphorylation site on the acceptor kinase will be less accessible to MAP kinase. It also appears that additional residues may be important for the MAP kinase-mediated desensitization mechanism and identification of these residues will be important.

Thr-669 in the recent crystal structure determined by Red Brewer et al. points away from the C-lobe of the donor kinase (Figure 3.2) (39). This may seem contradictory to an interaction with Asp-960 and/or Glu-961 during MAP kinase-mediated desensitization. However, phosphorylated Thr-669 may negatively interact with Asp-960 and/or Glu-961 in a transitory state that exists as the acceptor kinase is forming the cradle around the C-lobe of the donor kinase. The structure observed by Red Brewer et al. would then form when Thr-669 is not phosphorylated.

The data presented in this Chapter describe, for the first time, the mechanism that MAP kinase utilizes to desensitize the EGF receptor through phosphorylation on Thr-669. This mechanism of blocking asymmetric dimer formation is not unique, since Mig6, a protein transcriptionally activated by the EGF receptor, has also been reported to block EGF receptor activation by blocking asymmetric dimer formation (89). It will be interesting to see if additional modulators of EGF receptor activity function through a similar mechanism of blocking asymmetric dimer formation.

Experimental Procedures

Reagents—Murine EGF was purchased from Biomedical Technologies, Inc. and was dissolved in sterile water. U0126 (EMD Chemicals) was dissolved in DMSO.

Doxycycline was from Clontech and was dissolved in sterile water. D-Luciferin (Biosynth) was dissolved in PBS and coelenterazine (Sigma) was dissolved in ethanol. The MAP kinase and phospho-specific Thr-669 antibodies were from Upstate. The phospho-specific MAP kinase antibody was from Promega and the phosphotyrosine (PY20) antibody was from BD Biosciences. A mixture of EGF receptor antibodies from Cell signaling and Santa Cruz were used to detect the EGF receptor.

DNA Constructs—The wild type EGF receptor construct (127) was subcloned from pcDNA3.1(-) (Invitrogen) into pcDNA5/FRT (Invitrogen) using the NheI and HindIII restriction enzyme sites. Using the wild type EGF receptor (pcDNA3.1(-)) as the template, QuikChange site-directed mutagenesis (Stratagene) was used to generate the D950A and D960A/E961A mutants. Mutants were digested with the BstEII and HindIII restriction enzyme sites and were ligated into the wild type EGF receptor construct (pcDNA5/FRT) cut with the same enzymes. All mutants were sequenced in their entirety.

The D950A/D960A/E961A mutant was generated using QuikChange site-directed mutagenesis with the D960A/E961A-EGF receptor mutant (pcDNA3.1(-)) as the template. The D950A/D960A/E961A-EGF receptor pcDNA5/FRT construct was subcloned into the wild type pcDNA5/FRT construct using the BstEII and HindIII restriction sites and was sequenced.

The T669A-CLuc construct was made using QuikChange site-directed mutagenesis of the EGFR-CLuc (pcDNA6/V5-HisB) construct (Chapter 2). The product was re-ligated into the same vector using the NheI and BsiWI restriction enzyme sites. The T669A-EGF receptor (pcDNA5/FRT) construct was subsequently generated by

digesting the T669A-CLuc (pcDNA6/V5-HisB) and wild type EGF receptors (pcDNA5/FRT) with NheI and BstEII. The product was sequenced to verify the mutation.

QuikChange site-directed mutagenesis was used to make the T669A/D950A-EGF receptor mutation, with the T669A-EGF receptor (pcDNA5/FRT) construct as the template. Following mutagenesis, the construct was re-ligated into the T669A-EGF receptor construct using the NheI and NotI restriction enzyme sites. Sequencing confirmed the mutation.

The L680N-EGF receptor mutant was made using QuikChange site-directed mutagenesis in the wild type EGF receptor pcDNA5/FRT construct as described previously (136). The mutant was sequenced and then digested with NheI and EcoRV and ligated into MCS1 of the pBI-Tet vector (Clontech).

QuikChange site-directed mutagenesis was used to make the T669E-, T669R-, and T669D-EGF receptor constructs with the wild type EGF receptor (pcDNA5/FRT) as the template. Mutants were digested with NheI and BstEII and were ligated into the wild type EGF receptor pcDNA5/FRT plasmid cut with the same enzymes. Mutations were verified by sequencing.

The D950A-CLuc and D960A/E961A-CLuc mutants were made by QuikChange site directed mutagenesis of the EGFR-CLuc pcDNA6/V5-HisB construct. Mutants were digested with BstEII and BsiWI and were re-ligated into the EGFR-CLuc pcDNA6/V5-HisB construct. The D950A-NLuc and D960A/E961A-NLuc constructs were first made by digesting the D950A-CLuc and D960A/E961A-CLuc constructs with NheI and BsiWI, followed by ligation into the EGFR-NLuc pBI-Tet construct. These NLuc

mutants were later subcloned into the pcDNA5/FRT vector using the BstEII and EcoRV restriction enzyme sites in the mutants and the BstEII and KpnI sites in the wild type EGF receptor pcDNA5/FRT construct.

T669A-NLuc in pcDNA5FRT was generated by restriction enzyme digest of the EGFR-NLuc pcDNA3.1TOPO plasmid with BstEII and KpnI, followed by ligation into T669A-EGF receptor pcDNA5/FRT.

The K721A-EGFR-CLuc construct was made using QuikChange site-directed mutagenesis (Stratagene) in the EGFR-CLuc pcDNA6/V5-His B construct. The K721A-EGFR-NLuc construct was made by digesting EGFR-NLuc (pcDNA3.1 TOPO) with BstEII and KpnI. The insert was ligated into the K721A pcDNA5.FRT (Invitrogen) construct digested with the same enzymes.

Cell Lines—FI CHO cells (Invitrogen) were co-transfected with pOG44 (Invitrogen) and the wild type or mutant EGF receptors (pcDNA5/FRT) using Lipofectamine 2000 (Invitrogen). Stable clones were isolated by selection in 600 µg/ml hygromycin (InvivoGen). Cells were maintained in F-12 containing 10% FetalPlex, 1000 µg/ml penicillin/streptomycin, and 100 µg/ml hygromycin. CHO-K1 Tet-On cells were grown in DMEM containing 10% FetalPlex, 1000 µg/ml penicillin/streptomycin, and 200 µg/ml G418. The EGFR-NLuc/EGFR-CLuc, T669A-NLuc/T669A-CLuc, D950A-NLuc/D950A-CLuc, D960A/E961A-NLuc/D960A/E961A-CLuc, and K721A-NLuc/K721A-CLuc constructs were transiently transfected into CHO-K1 Tet-On cells 24 hrs prior to luciferase fragment complementation imaging using Lipofectamine 2000. Transfection efficiency was determined by co-transfection of renilla luciferase (pRLuc-N1, Packard Bioscience).

Kinase activation and Western Blotting—FI CHO EGF receptor wild type or mutant cells were grown to confluence in 35 mm dishes. Cells were serum-starved in F-12 containing 1 mg/ml BSA for 2 hr. Cells were washed twice in ice-cold PBS and were then scraped into RIPA buffer (150 mM NaCl, 10 mM Tris pH 7.2, 0.1% sodium dodecylsulfate, 1% Triton X-100, 17 mM deoxycholate, and 2.7 mM EDTA) containing 20 mM p-nitrophenyl phosphate, 1 mM sodium orthovanadate, and protease inhibitors. Equal amounts of protein (BCA assay, Pierce) were loaded onto a 9% SDS-polyacrylamide gel and then transferred to PVDF (Millipore). Western blots were blocked for 1 hour in TBST/10% nonfat milk. The blots were incubated in primary antibody for 1 hr (overnight at 4°C for EGF receptor and phospho-Thr-669 antibodies), washed in TBST/0.1% BSA, incubated in secondary antibody for 45 min and washed three times in TBST/0.1% BSA. Western blots were detected using the ECL reagent from GE Healthcare.

¹²⁵I-EGF Internalization—Murine EGF was radioiodinated as described previously (102). Cells were plated 48 hrs prior to assay in six-well dishes. Cells were washed twice in HBSS (37°C) and were then incubated for the indicated lengths of time in 1 nM ¹²⁵I-EGF at 37°C in F-12 media containing 40 mM Hepes and 0.1% bovine serum albumin. Nonspecific binding was determined by addition of 100 nM unlabeled EGF. At each time point, half of the cultures were washed three times in HBSS, the monolayers were dissolved in 1N NaOH, and the radioactivity was determined by γ -counting. This yields the total cell-associated ¹²⁵I-EGF. The other half of the cultures were washed twice (2 min each) in acid wash buffer (50 mM glycine, 100 mM NaCl, pH3) to remove any cell-surface ¹²⁵I-EGF (137). Monolayers were then dissolved in 1N

NaOH and were counted in a γ -counter. This yields the internalized ^{125}I -EGF and subtraction from the total ^{125}I -EGF yields the amount of surface ^{125}I -EGF.

Luciferase complementation imaging—Cells were plated 48 hr prior to use at 5×10^3 cells per well in DMEM in a black-wall 96-well plate. On the day of the assay, cells were serum-starved for 2 hr and then incubated for 20 min in 175 μl DMEM without phenol red, containing 1 mg/ml BSA, 25 mM HEPES, and 0.6 mg/ml D-luciferin at 37°C . To establish a baseline, cell radiance (photons/second/ cm^2/sr) was measured using a cooled CCD camera and imaging system at 37°C (IVIS 50; Caliper) (30 sec exposure; binning, 8; no filter; f-stop, 1; field of view, 12 cm). EGF was added in a volume of 25 μl in the same media (DMEM, 1mg/ml BSA, 25mM HEPES, 0.6mg/ml D-Luciferin). Radiance was measured sequentially as described above. Transfection efficiency was assessed by monitoring renilla luciferase expression. Media was replaced on cells with DMEM (no phenol red) containing 1 mg/ml BSA, 25 mM HEPES, and 400 nM coelenterazine. Radiance was immediately measured as described above except the filter was set to <510 .

Data Analysis—Data was collected in quadruplicate for each condition. A flat-field correction was done to correct for differences in the baseline photon flux. Light production expressed as photon flux (photons/sec) was determined from regions-of-interest defined over wells using LIVINGIMAGE (Xenogen) and IGOR (Wavemetrics) software. Changes in photon flux were calculated by subtracting values from untreated cells from those of EGF-treated cells. Standard errors were determined using the formula for the unpooled standard error.

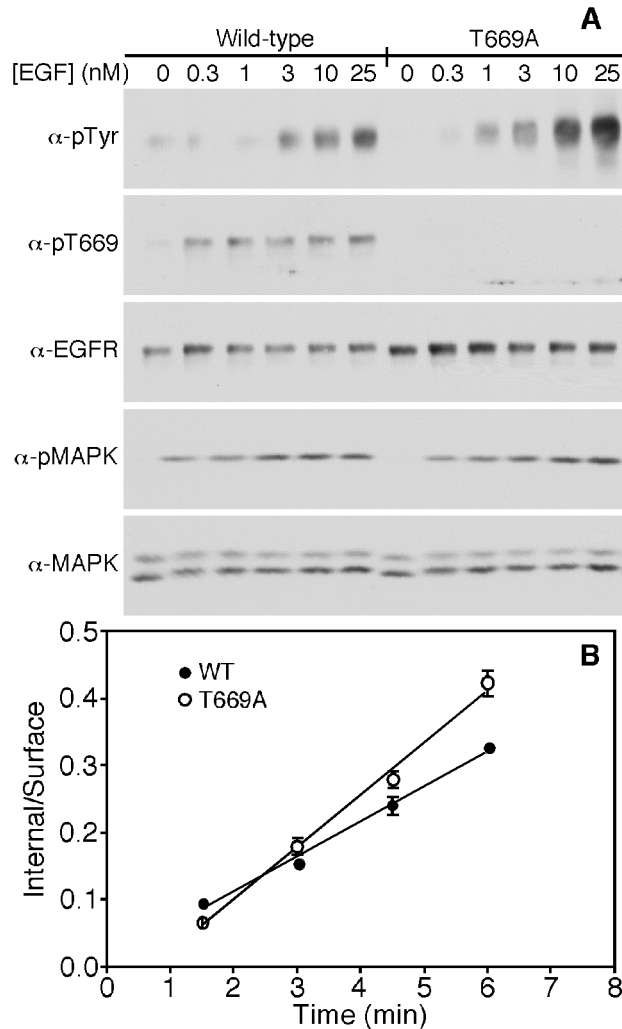


Figure 3.1. Effect of Thr-669 mutation on EGF receptor autophosphorylation and internalization. FI CHO cells expressing the wild type or T669A-EGF receptor were plated 48 hr prior to assay in six-well dishes. Cells were serum-starved prior to assay. A) Cells were stimulated with the indicated concentrations of EGF for 5 min at 37°C. Cells were lysed, run on an SDS-PAGE gel, and Western blot analysis was done with the indicated antibodies. B) Cultures were incubated for the indicated lengths of time in 1 nM ^{125}I -EGF. Total ^{125}I -EGF was determined by washing cultures three times in HBSS, while internalized ^{125}I -EGF was determined by washing cultures twice in acid wash. Monolayers were dissolved in 1N NaOH followed by γ -counting. Surface ^{125}I -EGF was determined by subtraction of total and internalized ^{125}I -EGF. Internalized/surface ^{125}I -EGF was plotted as a function of time to determine the internalization rate for the wild type (closed circles, $0.052 \pm 0.003 \text{ min}^{-1}$) and T669A-EGF receptors (open circles, $0.078 \pm 0.004 \text{ min}^{-1}$).

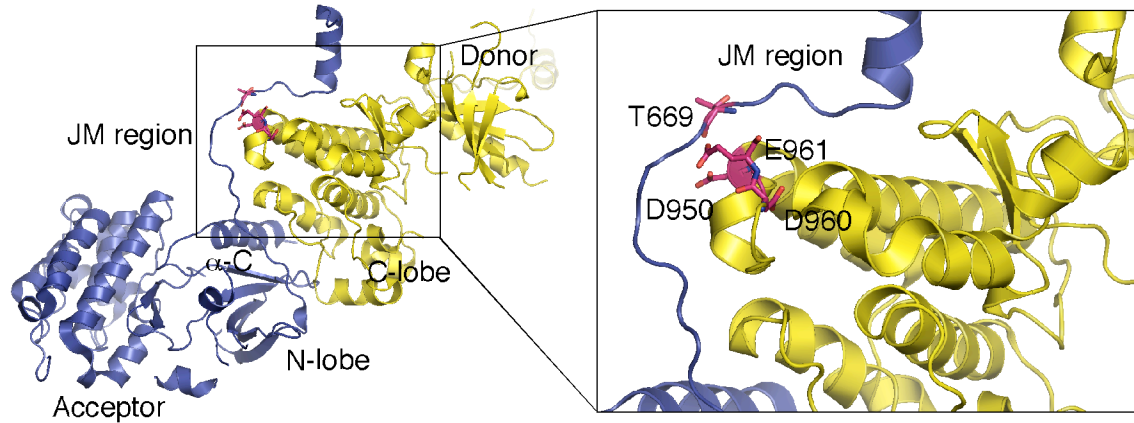


Figure 3.2. Crystal structure of the EGF receptor juxtamembrane and kinase domain asymmetric dimer interface, highlighting the residues surrounding Thr-669. The acceptor EGF receptor kinase monomer is shown in blue and the donor kinase is shown in yellow. The juxtamembrane region of the acceptor/blue kinase monomer is shown forming a cradle around the C-lobe of the donor/yellow kinase monomer in the asymmetric dimer. Shown magnified is the position of the Thr-669 residue in the juxtamembrane domain of the acceptor/blue monomer. Highlighted in the C-lobe of the donor/yellow monomer are acidic residues (Asp-950, Asp-960, Glu-961) that lie in close proximity to Thr-669. The PDB coordinates for this structure are 3GOP (39).

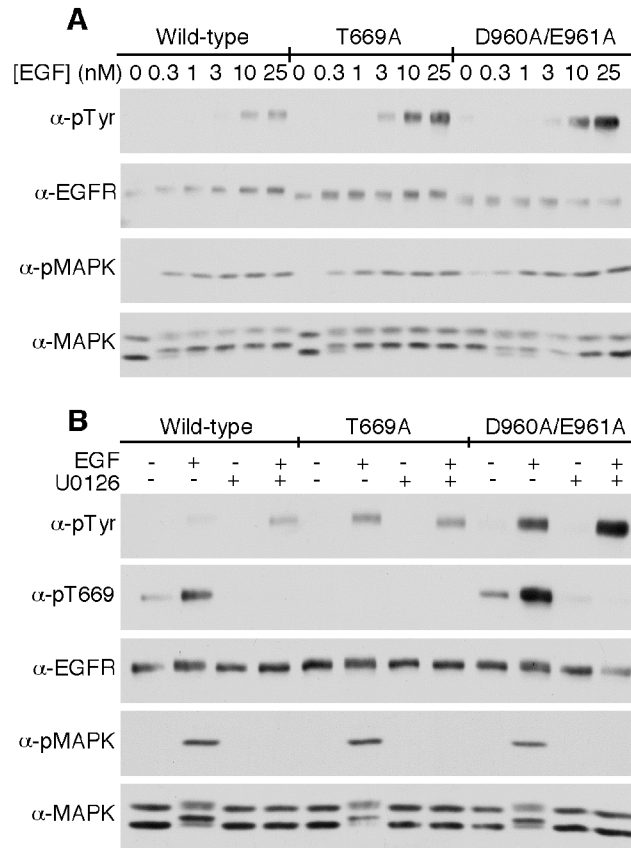


Figure 3.3. EGF receptor autophosphorylation in wild type, T669A, and D960A/E961A mutants. FI CHO cells stably expressing the wild type, T669A, or D960A/E961A-EGF receptor were plated 48 hrs prior to assay in six-well dishes. Cells were serum-starved 2 hrs prior to assay. A) The indicated concentrations of EGF were added to cells for 5 min at 37°C. Cells were lysed, loaded for equal EGF receptor expression, and were run on a 9% SDS-PAGE gel. Western blot analysis was performed with the indicated antibodies. B) Cells were incubated for 20 min at 37°C without or with 10 μ M U0126, followed by stimulation with 1 nM EGF for 5 min. Cells were immediately lysed, equal EGF receptor levels were run on an SDS-PAGE gel and Western blotting was done with the indicated antibodies.

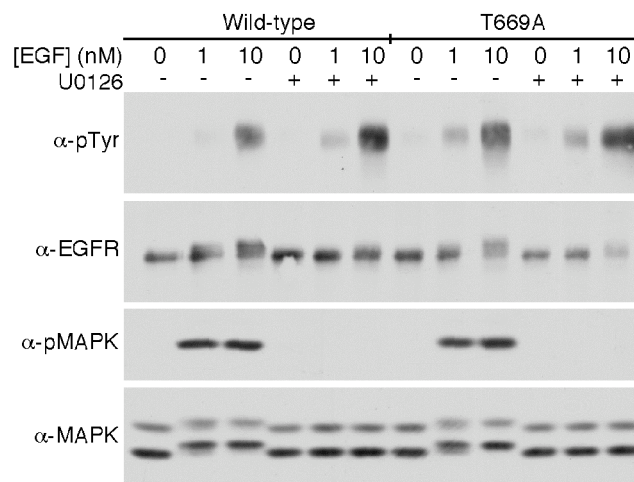


Figure 3.4. Effect of blocking MAP kinase activation on wild type or T669A-EGF receptor autophosphorylation. FI CHO cells stably expressing the wild type or T669A-EGF receptor were plated 48 hrs before assaying in six-well plates. On the day of the assay, cells were serum-starved for 2 hrs. Cells were pre-incubated in the absence or presence of 10 μ M U0126 for 20 min at 37°C, followed by stimulation for 5 min with 1 or 10 nM EGF. Lysates were immediately made of the cells and equal proteins were loaded on an SDS-PAGE gel. Western blots were analyzed with the indicated antibodies.

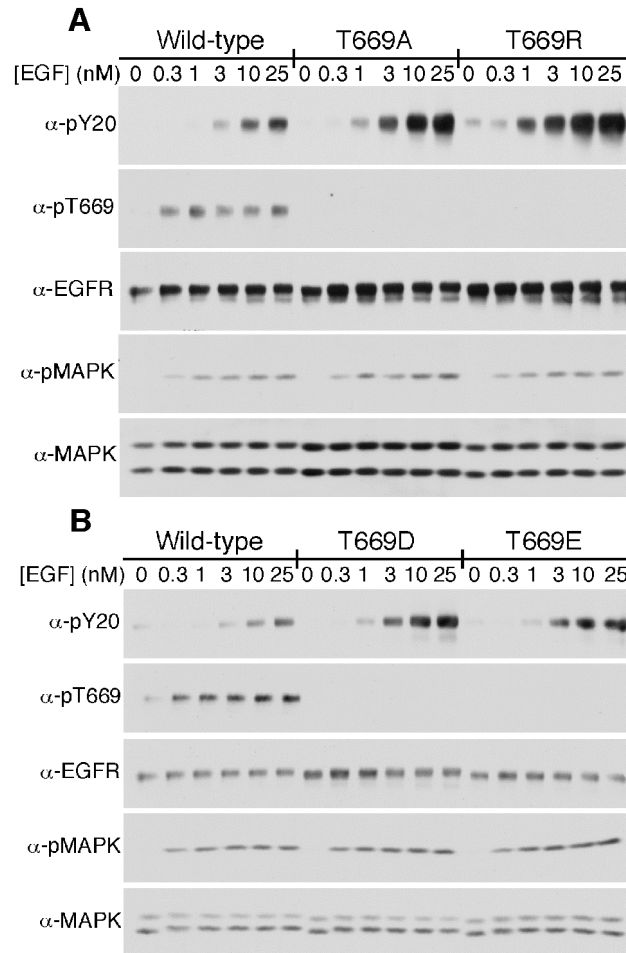


Figure 3.5. Dose-response to EGF in cells expressing wild type, T669A, T669R, T669D, and T669E-EGF receptor mutants. Cells stably expressing the wild type or EGF receptor mutants were plated 48 hrs prior to assay in six-well dishes. Cells were serum-starved 2 hr prior to assay. The indicated concentrations of EGF were added to cells for 5 min at 37°C. Cells were immediately lysed, equal proteins were loaded on a 9% SDS-PAGE gel and Western blot analysis was performed with the indicated antibodies. A) Wild type, T669A, and T669R-EGF receptors. B) Wild type, T669D, and T669E-EGF receptors.

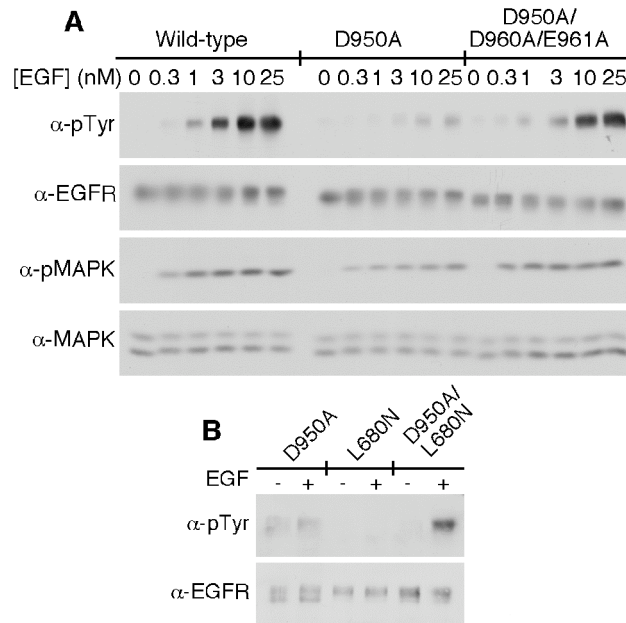


Figure 3.6. EGF receptor autophosphorylation in cells expressing wild type, D950A, D950A/D960A/E961A, L680N, or D950A/L680N mutations. A) FI CHO cells that stably express the wild type, D950A, or D950A/D960A/E961A-EGF receptor were plated 48 hrs before assaying in six-well dishes. Cells were serum-starved 2 hrs before assay. Cells were treated with the indicated concentrations of EGF for 5 min at 37°C and were immediately lysed. Lysates were loaded for equal EGF receptor expression and were run on an SDS-PAGE gel. Western blot analysis was done with the indicated antibodies. B) CHO-K1 Tet-On cells stably expressing the L680N-EGF receptor were plated 48 hrs prior to assay in the absence (D950A) or presence (L680N and D950A/L680N) of 500 ng/ml doxycycline to induce L680N-EGF receptor expression (pBI-Tet vector). 24 hrs prior to assay cells were transiently transfected with cDNA for the D950A-EGF receptor. Cells were serum-starved for 2 hrs and were then stimulated with 25 nM EGF for 5 min at 37°C. Cells were immediately lysed and equal proteins loaded on an SDS-PAGE gel. Western blotting was performed with the indicated antibodies.

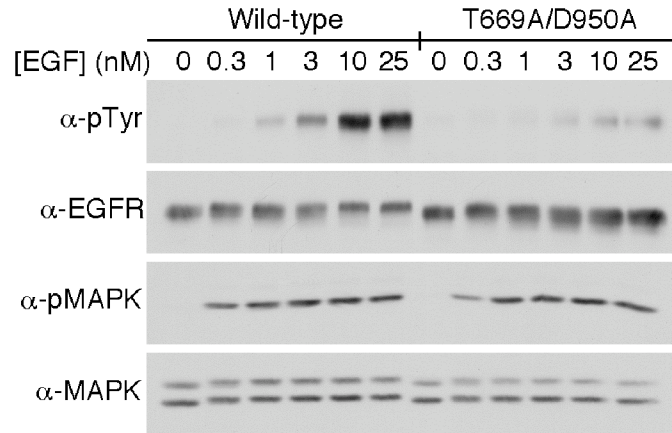


Figure 3.7. EGF dose response in cells expressing wild type or T669A/D950A EGF receptors. FI CHO cells stably expressing the wild type or T669A/D950A-EGF receptor were plated in six-well dishes 48 hrs prior to assay. Cells were serum-starved 2 hr prior to assay, followed by stimulation for 5 min at 37°C with the indicated concentrations of EGF. Cells were lysed and equal proteins were loaded on an SDS-PAGE gel. Western blot analysis was done with the indicated antibodies.

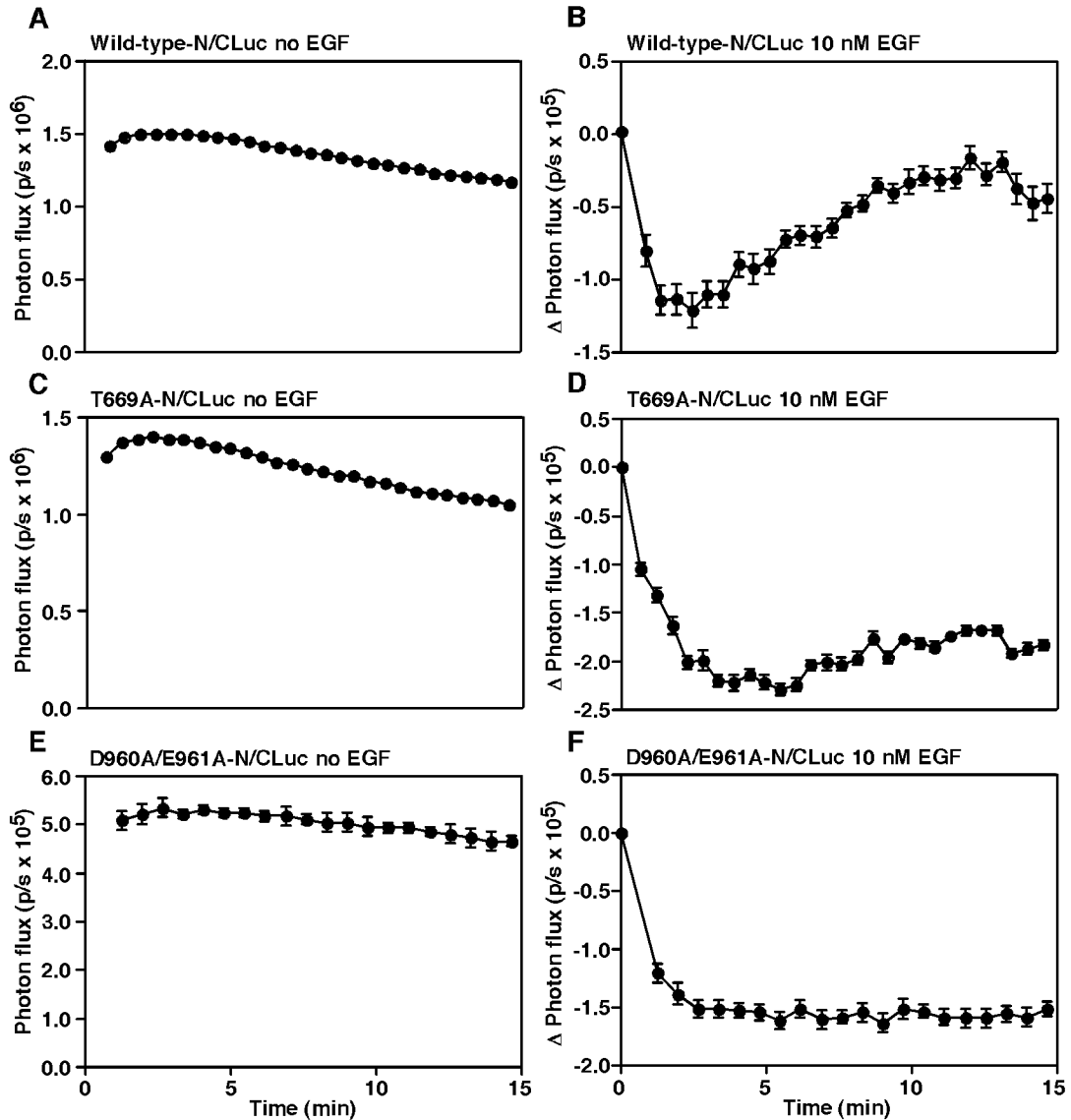


Figure 3.8. Reconstitution of luciferase activity in cells expressing wild type, T669A, or D960A/E961A luciferase constructs. CHO-K1 Tet-On cells were plated in 96-well plates 48 hrs prior to luciferase complementation imaging. 24 hrs prior to imaging, cells were transiently transfected with the cDNA encoding the wild type, T669A, or D960A/E961A-EGF receptor NLuc and CLuc luciferase constructs. On the day of imaging, cells were serum-starved for 2 hrs followed by pre-incubation in 0.6 mg/ml D-luciferin for 20 min. A, C, E) Photon flux (photons/sec; p/s) in the absence of EGF. B, D, F) Change in photon flux following addition of 10 nM EGF. Data represent the average of four independent replicates and standard error is shown.

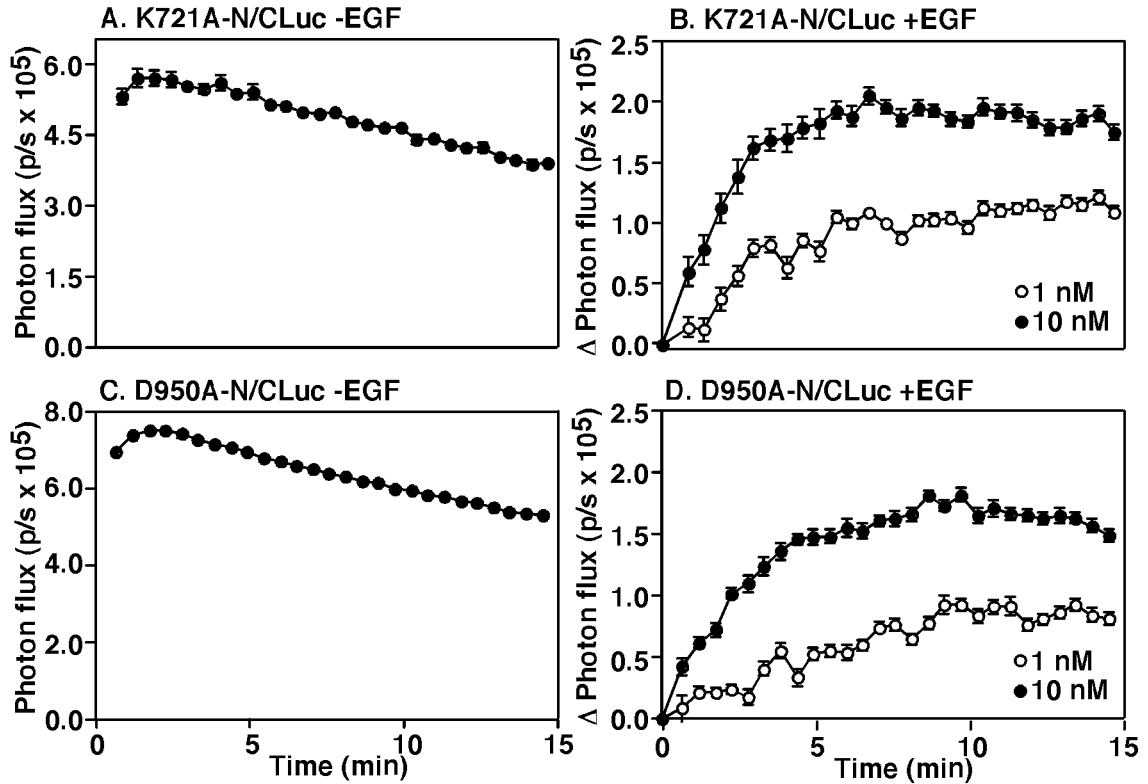


Figure 3.9. Reconstitution of luciferase activity in cells expressing D950A and K721A EGF receptor luciferase constructs. CHO-K1 Tet-On cells were plated in a 96-well plate 48 hrs prior to imaging. Cells were transiently transfected with the cDNA encoding the K721A-EGF receptor or D950A-EGF receptor NLuc and CLuc constructs 24 hrs prior to imaging. On the day of imaging, cells were serum-starved for 2 hrs, followed by a 20 min incubation with 0.6 mg/ml D-luciferin. A and C) Photon flux (photons/sec; p/s) in the absence of ligand. B and D) Change in photon flux following addition of 1 (open circles) or 10 nM EGF (closed circles).

	669		950	960
EGFR	ELVEPLTPSGEAPNQALL	EGFR	EFSKMARDPQRYLVIQGD [•] ER-MHLPSPT	
ErbB2	ELVEPLTPSGAMPNQAQM	ErbB2	EFSKMARDPQRFVVIQ-NE [•] D-LGPASPL	
ErbB3	ESIEPLDPS-EKANKVLA	ErbB3	EFTRMARDPPRYLVIKRE [•] SGPGIAPGPE	
ErbB4	ELVEPLTPSGTAPNQAQL	ErbB4	EFSRMARDPQRYLVIQGD [•] DR-MKLPSPN	
human	ELVEPLTPSGEAPNQALL	human	EFSKMARDPQRYLVIQGD [•] ERMHLPSPT	
mouse	ELVEPLTPSGEAPNQAHL	mouse	EFSKMARDPQRYLVIQGD [•] ERMHLPSPT	
pig	ELVEPLTPSGEAPNQALL	pig	EFSKMARDPQRYLVIQGD [•] ERMHLPSPT	
chicken	ELVEPLTPSGEAPNQAHL	chicken	EFSKMARDPPRYLVIQGD [•] ERMHLPSPT	
zebra	ELVEPLTPSGEAPNQALL	zebra	EFTKMARDPSRYLVIQGD [•] DRMHLPSPS	
drosophila	EDSEPLRPSNIGANLCKL	drosophila	VFAEFARDPGRYLAI [•] PGDK [•] FTRLPAYT	

Figure 3.10. Sequence alignment of the region surrounding EGF receptor Thr-669 and the acidic amino acids Asp-950, Asp-960, and Glu-961. The top panels show the sequence alignment of the human EGF receptor family members (EGFR, ErbB2, ErbB3, ErbB4), while the bottom panel shows the sequence alignment of the EGF receptor in various species. The left panels show the residues surrounding Thr-669, while the right panels show the residues surrounding Asp-950 and Asp-960/Glu-961 on the EGF receptor. Highlighted in pink are residues that are conserved among family members/species. Turquoise shows residues that are not conserved compared to the other family members/species, while blue shows residues that are not conserved, but carry the same charge compared to other family members/species.

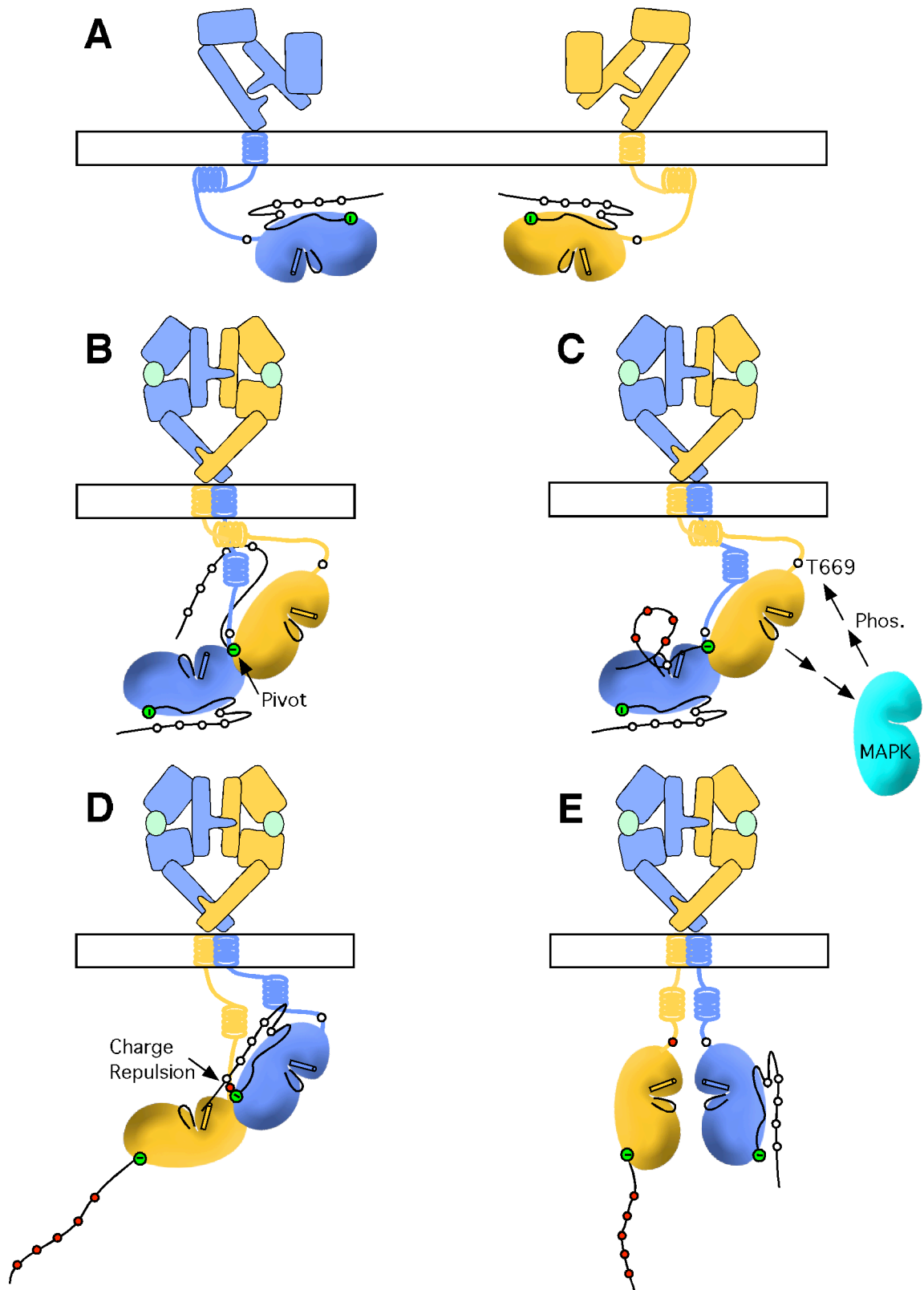


Figure 3.11. Model for the mechanism of MAP kinase-mediated EGF receptor desensitization. A) Conformation of the EGF receptor in the absence of ligand with the extracellular domain held in the tethered conformation. B) Ligand binding induces a dramatic extracellular domain conformational change, facilitating EGF receptor dimerization, and bringing into proximity the kinase domains to form the activating asymmetric dimer (yellow = donor kinase, blue = acceptor kinase). Formation of the juxtamembrane domain cradle by the blue/acceptor kinase may displace the C-terminal tail of the yellow/donor kinase so that it can be phosphorylated. C) Phosphorylation of the C-terminal tail of the yellow/donor kinase provides a scaffold for activation of downstream signaling pathways, particularly the MAP kinase pathway. MAP kinase is engaged in a feedback loop with the EGF receptor through phosphorylation on Thr-669. D) Following phosphorylation of the donor/yellow kinase C-terminal tail, the kinase domains may attempt to switch roles so the donor becomes the acceptor and vice versa. When the yellow kinase tries to engage the acceptor kinase role, the phosphorylated Thr-669 interacts unfavorably with negatively charged residues (Asp-960 and/or Glu-961), resulting in a charge repulsion. E) Because of the charge repulsion, the yellow kinase could not adopt the acceptor role and therefore could not become activated via the allosteric asymmetric dimer mechanism.

CHAPTER 4. Examining the Differential Effects of the EGF Family of Growth Factors using the Luciferase Fragment Complementation Imaging Assay

Introduction

Signaling from the EGF receptor family members is first initiated by binding of the EGF-like family of growth factor ligands. There are 11 known ligands that bind to the EGF receptor family. These ligands are synthesized as transmembrane precursors that can mediate either juxtacrine effects and/or both autocrine and paracrine effects upon ectodomain shedding (47, 138, 139). The soluble growth factors subsequently bind to and initiate the formation of both homo- and hetero-dimeric receptor complexes as depicted in Figure 4.1 (47, 140).

The number of possible ligand and receptor combinations suggests a layer of complexity in the initialization of the signaling network (48, 66, 140). It was originally thought that different ligands induce different combinations of ErbB receptor dimerization. However, the discoveries that EGF receptor or ErbB4 homodimers can initiate different cellular responses upon binding to different ligands (141, 142) suggested that signal diversification is not achieved simply by ligand-induced dimer combination, but rather additionally regulated by subtle differences in the transmission of signals from ligands to receptor activation.

In addition to EGF, the ligand amphiregulin (AR) is specific for the EGF receptor and can induce tyrosine phosphorylation of the receptor (143, 144). AR was first discovered in 1988 in the media of MCF7 breast cancer cells treated with 12-O-tetradecanoylphorbol 13-acetate (143). Shoyab et al. termed the new growth factor “amphi”-regulin because of its ability to be stimulating in some cells, while inhibitory in

others. However, these inhibitory properties of AR have not yet been validated. Amphiregulin exhibits significantly lower affinity for the EGF receptor compared to EGF— AR can only compete 50-75% of the ^{125}I -EGF (143). Studies have indicated that the decreased affinity of AR may be due to the absence of a critical Leu residue in the C-terminal region of the growth factor that is important for high affinity binding in both EGF and TGF- α (145).

Both EGF and AR are specific for the EGF receptor, while the growth factor betacellulin (BTC) and neuregulin2 β are considered as pan-ErbB ligands because they can induce all combinations of receptors through binding to either the EGF receptor or ErbB4 (146). Unlike AR, BTC has comparable ability to compete for ^{125}I -EGF binding as EGF itself ($\text{IC}_{50} \sim 1.4 \text{ nM}$ for BTC versus $\sim 1.9 \text{ nM}$ for EGF) (50). The observations that these distinct ligands are able to induce different tyrosine phosphorylation patterns on either the EGF receptor or ErbB4 (141, 142) suggests a plausible mechanism for the initiation of distinct signaling pathways which ultimately lead to distinct cellular outcomes.

Clearly the ligands for the EGF receptor, while structurally similar, are able to mediate a distinct and complex set of signaling outputs. However, there have been few studies capturing the differences in their abilities to induce homo- and heterodimerization due to lack of an appropriate assay. This Chapter examines the dimerization potential of these EGF-like ligands and the consequential impact on the intracellular domain conformational changes in the full length EGF receptor. By utilizing the luciferase imaging assay, we focus on comparing the hierarchy of these ligands by

measuring both the magnitudes and rates of extracellular-mediated dimer formation and the intracellular domain conformational changes.

Results

Identification of the saturation point in luciferase activity following stimulation with EGF, BTC, or AR in Δ C-EGF receptor cells

In order to compare the dimerization potential of ligands, we first determined the concentration at which each ligand is saturating to dimerization by measuring the luciferase activity dose-response to EGF, BTC, or AR in cells stably expressing the intracellular-domain-lacking EGF receptor (Δ C-EGFR-NLuc/CLuc cell line). As with data presented in Chapter 2 (Figure 2.1), a baseline level of luciferase activity was observed in these cells in the absence of ligands (Figure 4.2A, C, E) consistent with the notion of pre-formed dimers (42, 114, 115).

When increasing concentrations of EGF were added to Δ C-EGFR-NLuc/CLuc cells, a rapid increase in luciferase activity was observed (Figure 4.2B). Luciferase activity reached a plateau 10-15 min after addition of 10 or 25 nM EGF, while no plateau was observed during the observation period after addition of lower concentrations of EGF (<2 nM). Qualitatively 10 nM EGF appears to be sufficient to induce maximal luciferase activity (Figure 4.2B). This is confirmed by comparing the Y_{\max} values for a one-phase exponential association curve fit to these data with GraphPad Prism (p-value > 0.05, Table 4.1).

Similarly, when Δ C-EGFR-NLuc/CLuc cells were stimulated with increasing concentrations of BTC, a rapid increase in luciferase activity was observed (Figure 4.2D). In this experiment, luciferase activity appeared to reach a plateau 15-20 min after

addition of 25 nM BTC, with no plateau observed during this time in cells treated with less than 2 nM BTC. Again, the one-phase exponential association curve fit to the 10 and 25 nM BTC data indicated that the Y_{\max} values were not significantly different for these two concentrations of ligand (p -value > 0.05 , Table 4.1), suggesting that these concentrations of ligand represent a saturation point in luciferase activity.

Δ C-EGFR-NLuc/CLuc cells treated with increasing concentrations of AR also exhibited a rapid increase in luciferase activity (Figure 4.2E). Because of the decreased affinity of the EGF receptor for AR, higher concentrations of ligand were used to observe the changes in luciferase activity (143). Addition of high concentrations of AR (100 and 250 nM) led to a rapid plateau in luciferase activity (5-10 min). However, in stark contrast to the results obtained with EGF and BTC, addition of increasing concentrations of AR resulted in an initial increase in luciferase activity, followed by a decrease. This unexpected result made it impossible to determine the saturating concentration of AR since it is unclear where, if any, saturation point exists.

From these dose-response data on Δ C-EGFR-NLuc/CLuc cells treated with EGF, BTC, or AR, a dose-response curve was generated by plotting the concentration of ligand versus the change in photon flux after 20 min of imaging (Figure 4.3). An estimate of the EC_{50} values for EGF and BTC was obtained by fitting the data to a sigmoidal dose-response curve using GraphPad Prism, yielding an EC_{50} of 1.8 nM and 0.8 nM for EGF and BTC, respectively (Figure 4.3A and B). The unique dose-response of Δ C-EGFR-NLuc/CLuc cells to AR exhibited a bell-shaped dose-response curve (Figure 4.3C). It is difficult to obtain EC_{50} values from a bell-shaped dose-response curve without a large

number of data points, so no values were obtained for AR. However, qualitatively the peak in luciferase activity occurs near 25 nM AR.

Ability of EGF, BTC, and AR to saturate Δ C-EGF receptor/ Δ C-ErbB2 hetero-dimerization

The effect of EGF, BTC, and AR was also examined in cells expressing the EGF receptor and ErbB2, both lacking the intracellular domains. Similar to the EGFR, ErbB2 consists of an extracellular domain with four subdomains, a single-pass α -helical region, and an intracellular domain (147). Unlike the EGFR, ErbB2 has no known high-affinity ligand and thus cannot undergo a ligand-induced conformational change. Instead, ErbB2 is thought to constitutively adopt an open/extended receptor conformation that is capable of undergoing dimerization (148-150). Heterodimers of EGFR and ErbB2 have been reported to exhibit more potent signaling than EGFR/EGFR homodimers and as a result are implicated in cancer progression (57, 66, 140, 151). It is therefore interesting to examine the hetero-dimerization induced by different EGF-like ligands, particularly because EGF receptor homodimers are capable of binding two ligands, while EGF receptor-ErbB2 hetero-dimers will have only one ligand bound in the dimer.

Because the luciferase fragment complementation imaging system utilizes two fragments of luciferase, we first wanted to determine if luciferase activity depended on which fragments were fused to the EGF receptor or ErbB2. The NLuc fragment was fused to either the EGF receptor or ErbB2 to produce Δ C-EGFR-NLuc or Δ C-ErbB2-NLuc. Similar constructs were made using the CLuc fragment. The following combinations of NLuc and CLuc fusion proteins were transiently transfected into CHO cells: Δ C-EGFR-NLuc/ Δ C-EGFR-CLuc, Δ C-ErbB2-NLuc/ Δ C-EGFR-CLuc, Δ C-EGFR-

NLuc/ Δ C-ErbB2-CLuc, and Δ C-ErbB2-NLuc/ Δ C-ErbB2-CLuc. The luciferase activity in the absence and presence of EGF was determined for each of these combinations and is shown in Figure 4.4.

For comparison, CHO cells were transiently transfected with the cDNA for Δ C-EGFR-NLuc and Δ C-EGFR-CLuc. Figure 4.4A shows the baseline photon flux in these cells. Similar to the results obtained in the cell line stably expressing Δ C-EGFR-NLuc/CLuc (Figure 4.2), this basal photon flux was not zero. Addition of EGF led to a rapid increase in luciferase activity that plateaued 10-15 min after stimulation (Figure 4.4B), comparable to earlier results (Figure 4.2 and Chapter 2, Figure 2.1).

When cells were transiently transfected with the Δ C-ErbB2-NLuc/ Δ C-EGFR-CLuc constructs, a basal luciferase activity was again observed (Figure 4.4C). This basal activity was somewhat higher than that observed in cells expressing just the Δ C-EGF receptor luciferase constructs, which may simply represent a difference in expression level of these constructs. EGF treatment led to a rapid increase in luciferase activity, with a plateau 10-15 min after addition of ligand (Figure 4.4D). While the maximum change in luciferase activity appears greater in the Δ C-ErbB2-NLuc/ Δ C-EGFR-CLuc cells compared to the Δ C-EGFR-NLuc/CLuc cells, the difference may again be due to variation in receptor expression levels.

Cells expressing the Δ C-EGFR-NLuc/ Δ C-ErbB2-CLuc constructs also displayed a baseline luciferase activity (Figure 4.4E). This baseline level was lower than that observed in the Δ C-ErbB2-NLuc/ Δ C-EGFR-CLuc constructs (Figure 4.4C), which may indicate a difference in expression level of the NLuc and CLuc constructs. Because the difference in baseline photon flux could affect interpretation of the ligand-induced

changes in photon flux, the baseline $\Delta\text{C-EGFR-NLuc}/\Delta\text{C-ErbB2-CLuc}$ photon flux was corrected to match that of cells expressing the $\Delta\text{C-ErbB2-NLuc}/\Delta\text{C-EGFR-CLuc}$ constructs. Stimulation with EGF again led to a rapid increase in luciferase activity (Figure 4.4F). Luciferase activity plateaued 10-15 min after addition of ligand. When the data was fit to a one-phase exponential association curve and compared to the $\Delta\text{C-ErbB2-NLuc}/\Delta\text{C-EGFR-CLuc}$ cells analyzed the same way, a small but statistically significant change in the Y_{max} was observed ($9.62 \pm 0.07 \times 10^5$ p/s vs $1.12 \pm 0.01 \times 10^6$ p/s, respectively). This may reflect a difference in the ability of the NLuc and CLuc fragments to complement when fused to the EGF receptor versus ErbB2. However, additional experiments using equal expression levels of all the EGF receptor and ErbB2 fusion proteins are necessary to properly assess the potential differences.

The $\Delta\text{C-ErbB2-NLuc}$ and $\Delta\text{C-ErbB2-CLuc}$ fusion proteins were expressed in cells in the absence of any EGF receptor. These cells also exhibited a baseline photon flux (Figure 4.4G). This is consistent with other reports that ErbB2 can homodimerize in the absence of ligand (152, 153). However, in contrast to both the homo- and hetero-dimerization examined here, the $\Delta\text{C-ErbB2-NLuc}/\text{CLuc}$ cells did not display any ligand-induced increase in luciferase activity when treated with EGF (Figure 4.4H). This result is entirely consistent with an inability of EGF to bind to ErbB2 and elicit any changes in dimerization (148-150).

To examine changes in hetero-dimerization mediated by EGF, BTC, or AR, a stable cell line was established that expressed $\Delta\text{C-EGFR-NLuc}$ and $\Delta\text{C-ErbB2-CLuc}$. Similar to the experiments done in the cell line expressing $\Delta\text{C-EGFR-NLuc}/\text{CLuc}$, the concentration of EGF, BTC, or AR needed to saturate luciferase activity was first

examined (Figure 4.5). Luciferase activity was detectable in the absence of ligand stimulation as previously demonstrated (Figure 4.5A, C, and E). Addition of increasing concentrations of EGF resulted in a dose-dependent increase in luciferase activity in the Δ C-EGFR-NLuc/ Δ C-ErbB2-CLuc cell line (Figure 4.5B). Luciferase activity increased with increasing concentration of ligand until ~3-10 nM EGF. This was confirmed by comparing the Y_{\max} from a one-phase exponential association curve fit at 10 and 25 nM EGF, yielding no significant difference in these values (Table 4.1, p-value >0.05).

The increase in luciferase activity following stimulation with BTC was also evaluated in cells expressing Δ C-EGFR-NLuc/ Δ C-ErbB2-CLuc. Saturation of luciferase activity occurred near 10 nM BTC, similar to cells expressing Δ C-EGFR-NLuc/CLuc (Figure 4.5D). Again, curve-fitting to a one-phase exponential association equation confirmed no detectable change in Y_{\max} upon addition of increasing concentrations of BTC (Table 4.1, p-value > 0.05).

When Δ C-EGFR-NLuc/ Δ C-ErbB2-CLuc cells were stimulated with AR, a different dose-dependent increase in luciferase activity was observed compared to the Δ C-EGFR-NLuc/CLuc cells (Figure 4.5F). In these cells addition of high ligand concentrations did not induce the same dramatic decrease in luciferase activity observed in the Δ C-EGFR-NLuc/CLuc cells. However, there were small differences in the maximum change in luciferase activity observed with the concentrations of AR above 1 nM, making assessment of the luciferase activity saturation point difficult.

Dose-response curves were generated for Δ C-EGFR-NLuc/ Δ C-ErbB2-CLuc cells stimulated with EGF and BTC (Figure 4.6). The data were fit to a sigmoidal dose-response curve to determine the EC_{50} after 20 min of stimulation with ligand. The EC_{50}

for EGF and BTC were very similar (0.7 nM and 1nM, respectively, Table 4.1), indicating these ligands elicited similar changes in luciferase activity in cells expressing EGF receptor/ErbB2 heterodimers. Similar to cells expressing only the EGF receptor, no EC_{50} was determined for ΔC -EGFR-NLuc/ ΔC -ErbB2-CLuc cells stimulated with AR. While a bell-shaped dose-response curve was not obtained in these cells, there were decreases in luciferase activity with mid-range concentrations of AR (~50 nM). Additional concentrations of AR will need to be examined before a well-defined dose-response curve can be generated.

Ability of EGF, BTC, and AR to induce homo- and hetero-dimerization

Based on the Y_{max} and EC_{50} values for the ΔC -EGFR-NLuc/CLuc and ΔC -EGFR-NLuc/ ΔC -ErbB2-CLuc cells, 10 and 25 nM were the saturating concentrations of ligand used in experiments to determine the ability of EGF, BTC, and AR to induce dimer formation. Consistent with other results, both the ΔC -EGFR-NLuc/CLuc and the ΔC -EGFR-NLuc/ ΔC -ErbB2-CLuc cell lines exhibited a non-zero baseline luciferase activity (Figure 4.7A and D). ΔC -EGFR-NLuc/CLuc and ΔC -EGFR-NLuc/ ΔC -ErbB2-CLuc cells were first stimulated with 10 nM EGF or BTC and the change in photon flux was assessed (Figure 4.7B and E). EGF stimulation yielded a greater change in photon flux than BTC in both ΔC -EGFR-NLuc/CLuc and ΔC -EGFR-NLuc/ ΔC -ErbB2-CLuc cells (compare Y_{max} in Table 4.2). The rate of change in luciferase activity was also lower in EGF-treated cells (Table 4.2). These differences were slightly smaller in the ΔC -EGFR-NLuc/ ΔC -ErbB2-CLuc cell line.

Luciferase activity in ΔC -EGFR-NLuc/CLuc and the ΔC -EGFR-NLuc/ ΔC -ErbB2-CLuc cells stimulated with 25 nM EGF, BTC, or AR was also examined (Figure

4.7C and F). Consistent with the 10 nM dose of EGF and BTC, EGF was able to induce the largest change in luciferase activity in both cell lines (Y_{\max} values, Table 4.2). AR was the least effective ligand in inducing an increase in luciferase activity in both cell lines (Table 4.2). The rate of change in luciferase activity was greatest in AR-treated cells (Table 4.2).

BTC enhances the recovery in luciferase activity in the full-length EGF receptor

In Chapter 2, luciferase fragment complementation imaging of the full-length EGF receptor revealed a series of ligand-induced conformational changes in the intracellular domain. The ability of EGF and BTC to induce these conformational changes was examined in CHO cells expressing the full-length EGFR-NLuc and EGFR-CLuc constructs (Figure 4.8). As expected, no difference in the basal photon flux was observed in these cells prior to ligand stimulation (Figure 4.8A). Increasing concentrations of EGF or BTC were added to cells and the change in photon flux over time was observed (Figure 4.8B-F). EGF was able to induce a decrease and recovery in luciferase complementation similar to what was previously observed (Chapter 2, Figure 2.3). At low concentrations of ligand (0.1 and 1 nM) little change in photon flux was observed (Figure 4.8B and C). Addition of higher concentrations of EGF or BTC resulted in both a decrease and recovery in luciferase activity (Figure 4.8D-F). The decrease in luciferase activity was essentially indistinguishable in cells treated with EGF or BTC. However, the magnitude of the recovery in luciferase activity was higher in cells treated with BTC, reflecting differences in the ability of these ligands to induce EGF receptor intracellular domain conformational changes.

Discussion

Luciferase fragment complementation imaging enabled characterization of ligand-induced conformational changes in both the extracellular and intracellular domains of the EGF receptor in response to different ligands of the EGF-like family. These ligands were able to induce dimerization to differing extents in the context of both homo- and hetero-dimerization of the EGF receptor extracellular domains.

Initially, dose-response curves were generated for cells expressing the luciferase fragments fused to either the EGF receptor alone or both the EGF receptor and ErbB2 truncated just beyond the transmembrane domain (Δ C-EGF receptor and Δ C-ErbB2). The EC_{50} for EGF and BTC were similar in both EGF receptor homo-dimerization and EGF receptor/ErbB2 hetero-dimerization. These values are similar to the IC_{50} values in experiments where these ligands competed with 125 I-EGF binding (50). This indicates that these receptors have similar responses to ligand in terms of both binding and dimerization. Unfortunately, without carefully matched receptor levels, the ability of EGF and BTC to induce homo- versus hetero-dimerization cannot be directly compared. Additional studies in which known amounts of receptors are expressed will be required to quantitatively compare the ability of these ligands to induce homo- and hetero-dimerization.

AR exhibited a unique bell-shaped dose-response curve in Δ C-EGF receptor cells. These data suggest that in the same cell, AR can function both as an agonist and antagonist to EGF receptor dimer formation. AR has previously been reported to be both stimulatory and inhibitory, but these functions were ascribed to its effect on different cell lines (143). Our findings that AR can be both stimulatory and inhibitory in the same cell

line suggest a possible unique self-regulatory role for this ligand. It is interesting to note that such a phenomenon has not been reported for AR-stimulated phosphorylation of the EGF receptor, indicating that this dose-response curve is unique to EGF receptor dimerization. The bell-shaped dose-response curve that is observed may indicate differential modes of binding to the EGF receptor, perhaps through additional binding sites other than the traditional subdomain I and III sites. Alternatively, additional ligand may bind between subdomains I and III making the binding site more open than normal and likely affecting subdomain II/dimerization arm interactions. This would then manifest as a decrease in dimerization upon addition of higher concentrations of ligand. It will be interesting to see if other EGF-like ligands exhibit similar bell-shaped dose-response curves.

The data presented here demonstrate that EGF, BTC, and AR exhibit a hierarchy in their ability to stimulate dimer formation, as measured by the maximum change in photon flux. In the context of both homo- and hetero-dimerization the order is EGF > BTC > AR in stimulating dimer formation. BTC may be slightly more effective in inducing dimer formation in cells expressing Δ C-EGF receptor and Δ C-ErbB2. In these cells, the percentage change in luciferase activity compared to EGF was ~30%, while there was a nearly 50% change in luciferase activity in cells expressing only the EGF receptor. These results are similar to a study by Wehrman et al. using a β -galactosidase enzyme complementation assay with a truncated EGF receptor and ErbB2 (152). In these studies BTC stimulated a lower level of dimer formation compared to EGF. Conversely, AR may be better at inducing dimer formation in cells expressing only the EGF receptor,

since the percentage change compared to EGF was ~55% in these cells compared to ~70% in cells expressing the Δ C-EGF receptor and Δ C-ErbB2.

In contrast to the ligand ranking for inducing EGF receptor dimerization, this hierarchy is switched when comparing the rate of ligand-induced dimerization. AR induces a faster rate of dimerization compared to BTC and EGF in cells expressing just the Δ C-EGF receptor or in combination with Δ C-ErbB2. This order for the rate of ligand-induced dimerization is consistent with the notion that AR induces a smaller number of homo- or hetero-dimers.

These data using the Δ C-EGF receptor and Δ C-ErbB2 indicate that there is a clear difference in the ability of a particular ligand to induce homo- or hetero-dimerization. Future studies correlating this with changes in the phosphorylation of specific tyrosine residues on the EGF receptor will be required to determine the ability of these ligands to initiate a particular signaling pathway. Previous studies indicate that AR may not stimulate the phosphorylation of the EGF receptor on Y1045 as well as EGF, possibly linking this ligand to reduced downregulation of the EGF receptor (154). It has been previously proposed that the differential phosphorylation patterns stimulated by a particular ligand may reflect subtle differences in the extracellular and intracellular domain interface upon binding of different ligands (Figure 4.9) (47, 138). Such subtle differences in the dimerization arm have been observed in crystal structures of the EGF receptor extracellular domain bound to EGF or TGF- α (32, 33). The data presented here are consistent with such a model in which ligand-induced dimerization is altered first on the extracellular domain interface. In addition to different EGF-like ligands initiating differences in the dimerization interfaces, the ligands may also selectively induce

formation of dimers or higher-order oligomers (138). This could conceivably alter the ability of the luciferase complementation assay to report on ligand-induced dimerization and could indicate the predominance of higher-order oligomers on stimulation with ligands other than EGF.

Conformational changes in the intracellular domain of the EGF receptor were also analyzed following addition of either EGF or BTC using the luciferase assay. The decrease in luciferase activity was very similar in cells treated with either EGF or BTC. However, cells treated with BTC displayed a clear enhancement in the magnitude of the recovery of luciferase activity. In Chapters 2 and 3 this recovery was shown to be dependent on MAP kinase activity (Figures 2.12, 2.13, and 3.8). Loss of MAP kinase activity completely ablated the recovery in luciferase activity. BTC has been reported to stimulate enhanced MAP kinase phosphorylation in cells compared EGF (142). This enhanced phosphorylation was mediated by enhanced phosphorylation of the EGF receptor on Y1068 and ultimately resulted in an inhibition of apoptosis in cells stimulated with BTC. The finding that BTC enhances MAP kinase phosphorylation is entirely consistent with the data presented here in which an enhanced recovery was observed compared to cells treated with EGF. It will be interesting to determine if BTC also enhances phosphorylation of the EGF receptor on Thr-669 and causes increased desensitization of the tyrosine kinase activity of the EGF receptor.

The results described in this chapter show that EGF-like ligands exhibit differences in the ability to induce EGF receptor homo- and hetero-dimerization and in the ability to induce intracellular domain conformational changes. This assay could be used in future studies to further examine the dimerization potential of additional EGF-like

ligands, as well as the ability of other ligands to affect changes in the EGF receptor intracellular domain, particularly through modulation of the MAP kinase pathway.

Experimental Procedures

Reagents—Murine EGF (Biomedical Technologies, Inc.), murine amphiregulin (Leinco Technologies, Inc.), and human betacellulin (Sigma) were dissolved in sterile water. Doxycycline was purchased from Clontech and was dissolved in sterile water. D-luciferin was from BioSynth and was dissolved in PBS. Coelenterazine was from Sigma and was dissolved in ethanol.

DNA constructs—The Δ C-EGFR-NLuc and Δ C-EGFR-CLuc and full-length EGFR-NLuc and EGFR-CLuc constructs were described previously in Chapter 2 (128). Δ C-ErbB2-CLuc (pcDNA6/V5-His B, Invitrogen) was made by inserting a BsiWI site just beyond the transmembrane domain in the ErbB2 pcDNA3.1 (+) construct (kind gift from Dr. G. Carpenter, Vanderbilt University) using QuikChange site-directed mutagenesis. The mutant was digested with the NheI and BsiWI restriction enzymes and was ligated into the Δ C-EGFR-CLuc (pcDNA6/V5-His B) construct digested with the same enzymes. This resulted in the following linker between the transmembrane domain and CLuc fragment: QQKTYASRGGGSSGGG (100, 101). The construct was verified by sequencing.

The Δ C-ErbB2-NLuc (pBI-Tet MCS1, Clontech) construct was generated by digesting the Δ C-ErbB2-CLuc (pcDNA6/V5-His B) construct with NheI and BsiWI. The insert was ligated into the ErbB2-NLuc pBI-Tet construct digested with the same enzymes. The truncation was verified by sequencing.

Cell Lines—CHO-K1 Tet-On cells (Clontech) were stably co-transfected with Δ C-EGFR-NLuc and pTK-Hyg (Clontech) using Lipofectamine 2000 (Invitrogen). Stable clones were isolated by selection in DMEM containing 600 μ g/ml hygromycin (InvivoGen). Double-stable cell lines were established by stably transfecting the Δ C-EGFR-NLuc cells with either Δ C-EGFR-CLuc or Δ C-ErbB2-CLuc. Clones stably expressing Δ C-EGFR-CLuc were selected in DMEM containing 400 μ g/ml Zeocin (Invitrogen). The Δ C-EGFR-NLuc/CLuc cells were grown in DMEM containing 10% FetalPlex, 1000 μ g/ml penicillin/streptomycin, 100 μ g/ml G418, 50 μ g/ml hygromycin, and 100 μ g/ml Zeocin. Clones stably expressing Δ C-ErbB2-CLuc were selected in DMEM containing 10 μ g/ml Blasticidin (InvivoGen). Cells were grown in DMEM with 1000 μ g/ml penicillin/streptomycin, 100 μ g/ml G418, 50 μ g/ml hygromycin, and 2 μ g/ml Blasticidin. For the transient transfection experiments with the Δ C-EGFR-NLuc, Δ C-EGFR-CLuc, Δ C-ErbB2-NLuc, and Δ C-ErbB2-CLuc constructs, cells were transfected 24 hrs prior to imaging using Lipofectamine 2000. Transfection efficiency was assessed by co-transfecting renilla luciferase (pRLuc-N1, Packard Bioscience).

Luciferase complementation imaging—48 hr prior to use cells were plated at 5×10^3 cells per well in DMEM containing doxycycline in a black-walled 96-well plate. On the day of the assay, cells were serum-starved for 2 hr and then incubated for 20 min in 175 μ l DMEM without phenol red, containing 1 mg/ml BSA, 25 mM HEPES, and 0.6 mg/ml D-luciferin at 37°C. To establish a baseline, cell radiance (photons/second/cm²/sr) was measured using a cooled CCD camera and imaging system at 37°C (IVIS 50; Caliper) (30 sec exposure; binning, 8; no filter; f-stop, 1; field of view, 12 cm). EGF was added in a volume of 25 μ l in the same media (DMEM, 1mg/ml BSA, 25mM HEPES,

0.6mg/ml D-Luciferin). Radiance was measured sequentially as described above. For experiments involving transient transfection, the transfection efficiency was assessed by monitoring renilla luciferase expression. Media was replaced on cells with DMEM (no phenol red) containing 1 mg/ml BSA, 25 mM Hepes, and 400 nM coelenterazine. Radiance was immediately measured as described above except the filter was set to <510.

Data Analysis—Data was collected in quadruplicate for each condition. A flat-field correction was done to correct for differences in the baseline photon flux. Light production expressed as photon flux (photons/sec) was determined from regions-of-interest defined over wells using LIVINGIMAGE (Xenogen) and IGOR (Wavemetrics) software. Changes in photon flux were calculated by subtracting values from untreated cells from those of EGF-treated cells. Standard errors were determined using the formula for the unpooled standard error.

Table 4.1. Comparison of the Y_{\max} and EC_{50} values following stimulation with EGF or BTC in cells expressing ΔC -EGFR-NLuc/CLuc or ΔC -EGFR-NLuc/ ΔC -ErbB2-CLuc. The Y_{\max} values were compared using GraphPad Prism and there was no difference between 10 nM and 25 nM for each ligand (p-value > 0.05).

		ΔC -EGFR-NLuc/CLuc		ΔC -EGFR-NLuc/ ΔC -ErbB2-CLuc	
		EGF	BTC	EGF	BTC
Y_{\max} (p/s)	10 nM	$2.50 \pm 0.02 \times 10^6$	$1.45 \pm 0.01 \times 10^6$	$1.39 \pm 0.11 \times 10^5$	$1.07 \pm 0.04 \times 10^5$
	25 nM	$2.54 \pm 0.01 \times 10^6$	$1.47 \pm 0.03 \times 10^6$	$1.50 \pm 0.04 \times 10^5$	$1.00 \pm 0.02 \times 10^5$
	EC_{50}	1.8 nM (95% CI 1.5-2.1 nM)	0.8 nM (95% CI 0.5-1.2 nM)	0.7 nM (95% CI 0.2-2 nM)	1 nM (95% CI 0.3-2.8 nM)

Table 4.2. Comparison of the effects of EGF, BTC, and AR on cells expressing ΔC -EGFR-NLuc/CLuc or ΔC -EGFR-NLuc/ ΔC -ErbB2-CLuc. Curves were fit to a one-phase exponential association curve using GraphPad Prism and the resulting parameters for Y_{\max} , rate (k), and $t_{1/2}$ are reported below.

		ΔC -EGFR-NLuc/CLuc			ΔC -EGFR-NLuc/ ΔC -ErbB2-CLuc		
		EGF	BTC	AR	EGF	BTC	AR
10 nM	Y_{\max} (p/s)	$1.36 \pm$ 0.01×10^6	$7.48 \pm$ 0.06×10^5	ND	$2.04 \pm$ 0.01×10^5	$1.51 \pm$ 0.01×10^5	ND
	Rate (k, min^{-1})	$0.161 \pm$ 0.004	$0.188 \pm$ 0.004	ND	$0.263 \pm$ 0.006	0.29 ± 0.01	ND
	$t_{1/2}$ (min)	4.32	3.69	ND	2.64	2.43	ND
25 nM	Y_{\max} (p/s)	$1.23 \pm$ 0.01×10^6	$7.00 \pm$ 0.04×10^5	$5.50 \pm$ 0.04×10^5	$2.00 \pm$ 0.01×10^5	$1.47 \pm$ 0.01×10^5	$6.62 \pm$ 0.10×10^4
	Rate (k, min^{-1})	$0.259 \pm$ 0.006	$0.316 \pm$ 0.007	$0.334 \pm$ 0.012	$0.360 \pm$ 0.012	$0.444 \pm$ 0.021	$0.636 \pm$ 0.068
	$t_{1/2}$ (min)	2.67	2.19	2.08	1.93	1.56	1.09

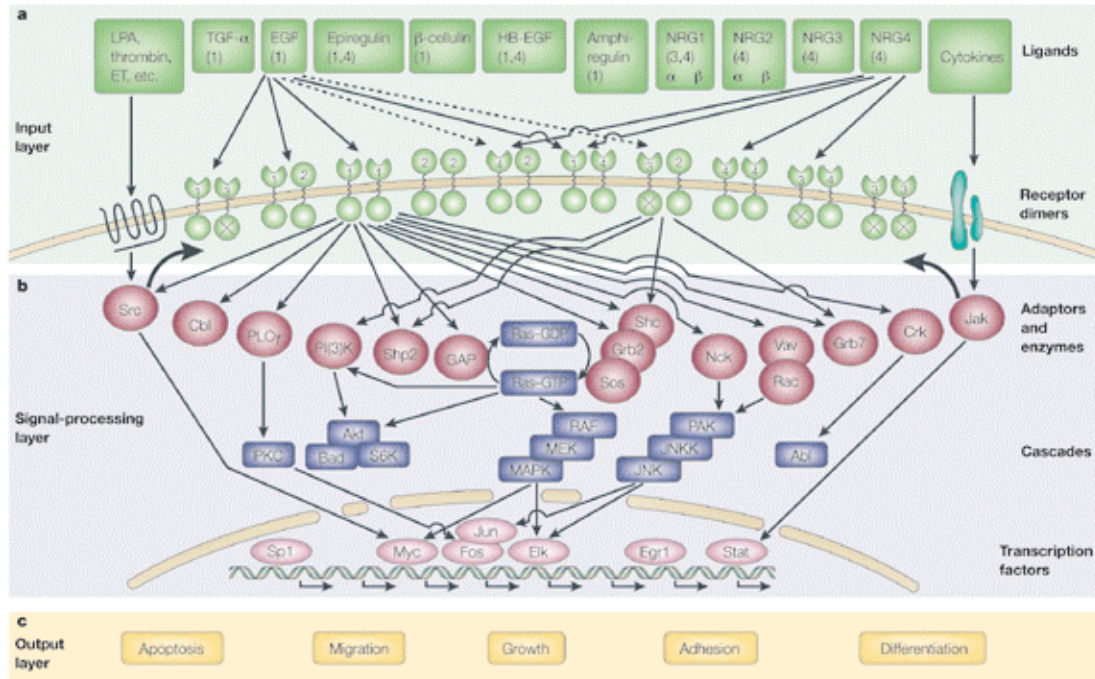


Figure 4.1. Complexity of the EGF receptor family signaling network. Schematic representation of the ligands belonging to the EGF-like growth factor family, as well as the possible combinations of EGF receptor family homo- and hetero-dimerization partners. The complexity of this signaling network is exemplified by the activation of diverse signaling pathways that ultimately lead to diverse biological outcomes (Figure from (140)).

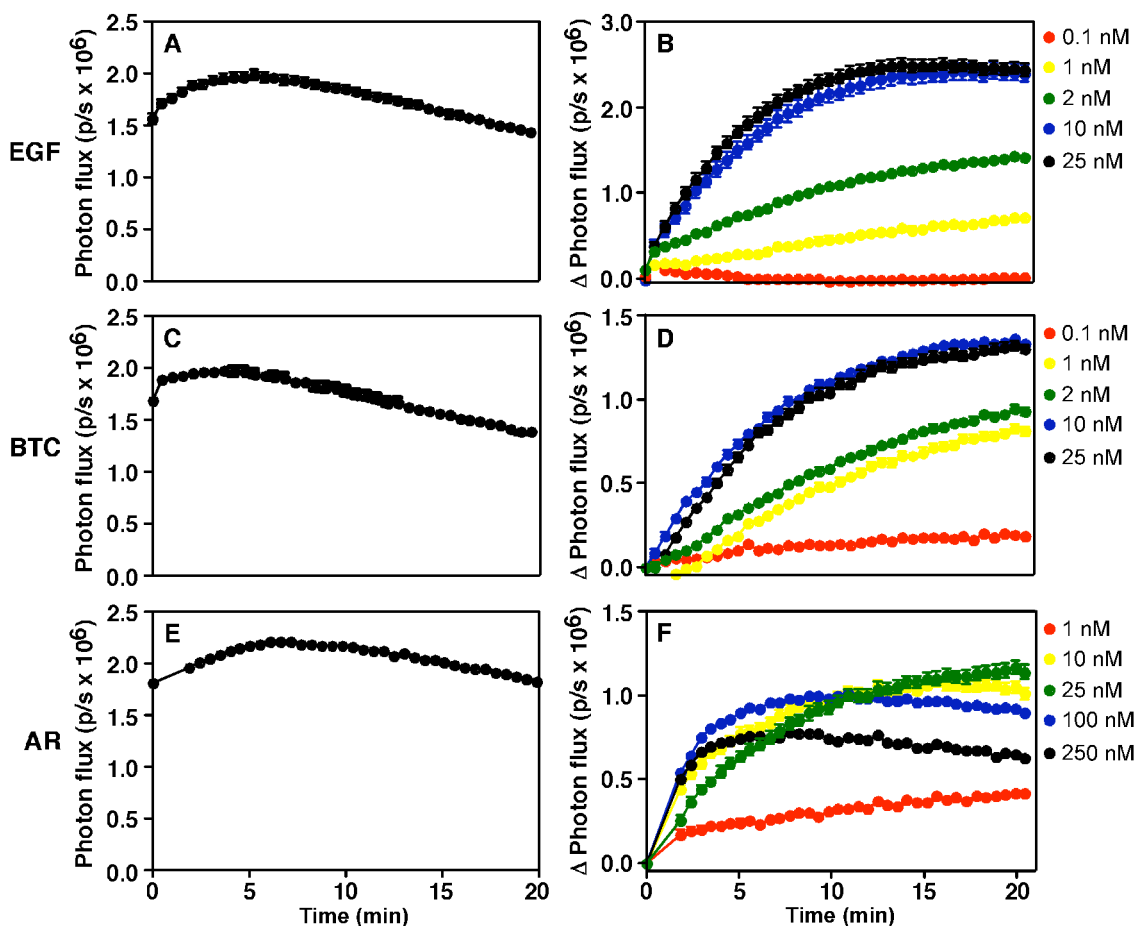


Figure 4.2. Ability of EGF, BTC, and AR to induce an increase in luciferase activity in Δ C-EGF receptor cells. CHO-K1 Tet-On cells stably expressing the Δ C-EGFR-NLuc and Δ C-EGFR-CLuc constructs were plated at 5×10^3 cells/well 48 hrs prior to imaging in 96-well plates containing 1 μ g/ml doxycycline. On the day of imaging, cells were serum-starved for 2 hrs followed by pre-treatment with 0.6 mg/ml D-Luciferin. A, C, E) Photon flux (photons/sec; p/s) in the absence of ligand. B, D, E) Change in photon flux (photons/sec; p/s) following addition of increasing concentrations of EGF, BTC, or AR, respectively. Error bars represent the standard error of data collected in quadruplicate.

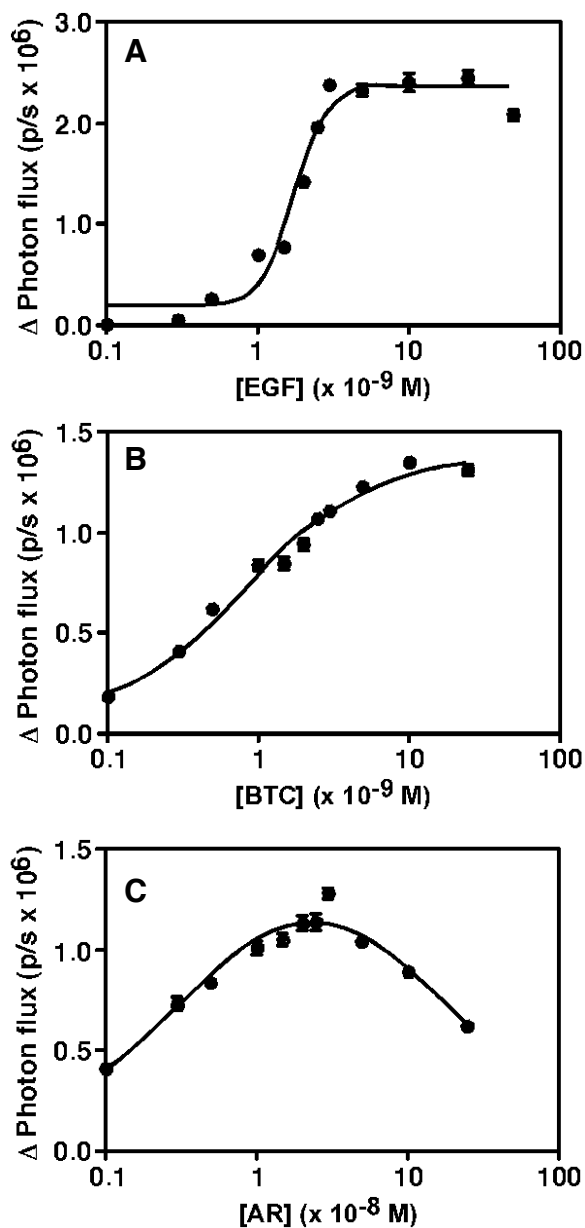


Figure 4.3. Dose-response to EGF, BTC, and AR in Δ C-EGF receptor cells. CHO-K1 Tet-On cells stably expressing Δ EGFR-NLuc and Δ EGFR-CLuc were plated at 5×10^3 cells per well in a 96-well plate 48 hrs prior to imaging in media containing 1 μ g/ml doxycycline. Cells were serum-starved 2 hr prior to imaging. 0.6 mg/ml D-luciferin was added to cells 20 min before imaging. These data represent the change in photon flux (photons/sec; p/s) at the 20 min imaging time point (Figure 4.2) after stimulation with increasing concentrations of EGF (A), BTC (B), or AR (C). The EGF (A) and BTC (B) data were fit to a sigmoidal dose-response curve using the GraphPad Prism software (EC_{50} values reported in Table 4.1). The curve through the AR data points (C) represents the data fit to a gaussian distribution, with no quantitative measurements taken from this curve fit. Error bars represent the standard error of data collected in quadruplicate.

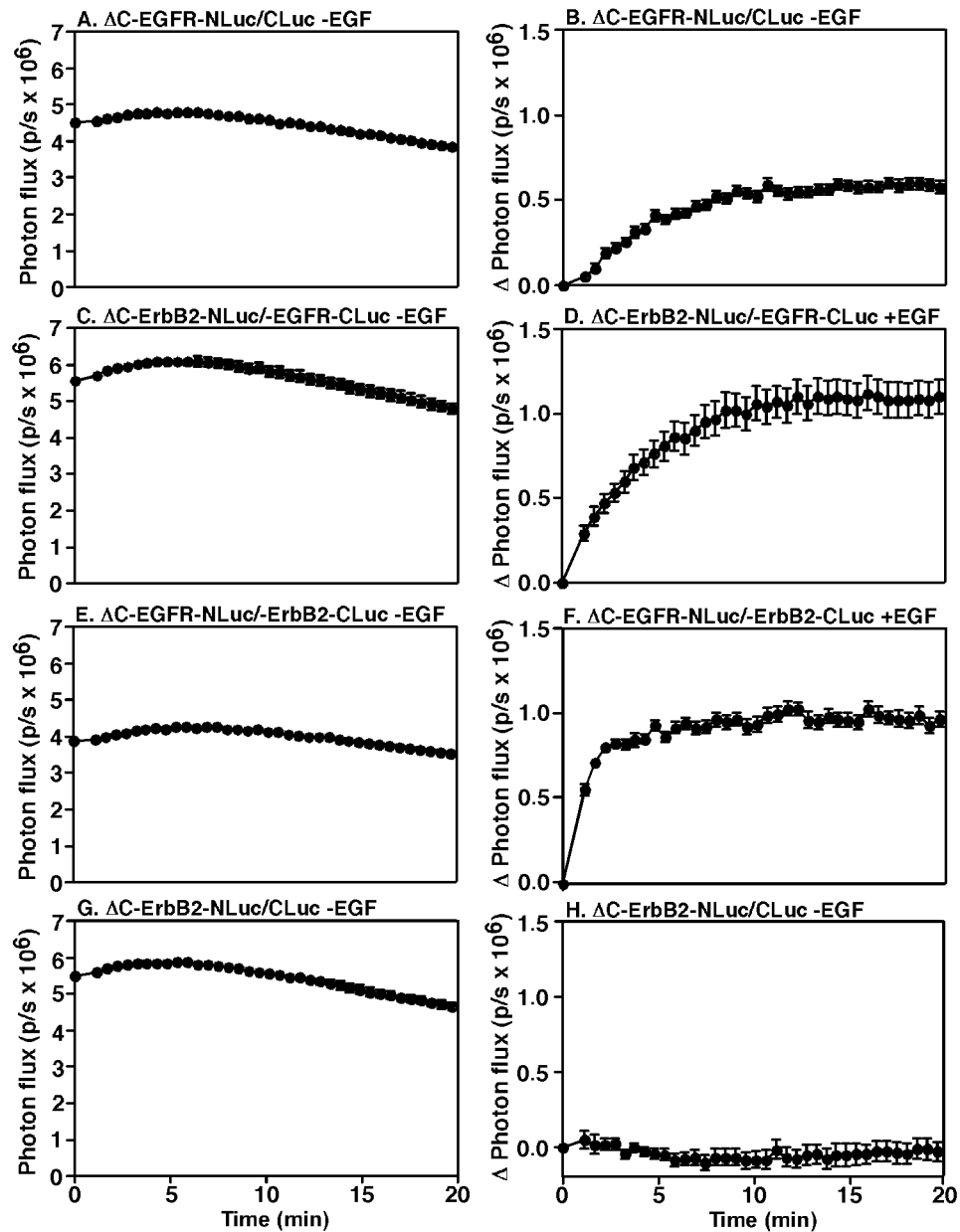


Figure 4.4. Characterization of Δ C-ErbB2-NLuc and Δ C-ErbB2-CLuc constructs. CHO-K1 Tet-On cells were plated at 5×10^3 cells/well in a 96-well plate 48 hrs before imaging in DMEM containing 1 μ g/ml doxycycline. 24 hrs prior to imaging, cells were transiently transfected with the cDNA encoding Δ C-EGFR-NLuc, Δ C-EGFR-CLuc, Δ C-ErbB2-NLuc, and Δ C-ErbB2-CLuc in the specified combinations. On the day of imaging, cells were serum-starved for 2 hrs, followed by a 20 min pre-treatment with 0.6 mg/ml D-Luciferin. A, C, E, G) Basal photon flux (photons/sec; p/s) for the indicated combinations of receptors. B, D, F, H) Change in photon flux (photons/sec; p/s) following addition of 10 nM EGF for the indicated receptor combinations. Error bars represent standard error of quadruplicate samples.

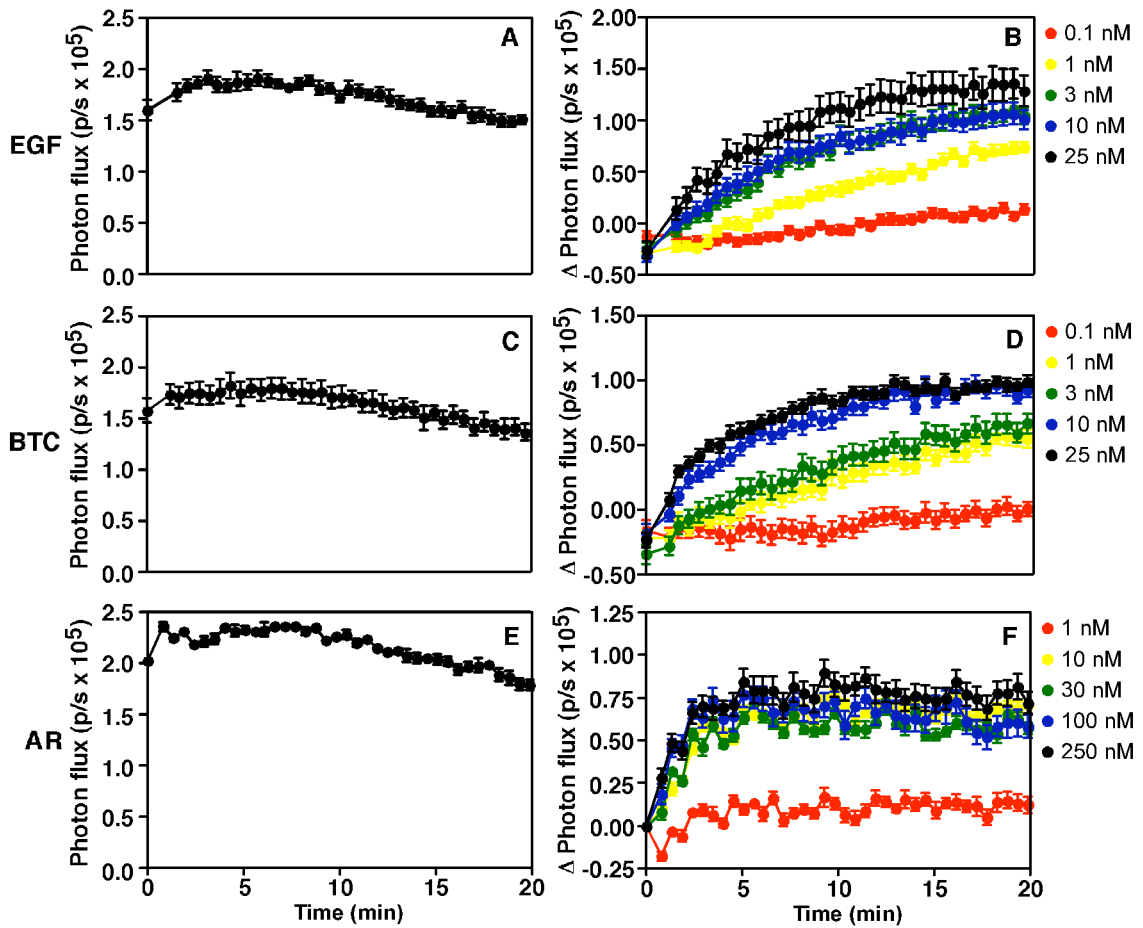


Figure 4.5. Ligand-induced increase in luciferase activity in Δ C-EGF receptor/ Δ C-ErbB2 cells. CHO-K1 Tet-On cells stably transfected with Δ C-EGFR-NLuc/ Δ C-ErbB2-CLuc were plated at 5×10^3 cells/well in DMEM containing 1 μ g/ml doxycycline 48 hrs prior to imaging. On the day of imaging cells were serum-starved 2 hrs and were pre-treated for 20 min with 0.6 mg/ml D-luciferin. A, C, E) Photon flux (photons/sec; p/s) in the absence of ligand. B, D, F) Change in photon flux (photons/sec; p/s) upon addition of increasing concentrations of EGF (B), BTC (D), or AR (F). Error bars represent the standard error of four measurements.

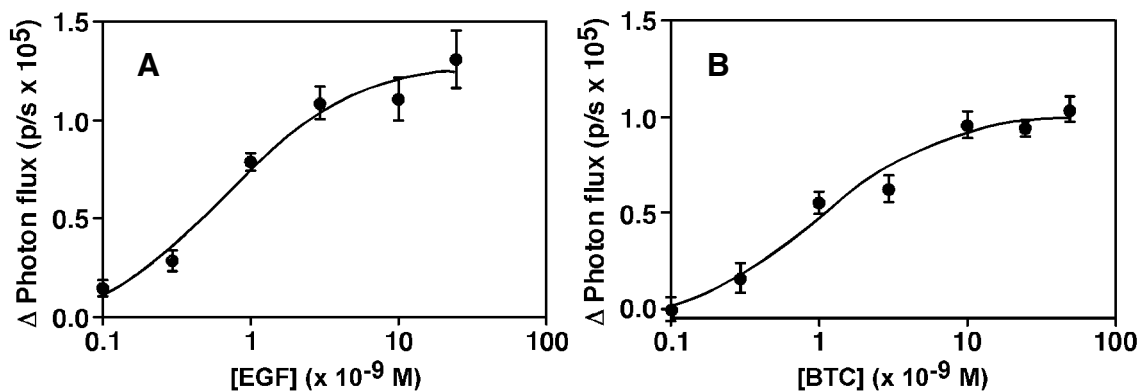


Figure 4.6. Dose-response to EGF and BTC in Δ C-EGF receptor/ Δ C-ErbB2 cells. CHO-K1 Tet-On cells stably expressing Δ C-EGFR-NLuc/ Δ C-ErbB2-CLuc were plated 48 hrs prior to imaging at 5×10^3 cells/well in DMEM containing 1 μ g/ml doxycycline. On the day of imaging, cells were serum-starved for 2 hrs, followed by a 20 min pre-incubation with 0.6 mg/ml D-luciferin. Data presented here (from Figure 4.5) represent the change in photon flux (photons/sec; p/s) at the 20 min imaging point following addition of varying concentrations of EGF (A) or BTC (B). Data were fit to a sigmoidal dose-response curve using GraphPad Prism, with the EC_{50} values listed in Table 4.1. Error bars represent the standard error from quadruplicate measurements.

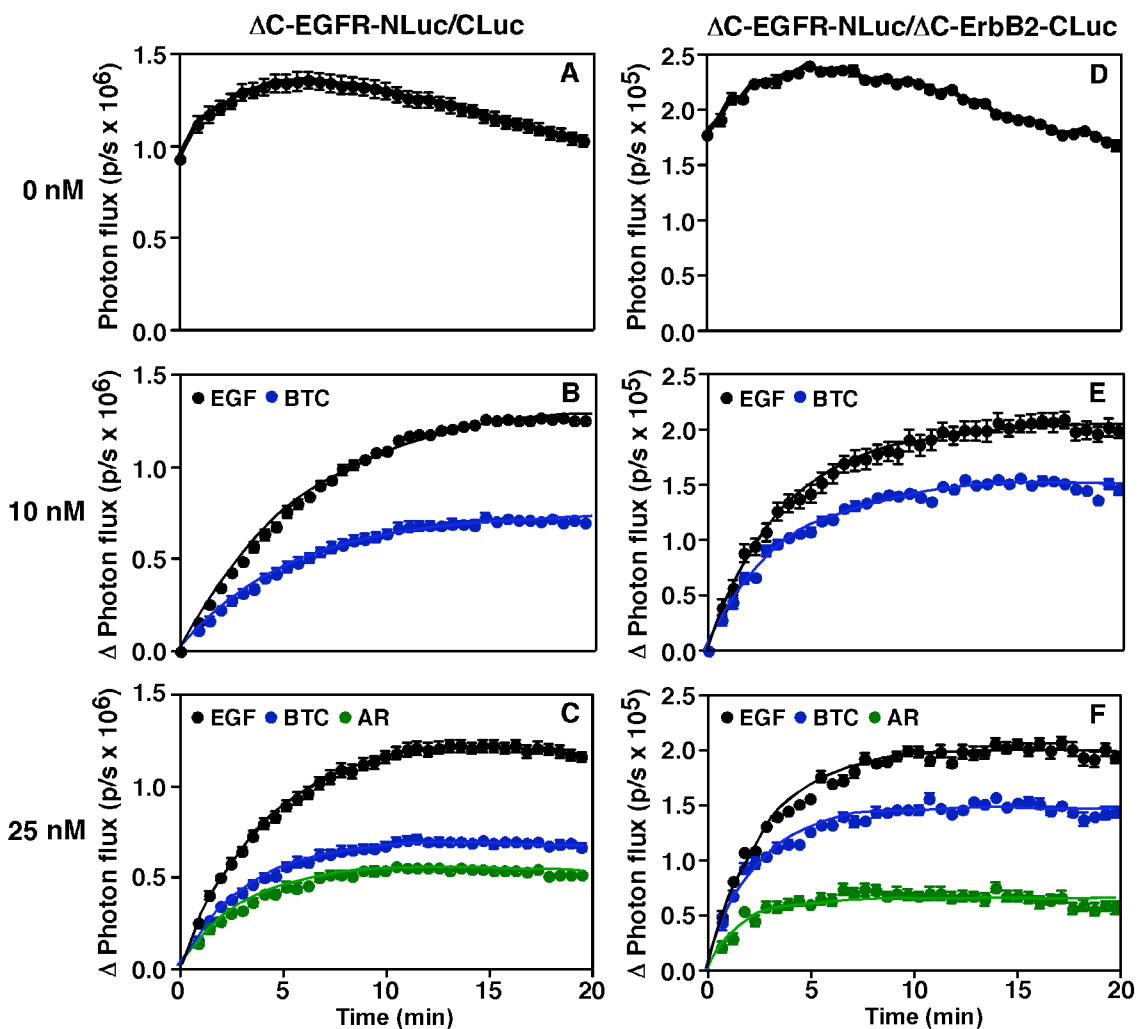


Figure 4.7. Ligand-induced changes in luciferase activity in cells expressing Δ C-EGF receptor alone or in addition to Δ C-ErbB2. CHO-K1 Tet-On cells stably expressing either Δ C-EGFR-NLuc/ Δ C-EGFR-CLuc or Δ C-EGFR-NLuc/ Δ C-ErbB2-CLuc were plated at 5×10^3 cells/well in 96-well plates containing 1 μ g/ml doxycycline 48 hrs prior to imaging. Cells were serum-starved 2 hrs on the day of the assay, followed by a 20 min pre-incubation period with 0.6 mg/ml D-luciferin. A, D) Photon flux (photons/sec; p/s) in the absence of ligand. B, C) Change in photon flux (photons/sec; p/s) in Δ C-EGFR-NLuc/ Δ C-EGFR-CLuc cells following addition of 10 nM EGF or BTC or 25 nM EGF, BTC, or AR. D, F) Change in photon flux (photons/sec; p/s) in Δ C-EGFR-NLuc/ Δ C-ErbB2-CLuc cells after addition of 10 nM EGF or BTC or 25 nM EGF, BTC, or AR. Standard error was determined based on quadruplicate measurements. Ligand-treated data were fit to a one-phase exponential association curve using GraphPad Prism. Results are listed in Table 4.2.

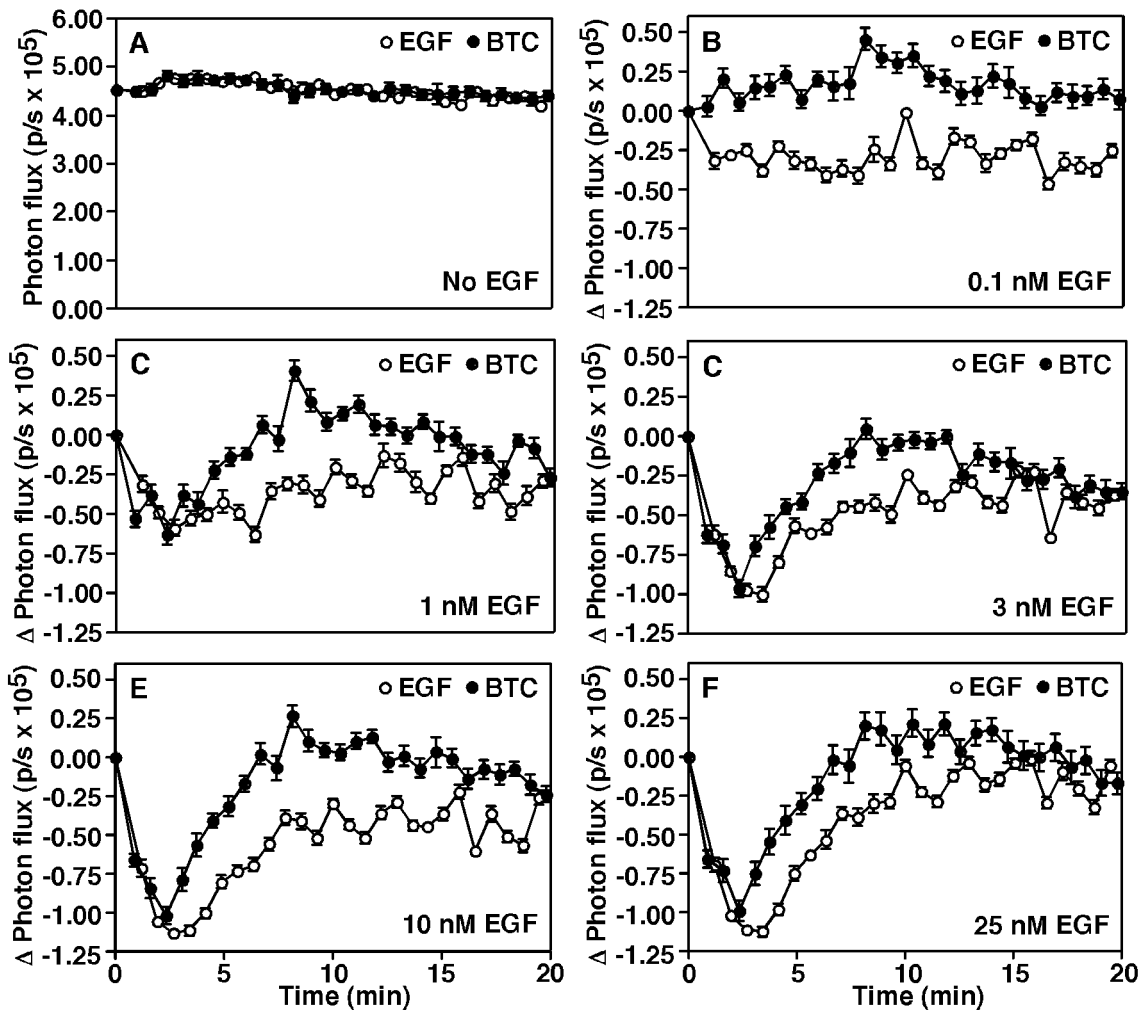


Figure 4.8. Effect of EGF and BTC on the ligand-induced conformational changes in the full-length EGF receptor.

CHO-K1 Tet-On cells stably expressing EGFR-NLuc and EGFR-CLuc were plated at 5×10^3 cells/well in a 96-well plate 48 hrs prior to imaging in DMEM containing $1 \mu\text{g/ml}$ doxycycline. 2 hrs prior to imaging cells were serum-starved and 20 min prior to imaging cells were treated with 0.6 mg/ml D-luciferin. A) Basal photon flux (photons/sec; p/s). B-F) Change in photon flux (photons/sec; p/s) after addition of increasing concentrations of either EGF (open circles) or BTC (closed circles). Error bars represent the standard error of measurements made in quadruplicate.

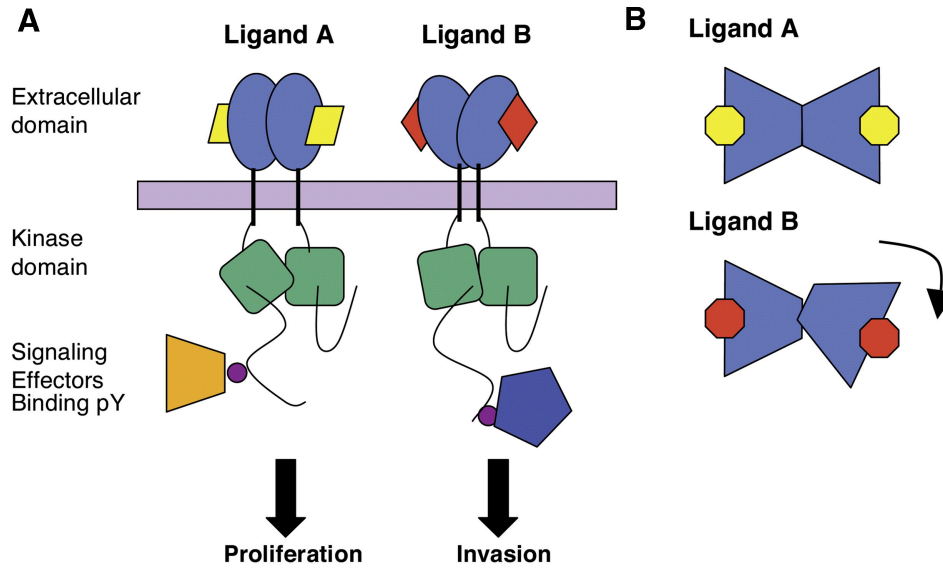


Figure 4.9. Model for differential regulation of EGF receptor dimerization, signaling, and biological effect mediated by different ligands. Schematic diagram indicating potential differences in ligand binding conformations to the extracellular domain of the EGF receptor (A and B). This extracellular difference in ligand binding may be propagated through the transmembrane region to the intracellular domain, mediating additional subtle differences in the binding interface. This could lead to phosphorylation of different tyrosine residues on the C-terminal tail of the EGF receptor, as well as recruitment of different downstream signaling proteins. Ultimately, the differences in ligand-receptor conformation at the cell surface could be propagated to elicit differences in the biological outcome of the cell (e.g. proliferation versus invasion) (From (47)).

CHAPTER 5. Discussion and Future Directions

Contributions to the EGF receptor field

In this thesis, I have described the development and utilization of a firefly luciferase fragment complementation imaging assay to examine the dynamics of the EGF receptor. This assay was used in two major ways: measuring the extracellular-domain-mediated dimerization and the conformational changes of the intracellular domains. Imaging an EGF receptor truncated just beyond the transmembrane domain followed ligand-induced EGF receptor dimerization. The ability of this assay to accurately follow the kinetics of ligand-induced dimerization in live cells is an improvement over existing assays that are performed under sub-optimal conditions and are unable to recapitulate the kinetics of ligand binding and dimerization.

Imaging the truncated EGF receptor in the context of homo- and hetero-dimerization with ErbB2 allowed detection of the differences in dimerization rate and extent of dimerization following stimulation with different EGF-like growth factors. These data compared the ability of these ligands to induce EGF receptor homo- and hetero-dimerization. In addition, amphiregulin was identified to have a unique ability to function as both an agonist and antagonist of dimerization.

Luciferase complementation imaging of the full-length EGF receptor identified sequential ligand-induced conformational changes that required kinase activity— a ligand-induced decrease followed by a recovery in luciferase activity. Several EGF receptor mutants were characterized to demonstrate that the decrease in luciferase activity involved re-arrangement of the kinase domains of the EGF receptor, while the recovery in luciferase activity was completely dependent on MAP kinase activity.

The intriguing dependence of the recovery in luciferase activity on MAP kinase activity is consistent with the previous reports that MAP kinase phosphorylation of the EGF receptor on Thr-669 results in desensitization of the kinase activity of the receptor. However, the mechanistic basis for the MAP kinase-dependent desensitization was unknown. In this thesis, I have established a model to explain how phosphorylation of the EGF receptor on Thr-669 results in desensitized kinase activity. Acidic amino acids in the C-lobe of the kinase domain were identified that lie in close proximity to the Thr-669 phosphorylation site on the juxtamembrane domain of the other kinase domain in an asymmetric dimer. The data presented here strongly suggest that these residues mediate a charge repulsion event with a phosphorylated Thr-669, resulting in a block in the allosteric asymmetric dimer that is required for kinase activation. This discovery underscores the critical role that the asymmetric dimer plays in mediating the kinase activity of the receptor and how this step in the receptor activation mechanism likely serves as an extremely important regulatory node in the EGF receptor signaling network.

Future Directions

The luciferase complementation imaging EGF receptor system provides a myriad of avenues for future research into the biology of the EGF receptor family. I will try and highlight a few of the ideas that I have regarding future studies with this assay. Given that the ErbB family members are validated cancer targets (48, 57, 66, 140, 151), one immediate application that carries promising clinical relevance would be its utility as a high-throughput screening assay to search for novel inhibitors of the EGF receptor with potential to expand current therapeutic strategies. For example, the luciferase complementation imaging assay with the truncated EGF receptor provides an excellent

opportunity to identify novel small molecule therapeutics targeting EGF receptor dimerization (R. Yang et al., manuscript submitted).

Small molecule inhibitors of EGF receptor family dimerization could also serve as chemical probes to further understand the biology of these receptors. For instance, it has been suggested that the EGF receptor and its family members not only exist as dimers, but also as higher-order oligomers. Inhibitors that target the “traditional” dimerization arm/interface could be used to examine alternative interfaces that may mediate higher-order oligomer formation. The luciferase complementation imaging assay is an excellent platform in which to identify small molecules targeting specific pairs of EGF receptor family homo- and hetero-dimers.

Luciferase complementation imaging with the full-length EGF receptor provides an opportunity to investigate the intracellular domain conformational changes that take place following ligand binding. The comparative analysis of the MAP kinase-mediated recovery in luciferase activity upon stimulation with EGF and betacellulin could lead to further characterization of other ligands in the same context.

I have demonstrated that MAP kinase is able to modulate the final conformation adopted by the EGF receptor, with the read-out being a recovery in luciferase activity. This recovery represents a dissociation of the asymmetric kinase dimer. I feel it would particularly interesting to apply a data-driven approach to this system to try and identify additional modulators of the recovery in luciferase activity. RNAi screening could be used with the full-length EGF receptor cells to identify proteins that are required for the recovery in luciferase activity. Besides MAP kinase, the MIG6 protein is likely a modulator of the recovery in luciferase activity, since it has been shown to block

formation of the asymmetric dimer interface (89, 90, 92). It appears that blocking asymmetric dimer formation may be a common mechanism to desensitize the kinase activity of the EGF receptor. Therefore, identification of additional asymmetric dimer interface modulators may provide additional insight into not only the biology of the ErbB receptors, but also expansion of therapeutic strategies.

Finally, the luciferase complementation imaging assay could be used to study the conformational changes in the intracellular domain of EGF receptor family heterodimers. Preliminary data not discussed here suggest that the luciferase activity of an EGF receptor/ErbB2 full-length hetero-dimer exhibits a similar pattern of a decrease and recovery in luciferase activity. It will be of interest to determine if there are receptor combinations that do not exhibit these characteristics. Particularly interesting may be the ErbB2/ErbB3 heterodimer in which ErbB2 lacks a known ligand and ErbB3 is intrinsically kinase-dead. This heterodimer may exhibit differences in the intracellular domain conformational changes, particularly because this complex signals more readily via the PI3-kinase pathway due to the presence of multiple phospho-tyrosine sites on ErbB3 that couple to this pathway.

I hope that I have highlighted not only the contributions this work has made to the EGF receptor field, but also the potential future contributions through the use of luciferase complementation imaging. This assay has provided a powerful tool to study the unique and complex protein-protein interactions that occur in the EGF receptor.

References

1. Levi-Montalcini, R., and Hamburger, V. (1951) Selective growth stimulating effects of mouse sarcoma on the sensory and sympathetic nervous system of the chick embryo, *J. Exp. Zool.* 116, 321-361.
2. Levi-Montalcini, R., and Hamburger, V. (1953) A diffusible agent of mouse sarcoma, producing hyperplasia of sympathetic ganglia and hyperneurotization of viscera in the chick embryo, *J. Exp. Zool.* 123, 233-288.
3. Levi-Montalcini, R., Meyer, H., and Hamburger, V. (1954) In vitro experiments on the effects of mouse sarcomas 180 and 37 on the spinal and sympathetic ganglia of the chick embryo, *Cancer Res.* 14, 49-57.
4. Cohen, S., Levi-Montalcini, R., and Hamburger, V. (1954) A Nerve Growth-Stimulating Factor Isolated from Sarcoma 37 and 180, *Proc Natl Acad Sci U S A* 40, 1014-1018.
5. Cohen, S., and Levi-Montalcini, R. (1956) A Nerve Growth-Stimulating Factor Isolated from Snake Venom, *Proc Natl Acad Sci U S A* 42, 571-574.
6. Cohen, S. (1962) Isolation of a mouse submaxillary gland protein accelerating incisor eruption and eyelid opening in the new-born animal, *J. Biol. Chem.* 237, 1555-1562.
7. Cohen, S. (1965) The stimulation of epidermal proliferation by a specific protein (EGF), *Dev. Biol.* 12, 394-407.
8. Carpenter, G., King, L., Jr., and Cohen, S. (1979) Rapid enhancement of protein phosphorylation in A-431 cell membrane preparations by epidermal growth factor, *J. Biol. Chem.* 254, 4884-4891.
9. King, L. E., Jr., Carpenter, G., and Cohen, S. (1980) Characterization by electrophoresis of epidermal growth factor stimulated phosphorylation using A-431 membranes, *Biochemistry* 19, 1524-1528.
10. Cohen, S., Carpenter, G., and King, L., Jr. (1980) Epidermal growth factor-receptor-protein kinase interactions. Co-purification of receptor and epidermal growth factor-enhanced phosphorylation activity, *J. Biol. Chem.* 255, 4834-4842.

11. Cohen, S., Ushiro, H., Stoscheck, C., and Chinkers, M. (1982) A native 170,000 epidermal growth factor receptor-kinase complex from shed plasma membrane vesicles, *J. Biol. Chem.* 257, 1523-1531.
12. Buhrow, S. A., Cohen, S., Garbers, D. L., and Staros, J. V. (1983) Characterization of the interaction of 5'-p-fluorosulfonylbenzoyl adenosine with the epidermal growth factor receptor/protein kinase in A431 cell membranes, *J. Biol. Chem.* 258, 7824-7827.
13. Buhrow, S. A., Cohen, S., and Staros, J. V. (1982) Affinity labeling of the protein kinase associated with the epidermal growth factor receptor in membrane vesicles from A431 cells, *J. Biol. Chem.* 257, 4019-4022.
14. Erneux, C., Cohen, S., and Garbers, D. L. (1983) The kinetics of tyrosine phosphorylation by the purified epidermal growth factor receptor kinase of A-431 cells, *J. Biol. Chem.* 258, 4137-4142.
15. Russo, M. W., Lukas, T. J., Cohen, S., and Staros, J. V. (1985) Identification of residues in the nucleotide binding site of the epidermal growth factor receptor/kinase, *J. Biol. Chem.* 260, 5205-5208.
16. Ushiro, H., and Cohen, S. (1980) Identification of phosphotyrosine as a product of epidermal growth factor-activated protein kinase in A-431 cell membranes, *J. Biol. Chem.* 255, 8363-8365.
17. Downward, J., Yarden, Y., Mayes, E., Scrace, G., Totty, N., Stockwell, P., Ullrich, A., Schlessinger, J., and Waterfield, M. D. (1984) Close similarity of epidermal growth factor receptor and v-erb-B oncogene protein sequences, *Nature* 307, 521-527.
18. Stein, R. A., and Staros, J. V. (2000) Evolutionary analysis of the ErbB receptor and ligand families, *J. Mol. Evol.* 50, 397-412.
19. Ullrich, A., Coussens, L., Hayflick, J. S., Dull, T. J., Gray, A., Tam, A. W., Lee, J., Yarden, Y., Libermann, T. A., Schlessinger, J., and et al. (1984) Human epidermal growth factor receptor cDNA sequence and aberrant expression of the amplified gene in A431 epidermoid carcinoma cells, *Nature* 309, 418-425.

20. Yarden, Y., and Schlessinger, J. (1987) Epidermal growth factor induces rapid, reversible aggregation of the purified epidermal growth factor receptor, *Biochemistry* 26, 1443-1451.
21. Boni-Schnetzler, M., and Pilch, P. F. (1987) Mechanism of epidermal growth factor receptor autophosphorylation and high-affinity binding, *Proc Natl Acad Sci U S A* 84, 7832-7836.
22. Fanger, B. O., Stephens, J. E., and Staros, J. V. (1989) High-yield trapping of EGF-induced receptor dimers by chemical cross-linking, *Faseb J* 3, 71-75.
23. Northwood, I. C., and Davis, R. J. (1988) Activation of the epidermal growth factor receptor tyrosine protein kinase in the absence of receptor oligomerization, *J. Biol. Chem.* 263, 7450-7453.
24. Fanger, B. O., Austin, K. S., Earp, H. S., and Cidlowski, J. A. (1986) Cross-linking of epidermal growth factor receptors in intact cells: detection of initial stages of receptor clustering and determination of molecular weight of high-affinity receptors, *Biochemistry* 25, 6414-6420.
25. Cochet, C., Kashles, O., Chambaz, E. M., Borrello, I., King, C. R., and Schlessinger, J. (1988) Demonstration of epidermal growth factor-induced receptor dimerization in living cells using a chemical covalent cross-linking agent, *J. Biol. Chem.* 263, 3290-3295.
26. Defize, L. H., Boonstra, J., Meisenhelder, J., Kruijer, W., Tertoolen, L. G., Tilly, B. C., Hunter, T., van Bergen en Henegouwen, P. M., Moolenaar, W. H., and de Laat, S. W. (1989) Signal transduction by epidermal growth factor occurs through the subclass of high affinity receptors, *J. Cell Biol.* 109, 2495-2507.
27. Yarden, Y., and Schlessinger, J. (1987) Self-phosphorylation of epidermal growth factor receptor: evidence for a model of intermolecular allosteric activation, *Biochemistry* 26, 1434-1442.
28. Spaargaren, M., Defize, L. H., Boonstra, J., and de Laat, S. W. (1991) Antibody-induced dimerization activates the epidermal growth factor receptor tyrosine kinase, *J. Biol. Chem.* 266, 1733-1739.
29. Honegger, A. M., Kris, R. M., Ullrich, A., and Schlessinger, J. (1989) Evidence that autophosphorylation of solubilized receptors for epidermal growth factor is

mediated by intermolecular cross-phosphorylation, *Proc Natl Acad Sci U S A* 86, 925-929.

30. Honegger, A. M., Schmidt, A., Ullrich, A., and Schlessinger, J. (1990) Evidence for epidermal growth factor (EGF)-induced intermolecular autophosphorylation of the EGF receptors in living cells, *Mol. Cell. Biol.* 10, 4035-4044.
31. Ferguson, K. M., Berger, M. B., Mendrola, J. M., Cho, H. S., Leahy, D. J., and Lemmon, M. A. (2003) EGF activates its receptor by removing interactions that autoinhibit ectodomain dimerization, *Mol. Cell* 11, 507-517.
32. Ogiso, H., Ishitani, R., Nureki, O., Fukai, S., Yamanaka, M., Kim, J. H., Saito, K., Sakamoto, A., Inoue, M., Shirouzu, M., and Yokoyama, S. (2002) Crystal structure of the complex of human epidermal growth factor and receptor extracellular domains, *Cell* 110, 775-787.
33. Garrett, T. P., McKern, N. M., Lou, M., Elleman, T. C., Adams, T. E., Lovrecz, G. O., Zhu, H. J., Walker, F., Frenkel, M. J., Hoyne, P. A., Jorissen, R. N., Nice, E. C., Burgess, A. W., and Ward, C. W. (2002) Crystal structure of a truncated epidermal growth factor receptor extracellular domain bound to transforming growth factor alpha, *Cell* 110, 763-773.
34. Walker, F., Orchard, S. G., Jorissen, R. N., Hall, N. E., Zhang, H. H., Hoyne, P. A., Adams, T. E., Johns, T. G., Ward, C., Garrett, T. P., Zhu, H. J., Nerrie, M., Scott, A. M., Nice, E. C., and Burgess, A. W. (2004) CR1/CR2 interactions modulate the functions of the cell surface epidermal growth factor receptor, *J. Biol. Chem.* 279, 22387-22398.
35. Zhang, X., Gureasko, J., Shen, K., Cole, P. A., and Kuriyan, J. (2006) An allosteric mechanism for activation of the kinase domain of epidermal growth factor receptor, *Cell* 125, 1137-1149.
36. Thiel, K. W., and Carpenter, G. (2007) Epidermal growth factor receptor juxtamembrane region regulates allosteric tyrosine kinase activation, *Proc Natl Acad Sci U S A* 104, 19238-19243.
37. Wood, E. R., Shewchuk, L. M., Ellis, B., Brignola, P., Brashear, R. L., Caferro, T. R., Dickerson, S. H., Dickson, H. D., Donaldson, K. H., Gaul, M., Griffin, R. J., Hassell, A. M., Keith, B., Mullin, R., Petrov, K. G., Reno, M. J., Rusnak, D. W., Tadepalli, S. M., Ulrich, J. C., Wagner, C. D., Vanderwall, D. E., Waterson, A. G., Williams, J. D., White, W. L., and Uehling, D. E. (2008) 6-Ethynylthieno[3,2-

d]- and 6-ethynylthieno[2,3-d]pyrimidin-4-anilines as tunable covalent modifiers of ErbB kinases, *Proc Natl Acad Sci U S A* 105, 2773-2778.

38. Jura, N., Endres, N. F., Engel, K., Deindl, S., Das, R., Lamers, M. H., Wemmer, D. E., Zhang, X., and Kuriyan, J. (2009) Mechanism for activation of the EGF receptor catalytic domain by the juxtamembrane segment, *Cell* 137, 1293-1307.
39. Red Brewer, M., Choi, S. H., Alvarado, D., Moravcevic, K., Pozzi, A., Lemmon, M. A., and Carpenter, G. (2009) The juxtamembrane region of the EGF receptor functions as an activation domain, *Mol. Cell* 34, 641-651.
40. Cadena, D. L., Chan, C. L., and Gill, G. N. (1994) The intracellular tyrosine kinase domain of the epidermal growth factor receptor undergoes a conformational change upon autophosphorylation, *J. Biol. Chem.* 269, 260-265.
41. Lee, N. Y., and Koland, J. G. (2005) Conformational changes accompany phosphorylation of the epidermal growth factor receptor C-terminal domain, *Protein Sci.* 14, 2793-2803.
42. Clayton, A. H., Walker, F., Orchard, S. G., Henderson, C., Fuchs, D., Rothacker, J., Nice, E. C., and Burgess, A. W. (2005) Ligand-induced dimer-tetramer transition during the activation of the cell surface epidermal growth factor receptor-A multidimensional microscopy analysis, *J. Biol. Chem.* 280, 30392-30399.
43. Saffarian, S., Li, Y., Elson, E. L., and Pike, L. J. (2007) Oligomerization of the EGF Receptor Investigated by Live Cell Fluorescence Intensity Distribution Analysis, *Biophys. J.*
44. Whitson, K. B., Beechem, J. M., Beth, A. H., and Staros, J. V. (2004) Preparation and characterization of Alexa Fluor 594-labeled epidermal growth factor for fluorescence resonance energy transfer studies: application to the epidermal growth factor receptor, *Anal. Biochem.* 324, 227-236.
45. Clayton, A. H., Tavarnesi, M. L., and Johns, T. G. (2007) Unligated Epidermal Growth Factor Receptor Forms Higher Order Oligomers within Microclusters on A431 Cells That Are Sensitive to Tyrosine Kinase Inhibitor Binding, *Biochemistry* 46, 4589-4597.

46. Linggi, B., and Carpenter, G. (2006) ErbB receptors: new insights on mechanisms and biology, *Trends Cell Biol.*
47. Wilson, K. J., Gilmore, J. L., Foley, J., Lemmon, M. A., and Riese, D. J., 2nd. (2009) Functional selectivity of EGF family peptide growth factors: implications for cancer, *Pharmacol. Ther.* 122, 1-8.
48. Holbro, T., and Hynes, N. E. (2004) ErbB receptors: directing key signaling networks throughout life, *Annu. Rev. Pharmacol. Tox.* 44, 195-217.
49. Harris, R. C., Chung, E., and Coffey, R. J. (2003) EGF receptor ligands, *Exp. Cell Res.* 284, 2-13.
50. Jones, J. T., Akita, R. W., and Sliwkowski, M. X. (1999) Binding specificities and affinities of egf domains for ErbB receptors, *FEBS Lett.* 447, 227-231.
51. Ferguson, K. M. (2004) Active and inactive conformations of the epidermal growth factor receptor, *Biochem. Soc. Trans.* 32, 742-745.
52. Ferguson, K. M. (2008) Structure-based view of epidermal growth factor receptor regulation, *Annu. Rev. Biophys.* 37, 353-373.
53. Burgess, A. W., Cho, H. S., Eigenbrot, C., Ferguson, K. M., Garrett, T. P., Leahy, D. J., Lemmon, M. A., Sliwkowski, M. X., Ward, C. W., and Yokoyama, S. (2003) An open-and-shut case? Recent insights into the activation of EGF/ErbB receptors, *Mol. Cell* 12, 541-552.
54. Hubbard, S. R. (2006) EGF receptor activation: push comes to shove, *Cell* 125, 1029-1031.
55. Hsuan, J. J., Totty, N., and Waterfield, M. D. (1989) Identification of a novel autophosphorylation site (P4) on the epidermal growth factor receptor, *Biochem. J.* 262, 659-663.
56. Jorissen, R. N., Walker, F., Pouliot, N., Garrett, T. P., Ward, C. W., and Burgess, A. W. (2003) Epidermal growth factor receptor: mechanisms of activation and signalling, *Exp. Cell Res.* 284, 31-53.

57. Olayioye, M. A., Neve, R. M., Lane, H. A., and Hynes, N. E. (2000) The ErbB signaling network: receptor heterodimerization in development and cancer, *EMBO J.* 19, 3159-3167.
58. Downward, J., Parker, P., and Waterfield, M. D. (1984) Autophosphorylation sites on the epidermal growth factor receptor, *Nature* 311, 483-485.
59. Margolis, B. L., Lax, I., Kris, R., Dombalagian, M., Honegger, A. M., Howk, R., Givol, D., Ullrich, A., and Schlessinger, J. (1989) All autophosphorylation sites of epidermal growth factor (EGF) receptor and HER2/neu are located in their carboxyl-terminal tails. Identification of a novel site in EGF receptor, *J. Biol. Chem.* 264, 10667-10671.
60. Walton, G. M., Chen, W. S., Rosenfeld, M. G., and Gill, G. N. (1990) Analysis of deletions of the carboxyl terminus of the epidermal growth factor receptor reveals self-phosphorylation at tyrosine 992 and enhanced in vivo tyrosine phosphorylation of cell substrates, *J. Biol. Chem.* 265, 1750-1754.
61. Biscardi, J. S., Maa, M. C., Tice, D. A., Cox, M. E., Leu, T. H., and Parsons, S. J. (1999) c-Src-mediated phosphorylation of the epidermal growth factor receptor on Tyr845 and Tyr1101 is associated with modulation of receptor function, *J. Biol. Chem.* 274, 8335-8343.
62. Stover, D. R., Becker, M., Liebetanz, J., and Lydon, N. B. (1995) Src phosphorylation of the epidermal growth factor receptor at novel sites mediates receptor interaction with Src and P85 alpha, *J. Biol. Chem.* 270, 15591-15597.
63. Tice, D. A., Biscardi, J. S., Nickles, A. L., and Parsons, S. J. (1999) Mechanism of biological synergy between cellular Src and epidermal growth factor receptor, *Proc Natl Acad Sci U S A* 96, 1415-1420.
64. Olayioye, M. A. (2001) Update on HER-2 as a target for cancer therapy: intracellular signaling pathways of ErbB2/HER-2 and family members, *Breast Cancer Res.* 3, 385-389.
65. Sudol, M. (1998) From Src Homology domains to other signaling modules: proposal of the 'protein recognition code', *Oncogene* 17, 1469-1474.
66. Citri, A., and Yarden, Y. (2006) EGF-ERBB signalling: towards the systems level, *Nat. Rev. Mol. Cell Biol.* 7, 505-516.

67. Batzer, A. G., Rotin, D., Urena, J. M., Skolnik, E. Y., and Schlessinger, J. (1994) Hierarchy of binding sites for Grb2 and Shc on the epidermal growth factor receptor, *Mol. Cell. Biol.* *14*, 5192-5201.
68. Sasaoka, T., Langlois, W. J., Leitner, J. W., Draznin, B., and Olefsky, J. M. (1994) The signaling pathway coupling epidermal growth factor receptors to activation of p21ras, *J. Biol. Chem.* *269*, 32621-32625.
69. Mendelsohn, J., and Baselga, J. (2003) Status of epidermal growth factor receptor antagonists in the biology and treatment of cancer, *J. Clin. Oncol.* *21*, 2787-2799.
70. Lowenstein, E. J., Daly, R. J., Batzer, A. G., Li, W., Margolis, B., Lammers, R., Ullrich, A., Skolnik, E. Y., Bar-Sagi, D., and Schlessinger, J. (1992) The SH2 and SH3 domain-containing protein GRB2 links receptor tyrosine kinases to ras signaling, *Cell* *70*, 431-442.
71. Olivier, J. P., Raabe, T., Henkemeyer, M., Dickson, B., Mbamalu, G., Margolis, B., Schlessinger, J., Hafen, E., and Pawson, T. (1993) A Drosophila SH2-SH3 adaptor protein implicated in coupling the sevenless tyrosine kinase to an activator of Ras guanine nucleotide exchange, Sos, *Cell* *73*, 179-191.
72. Li, N., Batzer, A., Daly, R., Yajnik, V., Skolnik, E., Chardin, P., Bar-Sagi, D., Margolis, B., and Schlessinger, J. (1993) Guanine-nucleotide-releasing factor hSos1 binds to Grb2 and links receptor tyrosine kinases to Ras signalling, *Nature* *363*, 85-88.
73. Gale, N. W., Kaplan, S., Lowenstein, E. J., Schlessinger, J., and Bar-Sagi, D. (1993) Grb2 mediates the EGF-dependent activation of guanine nucleotide exchange on Ras, *Nature* *363*, 88-92.
74. Buday, L., and Downward, J. (1993) Epidermal growth factor regulates p21ras through the formation of a complex of receptor, Grb2 adapter protein, and Sos nucleotide exchange factor, *Cell* *73*, 611-620.
75. Zhang, X. F., Settleman, J., Kyriakis, J. M., Takeuchi-Suzuki, E., Elledge, S. J., Marshall, M. S., Bruder, J. T., Rapp, U. R., and Avruch, J. (1993) Normal and oncogenic p21ras proteins bind to the amino-terminal regulatory domain of c-Raf-1, *Nature* *364*, 308-313.

76. Warne, P. H., Viciano, P. R., and Downward, J. (1993) Direct interaction of Ras and the amino-terminal region of Raf-1 in vitro, *Nature* 364, 352-355.
77. Vojtek, A. B., Hollenberg, S. M., and Cooper, J. A. (1993) Mammalian Ras interacts directly with the serine/threonine kinase Raf, *Cell* 74, 205-214.
78. Kyriakis, J. M., App, H., Zhang, X. F., Banerjee, P., Brautigan, D. L., Rapp, U. R., and Avruch, J. (1992) Raf-1 activates MAP kinase-kinase, *Nature* 358, 417-421.
79. Crews, C. M., Alessandrini, A., and Erikson, R. L. (1992) The primary structure of MEK, a protein kinase that phosphorylates the ERK gene product, *Science* 258, 478-480.
80. Ray, L. B., and Sturgill, T. W. (1988) Insulin-stimulated microtubule-associated protein kinase is phosphorylated on tyrosine and threonine in vivo, *Proc Natl Acad Sci U S A* 85, 3753-3757.
81. Carraway, K. L., 3rd, Yen, L., Ingalla, E., and Sweeney, C. (2008) Negative regulation of signaling by the EGFR family, in *EGFR signaling networks in cancer therapy* (Gullick, W. J., and Haley, J. D., Eds.), pp 161-178, Humana Press, New York.
82. Stoscheck, C. M., and Carpenter, G. (1984) Characterization of the metabolic turnover of epidermal growth factor receptor protein in A-431 cells, *J. Cell. Physiol.* 120, 296-302.
83. Stoscheck, C. M., and Carpenter, G. (1984) Down regulation of epidermal growth factor receptors: direct demonstration of receptor degradation in human fibroblasts, *J. Cell Biol.* 98, 1048-1053.
84. Sorkin, A. (2008) Internalization and degradation of the EGF receptor, in *EGFR signaling networks in cancer therapy* (Gullick, W. J., and Haley, J. D., Eds.), pp 45-59, Humana Press, New York.
85. Carpenter, G., and Cohen, S. (1976) 125I-labeled human epidermal growth factor. Binding, internalization, and degradation in human fibroblasts, *J. Cell Biol.* 71, 159-171.

86. Chinkers, M., and Garbers, D. L. (1986) Suppression of protein tyrosine kinase activity of the epidermal growth factor receptor by epidermal growth factor, *J. Biol. Chem.* *261*, 8295-8297.
87. Lai, W. H., Cameron, P. H., Doherty, J. J., 2nd, Posner, B. I., and Bergeron, J. J. (1989) Ligand-mediated autophosphorylation activity of the epidermal growth factor receptor during internalization, *J. Cell Biol.* *109*, 2751-2760.
88. McCune, B. K., Prokop, C. A., and Earp, H. S. (1990) Transient epidermal growth factor (EGF)-dependent suppression of EGF receptor autophosphorylation during internalization, *J. Biol. Chem.* *265*, 9715-9721.
89. Zhang, X., Pickin, K. A., Bose, R., Jura, N., Cole, P. A., and Kuriyan, J. (2007) Inhibition of the EGF receptor by binding of MIG6 to an activating kinase domain interface, *Nature* *450*, 741-744.
90. Anastasi, S., Baietti, M. F., Frosi, Y., Alema, S., and Segatto, O. (2007) The evolutionarily conserved EBR module of RALT/MIG6 mediates suppression of the EGFR catalytic activity, *Oncogene* *26*, 7833-7846.
91. Hackel, P. O., Gishizky, M., and Ullrich, A. (2001) Mig-6 is a negative regulator of the epidermal growth factor receptor signal, *Biol. Chem.* *382*, 1649-1662.
92. Xu, D., Makkinje, A., and Kyriakis, J. M. (2005) Gene 33 is an endogenous inhibitor of epidermal growth factor (EGF) receptor signaling and mediates dexamethasone-induced suppression of EGF function, *J. Biol. Chem.* *280*, 2924-2933.
93. Heisermann, G. J., Wiley, H. S., Walsh, B. J., Ingraham, H. A., Fiol, C. J., and Gill, G. N. (1990) Mutational removal of the Thr669 and Ser671 phosphorylation sites alters substrate specificity and ligand-induced internalization of the epidermal growth factor receptor, *J. Biol. Chem.* *265*, 12820-12827.
94. Li, X., Huang, Y., Jiang, J., and Frank, S. J. (2008) ERK-dependent threonine phosphorylation of EGF receptor modulates receptor downregulation and signaling, *Cell. Signal.* *20*, 2145-2155.
95. Heisermann, G. J., and Gill, G. N. (1988) Epidermal growth factor receptor threonine and serine residues phosphorylated in vivo, *J. Biol. Chem.* *263*, 13152-13158.

96. Countaway, J. L., Northwood, I. C., and Davis, R. J. (1989) Mechanism of phosphorylation of the epidermal growth factor receptor at threonine 669, *J. Biol. Chem.* 264, 10828-10835.
97. Takishima, K., Griswold-Prenner, I., Ingebritsen, T., and Rosner, M. R. (1991) Epidermal growth factor (EGF) receptor T669 peptide kinase from 3T3-L1 cells is an EGF-stimulated "MAP" kinase, *Proc Natl Acad Sci U S A* 88, 2520-2524.
98. Northwood, I. C., Gonzalez, F. A., Wartmann, M., Raden, D. L., and Davis, R. J. (1991) Isolation and characterization of two growth factor-stimulated protein kinases that phosphorylate the epidermal growth factor receptor at threonine 669, *J. Biol. Chem.* 266, 15266-15276.
99. Lee, N. Y., Hazlett, T. L., and Koland, J. G. (2006) Structure and dynamics of the epidermal growth factor receptor C-terminal phosphorylation domain, *Protein Sci.* 15, 1142-1152.
100. Luker, K. E., Smith, M. C., Luker, G. D., Gammon, S. T., Piwnica-Worms, H., and Piwnica-Worms, D. (2004) Kinetics of regulated protein-protein interactions revealed with firefly luciferase complementation imaging in cells and living animals, *Proc Natl Acad Sci U S A* 101, 12288-12293.
101. Villalobos, V., Naik, S., and Piwnica-Worms, D. (2007) Current state of imaging protein-protein interactions in vivo with genetically encoded reporters, *Annu. Rev. Biomed. Eng.* 9, 321-349.
102. Macdonald, J. L., and Pike, L. J. (2008) Heterogeneity in EGF-binding affinities arises from negative cooperativity in an aggregating system, *Proc. Natl. Acad. Sci. USA* 105, 112-117.
103. Friedman, B., Frackelton, A. R., Jr., Ross, A. H., Connors, J. M., Fujiki, H., Sugimura, T., and Rosner, M. R. (1984) Tumor promoters block tyrosine-specific phosphorylation of the epidermal growth factor receptor, *Proc Natl Acad Sci U S A* 81, 3034-3038.
104. Martin-Nieto, J., and Villalobo, A. (1998) The human epidermal growth factor receptor contains a juxtamembrane calmodulin-binding site, *Biochemistry* 37, 227-236.

105. Sengupta, P., Ruano, M. J., Tebar, F., Golebiewska, U., Zaitseva, I., Enrich, C., McLaughlin, S., and Villalobo, A. (2007) Membrane-permeable calmodulin inhibitors (e.g. W-7/W-13) bind to membranes, changing the electrostatic surface potential: dual effect of W-13 on epidermal growth factor receptor activation, *J. Biol. Chem.* 282, 8474-8486.
106. Li, H., Ruano, M. J., and Villalobo, A. (2004) Endogenous calmodulin interacts with the epidermal growth factor receptor in living cells, *FEBS Lett.* 559, 175-180.
107. Honegger, A. M., Szapary, D., Schmidt, A., Lyall, R., Van Obberghen, E., Dull, T. J., Ullrich, A., and Schlessinger, J. (1987) A mutant epidermal growth factor receptor with defective protein tyrosine kinase is unable to stimulate proto-oncogene expression and DNA synthesis, *Mol. Cell. Biol.* 7, 4568-4571.
108. Takishima, K., Griswold-Prenner, I., Ingebritsen, T., and Rosner, M. R. (1991) Epidermal growth factor (EGF) receptor T669 peptide kinase from 3T3-L1 cells is an EGF-stimulated "MAP" kinase, *Proc. Natl. Acad. Sci. USA* 88, 2520-2524.
109. Countaway, J. L., Northwood, I. C., and Davis, R. J. (1989) Mechanism of phosphorylation of the epidermal growth factor receptor at threonine 669, *J. Biol. Chem.* 264, 10828-10835.
110. Northwood, I. C., Gonzalez, F. A., Wartmann, M., Raden, D. L., and Davis, R. J. (1991) Isolation and characterization of two growth factor-stimulated protein kinases that phosphorylate the epidermal growth factor receptor at threonine 669, *J. Biol. Chem.* 266, 15266-15276.
111. Blakely, B. T., Rossi, F. M. V., Tillotson, B., Palmer, M., Estelles, A., and Blau, H. M. (2000) Epidermal Growth Factor Receptor Dimerization Monitored in Live Cells, *Nat. Biotechnol.* 18, 218-222.
112. Wehrman, T. S., Raab, W. J., Casipit, C. L., Doyonnas, R., Pomerantz, J. H., and Blau, H. M. (2006) A System for Quantifying Dynamic Protein Interactions Defines a Role for Herceptin in Modulating ErbB2 Interactions, *Proc. Natl. Acad. Sci. U.S.A.* 103, 19063-19068.
113. Chantry, A. (1995) The Kinase Domain and Membrane Localization Determine Intracellular Interactions between Epidermal Growth Factor Receptors, *J. Biol. Chem.* 270, 3068-3073.

114. Martin-Fernandez, M., Clarke, D. T., Tobin, M. J., Jones, S. V., and Jones, G. R. (2002) Preformed oligomeric epidermal growth factor receptors undergo an ectodomain structure change during signaling, *Biophys. J.* *82*, 2415-2427.
115. Yu, X., Sharma, K. D., Takahashi, T., Iwamoto, R., and Mekada, E. (2002) Ligand-independent dimer formation of epidermal growth factor receptor (EGFR) is a step separable from ligand-induced EGFR signaling, *Mol. Biol. Cell* *13*, 2547-2557.
116. Arteaga, C. L., Ramsey, T. T., Shawver, L. K., and Guyer, C. A. (1997) Unliganded Epidermal Growth Factor Receptor Dimerization Induced by Direct Interaction of Quinazolines with the ATP Binding Site, *J. Biol. Chem.* *272*, 23247-23254.
117. Lichtner, R. B., Menrad, A., Sommer, A., Klar, U., and Schneider, M. R. (2001) Signaling-inactive Epidermal Growth Factor Receptor/Ligand Complexes in Intact Carcinoma Cells by Quinazoline Tyrosine Kinase Inhibitors, *Cancer Res.* *61*, 5790-5795.
118. Gan, H. K., Walker, F., Burgess, A. W., Rigopoulos, A., and Scot, A. M. (2007) The Epidermal Growth Factor Receptor (EGFR) Tyrosine Kinase Inhibitor AG1478 Increases the Formation of Inactive Untethered EGFR Dimers, *J. Biol. Chem.* *282*, 2840-2850.
119. Liu, P., Sudhakaran, T., Koh, R. M. L., Hwang, L. C., Ahmed, S., Maruyama, I. N., and Wohland, T. (2007) Investigation of the Dimerization of Proteins from the Epidermal Growth Factor Receptor Family by Single Wavelength Fluorescence Cross-Correlation Spectroscopy, *Biophys. J.* *93*, 684-698.
120. McLaughlin, S., Smith, S. O., Hayman, M. J., and Murray, D. (2005) An electrostatic engine model for autoinhibition and activation of the epidermal growth factor receptor (EGFR/ErbB) family, *J. Gen. Physiol.* *126*, 41-53.
121. Li, X., Huang, Y., Jiang, J., and Frank, S. J. (2008) ERK-dependent threonine phosphorylation of EGF receptor modulates receptor downregulation and signaling, *Cell. Signal.* *20*, 2145-2155.
122. Lichtner, R. B., Menrad, A., Sommer, A., Klar, U., and Schneider, M. R. (2001) Signaling-inactive epidermal growth factor receptor/ligand complexes in intact carcinoma cells by quinazoline tyrosine kinase inhibitors, *Cancer Res.* *61*, 5790-5795.

123. Gan, H. K., Walker, F., Burgess, A. W., Rigopoulos, A., Scott, A. M., and Johns, T. G. (2006) The EGFR tyrosine kinase inhibitor AG1478 increases the formation of inactive untethered EGFR dimers: Implications for combination therapy with mab 806, *J. Biol. Chem.*
124. Liu, P., Sudhaharan, T., Koh, R. M., Hwang, L. C., Ahmed, S., Maruyama, I. N., and Wohland, T. (2007) Investigation of the dimerization of proteins from the epidermal growth factor receptor family by single wavelength fluorescence cross-correlation spectroscopy, *Biophys. J.* 93, 684-698.
125. Li, W., Li, F., Huang, Q., Frederick, B., Bao, S., and Li, C. Y. (2008) Noninvasive imaging and quantification of epidermal growth factor receptor kinase activation *in vivo*, *Cancer Res.* 68, 4990-4997.
126. Saffarian, S., Li, Y., Elson, E. L., and Pike, L. J. (2007) Oligomerization of the EGF receptor investigated by live cell fluorescence intensity distribution analysis, *Biophys. J.* 93, 1021-1031.
127. Macdonald, J., Li, Z., Su, W., and Pike, L. J. (2006) The membrane proximal disulfides of the EGF receptor extracellular domain are required for high affinity binding and signal transduction but do not play a role in the localization of the receptor to lipid rafts, *Biochim. Biophys. Acta* 1763, 870-878.
128. Yang, K. S., Ilagan, M. X., Piwnicka-Worms, D., and Pike, L. J. (2009) Luciferase fragment complementation imaging of conformational changes in the epidermal growth factor receptor, *J. Biol. Chem.* 284, 7474-7482.
129. Wood, E. R., Truesdale, A. T., McDonald, O. B., Yuan, D., Hassell, A., Dickerson, S. H., Ellis, B., Pennisi, C., Horne, E., Lackey, K., Allgood, K. J., Rusnak, D. W., Gilmer, T. M., and Shewchuk, L. (2004) A unique structure for epidermal growth factor receptor bound to GW572016 (Lapatinib): relationships among protein conformation, inhibitor off-rate, and receptor activity in tumor cells, *Cancer Res.* 64, 6652-6659.
130. Stamos, J., Sliwkowski, M. X., and Eigenbrot, C. (2002) Structure of the epidermal growth factor receptor kinase domain alone and in complex with a 4-anilinoquinazoline inhibitor, *J. Biol. Chem.* 277, 46265-46272.
131. Yun, C. H., Boggon, T. J., Li, Y., Woo, M. S., Greulich, H., Meyerson, M., and Eck, M. J. (2007) Structures of lung cancer-derived EGFR mutants and inhibitor

complexes: mechanism of activation and insights into differential inhibitor sensitivity, *Cancer Cell* 11, 217-227.

132. Morrison, P., Takishima, K., and Rosner, M. R. (1993) Role of threonine residues in regulation of the epidermal growth factor receptor by protein kinase C and mitogen-activated protein kinase, *J. Biol. Chem.* 268, 15536-15543.
133. Liu, P., Roush, E. D., Bruno, J., Osawa, S., and Weiss, E. R. (2004) Direct binding of visual arrestin to a rhodopsin carboxyl terminal synthetic phosphopeptide, *Mol. Vision* 10, 712-719.
134. Soufi, A., Noy, P., Buckle, M., Sawasdichai, A., Gaston, K., and Jayaraman, P. S. (2009) CK2 phosphorylation of the PRH/Hex homeodomain functions as a reversible switch for DNA binding, *Nucleic Acids Res.* 37, 3288-3300.
135. Na, H., Rho, J. K., Choi, Y. J., Kim, C. H., Park, J. H., Koh, J. S., Ryoo, B. Y., Yang, S. H., and Lee, J. C. (2007) The survival outcomes of patients with resected non-small cell lung cancer differ according to EGFR mutations and the P21 expression, *Lung Cancer (Amsterdam, Netherlands)* 57, 96-102.
136. Macdonald, J. L., and Pike, L. J. (2008) Heterogeneity in EGF-binding affinities arises from negative cooperativity in an aggregating system, *Proc Natl Acad Sci U S A* 105, 112-117.
137. Haigler, H. T., Maxfield, F. R., Willingham, M. C., and Pastan, I. (1980) Dansylcadaverine inhibits internalization of 125I-epidermal growth factor in BALB 3T3 cells, *J. Biol. Chem.* 255, 1239-1241.
138. Sweeney, C., and Carraway, K. L., 3rd. (2000) Ligand discrimination by ErbB receptors: differential signaling through differential phosphorylation site usage, *Oncogene* 19, 5568-5573.
139. Willmarth, N. E., and Ethier, S. P. (2008) Amphiregulin as a novel target for breast cancer therapy, *J. Mammary Gland Biol. Neoplasia* 13, 171-179.
140. Yarden, Y., and Sliwkowski, M. X. (2001) Untangling the ErbB signalling network, *Nat. Rev. Mol. Cell Biol.* 2, 127-137.

141. Sweeney, C., Lai, C., Riese, D. J., 2nd, Diamonti, A. J., Cantley, L. C., and Carraway, K. L., 3rd. (2000) Ligand discrimination in signaling through an ErbB4 receptor homodimer, *J. Biol. Chem.* 275, 19803-19807.
142. Saito, T., Okada, S., Ohshima, K., Yamada, E., Sato, M., Uehara, Y., Shimizu, H., Pessin, J. E., and Mori, M. (2004) Differential activation of epidermal growth factor (EGF) receptor downstream signaling pathways by betacellulin and EGF, *Endocrinology* 145, 4232-4243.
143. Shoyab, M., McDonald, V. L., Bradley, J. G., and Todaro, G. J. (1988) Amphiregulin: a bifunctional growth-modulating glycoprotein produced by the phorbol 12-myristate 13-acetate-treated human breast adenocarcinoma cell line MCF-7, *Proc Natl Acad Sci U S A* 85, 6528-6532.
144. Johnson, G. R., Kannan, B., Shoyab, M., and Stromberg, K. (1993) Amphiregulin induces tyrosine phosphorylation of the epidermal growth factor receptor and p185erbB2. Evidence that amphiregulin acts exclusively through the epidermal growth factor receptor at the surface of human epithelial cells, *J. Biol. Chem.* 268, 2924-2931.
145. Adam, R., Drummond, D. R., Solic, N., Holt, S. J., Sharma, R. P., Chamberlin, S. G., and Davies, D. E. (1995) Modulation of the receptor binding affinity of amphiregulin by modification of its carboxyl terminal tail, *Biochim. Biophys. Acta* 1266, 83-90.
146. Dunbar, A. J., and Goddard, C. (2000) Structure-function and biological role of betacellulin, *Int. J. Biochem. Cell Biol.* 32, 805-815.
147. Holmes, W. E., Sliwkowski, M. X., Akita, R. W., Henzel, W. J., Lee, J., Park, J. W., Yansura, D., Abadi, N., Raab, H., Lewis, G. D., and et al. (1992) Identification of heregulin, a specific activator of p185erbB2, *Science* 256, 1205-1210.
148. Franklin, M. C., Carey, K. D., Vajdos, F. F., Leahy, D. J., de Vos, A. M., and Sliwkowski, M. X. (2004) Insights into ErbB signaling from the structure of the ErbB2-pertuzumab complex, *Cancer Cell* 5, 317-328.
149. Garrett, T. P., McKern, N. M., Lou, M., Elleman, T. C., Adams, T. E., Lovrecz, G. O., Kofler, M., Jorissen, R. N., Nice, E. C., Burgess, A. W., and Ward, C. W. (2003) The crystal structure of a truncated ErbB2 ectodomain reveals an active conformation, poised to interact with other ErbB receptors, *Mol. Cell* 11, 495-505.

150. Sliwkowski, M. X., Schaefer, G., Akita, R. W., Lofgren, J. A., Fitzpatrick, V. D., Nuijens, A., Fendly, B. M., Cerione, R. A., Vandlen, R. L., and Carraway, K. L., 3rd. (1994) Coexpression of erbB2 and erbB3 proteins reconstitutes a high affinity receptor for heregulin, *J. Biol. Chem.* *269*, 14661-14665.
151. Hynes, N. E., and Lane, H. A. (2005) ERBB receptors and cancer: the complexity of targeted inhibitors, *Nat. Rev. Cancer* *5*, 341-354.
152. Wehrman, T. S., Raab, W. J., Casipit, C. L., Doyonnas, R., Pomerantz, J. H., and Blau, H. M. (2006) A system for quantifying dynamic protein interactions defines a role for Herceptin in modulating ErbB2 interactions, *Proc Natl Acad Sci U S A* *103*, 19063-19068.
153. Lemmon, M. A. (2009) Ligand-induced ErbB receptor dimerization, *Exp. Cell Res.* *315*, 638-648.
154. Willmarth, N. E., Baillo, A., Dziubinski, M. L., Wilson, K., Riese, D. J., 2nd, and Ethier, S. P. (2009) Altered EGFR localization and degradation in human breast cancer cells with an amphiregulin/EGFR autocrine loop, *Cell. Signal.* *21*, 212-219.